

# Higgs measurements in 3rd generation decay channels (excl. ttH) with ATLAS and CMS



On behalf of the ATLAS & CMS Collaborations

Stephen Jiggins

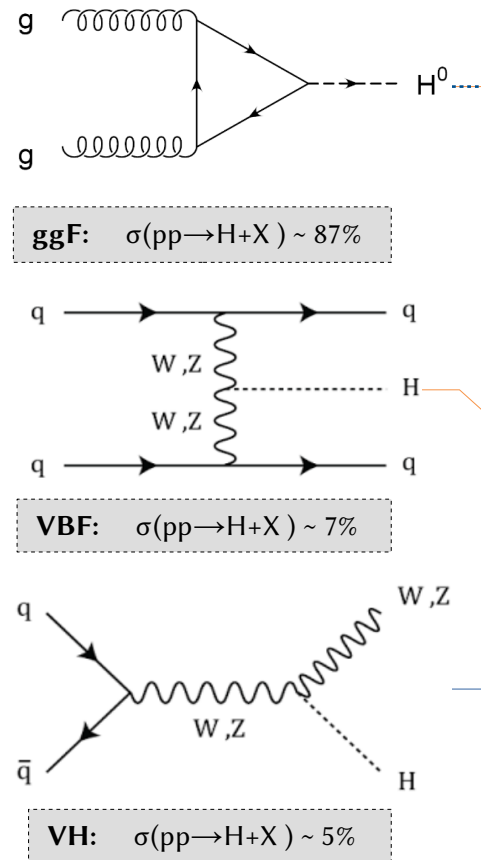
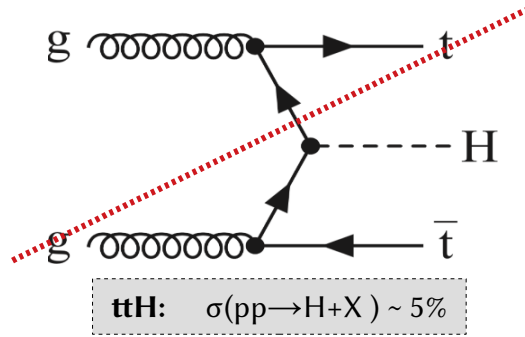
28/05/20

# Introduction

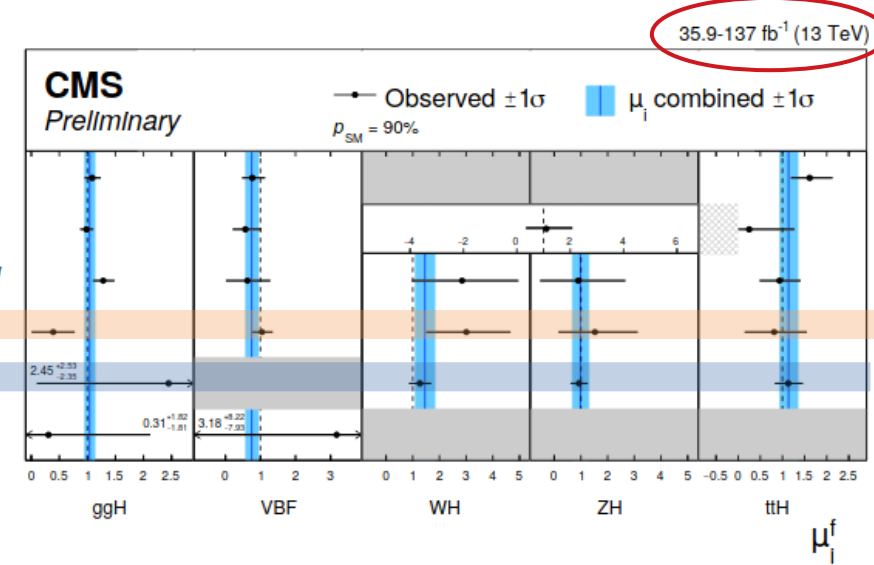
→ Summary of the latest **ATLAS & CMS 3<sup>rd</sup>** generation decay channel Higgs measurements

→ Talk will **only** address 3<sup>rd</sup> generation Higgs decays: **H → [bb, ττ]**

→ Associated top + higgs (ttH) production excluded:



Source: [HIG-19-005](#)



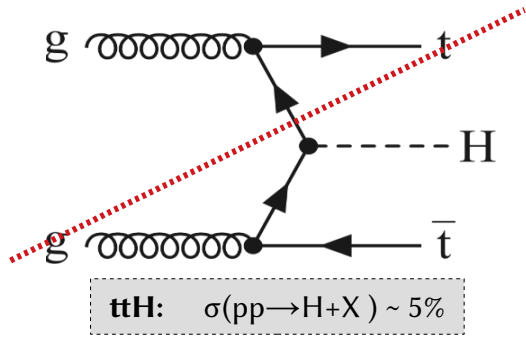
# Introduction

→ Summary of the latest **ATLAS & CMS 3<sup>rd</sup>** generation decay channel Higgs measurements

→ Talk will **only** address **3<sup>rd</sup> generation** Higgs decays: **H → [bb,ττ]**

Source: [PhysRevD 101.012002](https://arxiv.org/abs/101.012002)

→ Associated top + higgs (ttH) production excluded:



→ **Direct H → bb** measurement of **ggF** production?

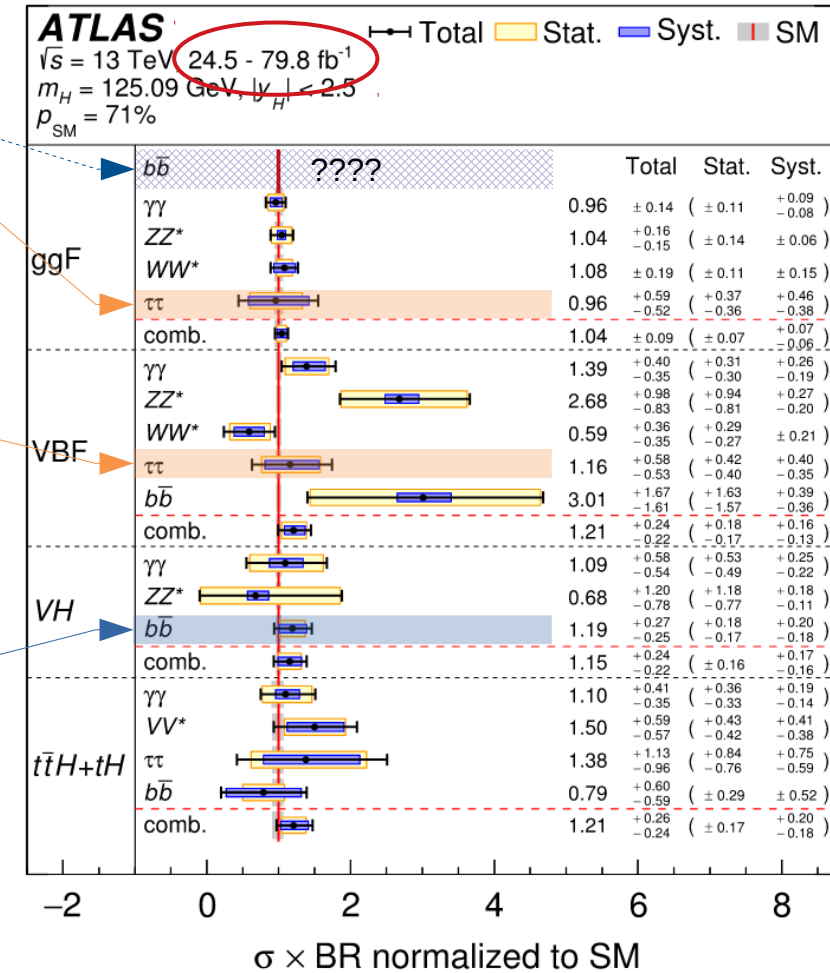
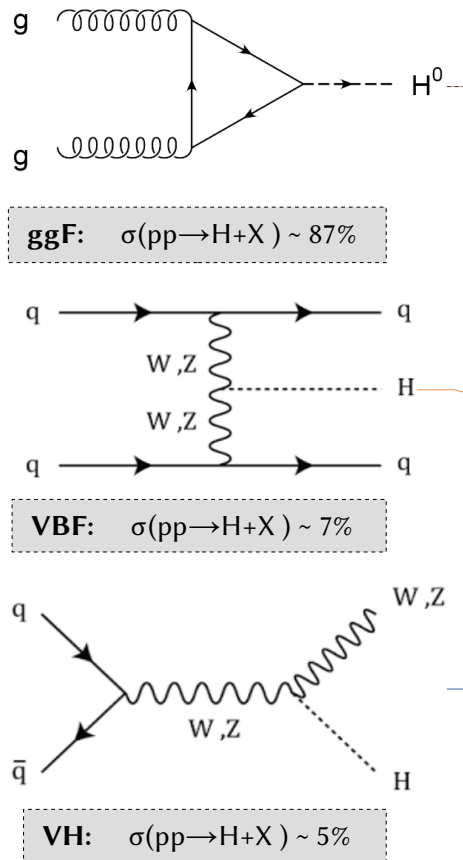
→ QCD background dominant  $\sim 10^7 >$  signal

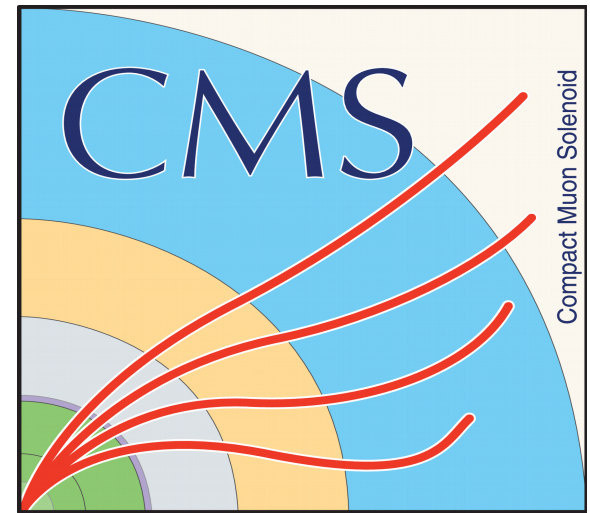
→ Limited by ggF ZH theoretical accuracy

→ See X, Chen talk

→ ....

→ Hopefully a new  $\sigma_{bb}^{ggF}$  entry soon...





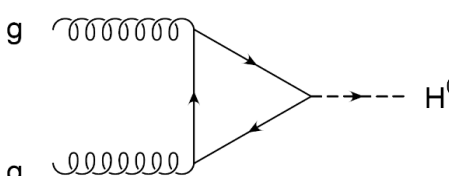
H → bb



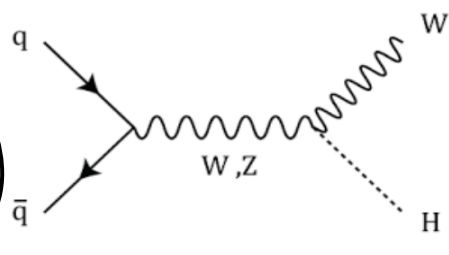
# H → bb Searches in ATLAS & CMS

→ Will cover **new** analyses only!

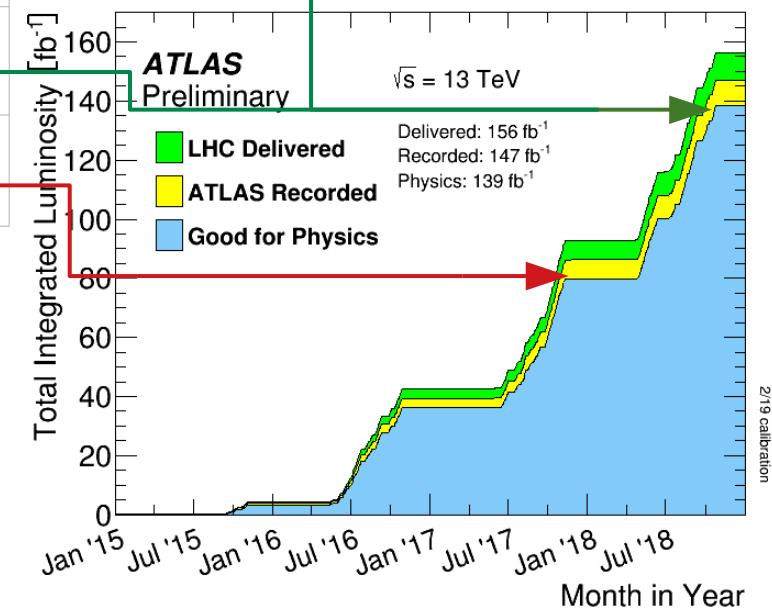
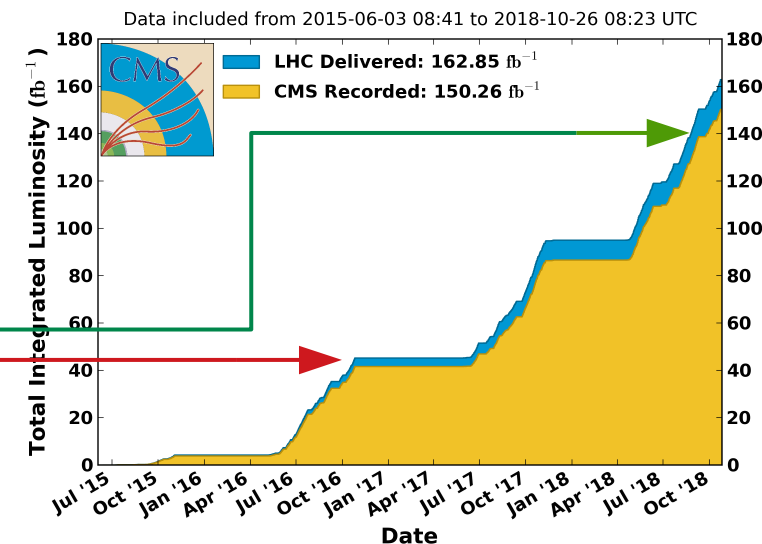
## CMS Publications

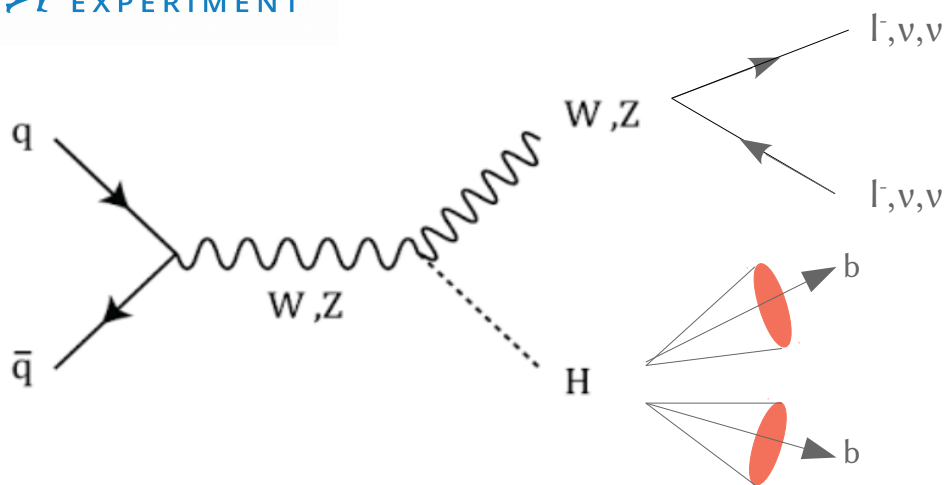
Paper	Luminosity	Signal Process	Date
HIG-19-003 <i>New</i>	137 fb <sup>-1</sup>		April 2020
PhysRevLett. 120, 071802	35.9 fb <sup>-1</sup>		Feb. 2018

## ATLAS Publications

ATLAS-CONF-2020-007 <i>New</i>	139 fb <sup>-1</sup>		April 2020
ATLAS-CONF-2020-006 <i>New</i>	139 fb <sup>-1</sup>		April 2020
JHEP 05 (2019) 141	79.8 fb <sup>-1</sup>		May 2019

CMS Integrated Luminosity, pp,  $\sqrt{s} = 13$  TeV

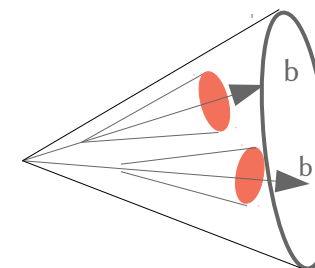




## W/Z-Boson Candidate Reconstruction:

- **0-lepton:** Large missing transverse energy (MET)
- **1-lepton:** 1 charged leptons:  $l = [e, \mu] + \text{MET from neutrino } (\nu)$
- **2-lepton:** 2 charged leptons:  $ll = [ee, \mu\mu] + m_{ll} \sim m_Z$

Increase  $p_T^H$



## Higgs Candidate Reco.:

### Resolved Analysis: $p_T^H > \sim 60$ GeV

- 2 anti- $k_t$   $R=0.4$  jets - AK4
- Exactly 2 b-tagged AK4 jets

### Boosted Analysis: $p_T^H > \sim 250$ GeV

- 1 anti- $k_t$   $R = 1.0$  jet - AK10
- $\geq 2$  matched anti- $k_t$  track jets
- 2 leading track jets b-tagged

More info in poster by K.A.I Khoury → ATLAS-CONF-2020-006

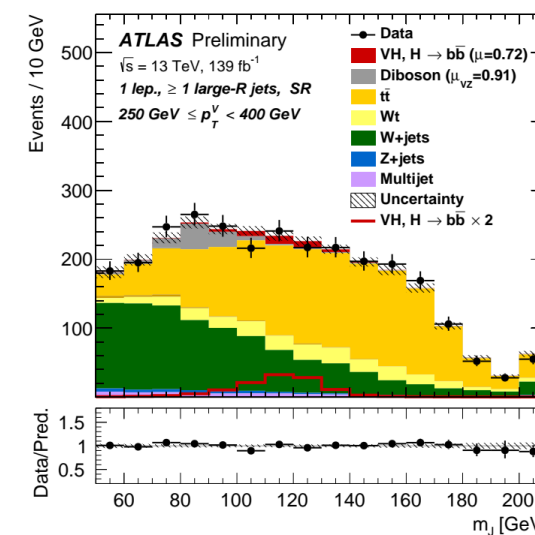
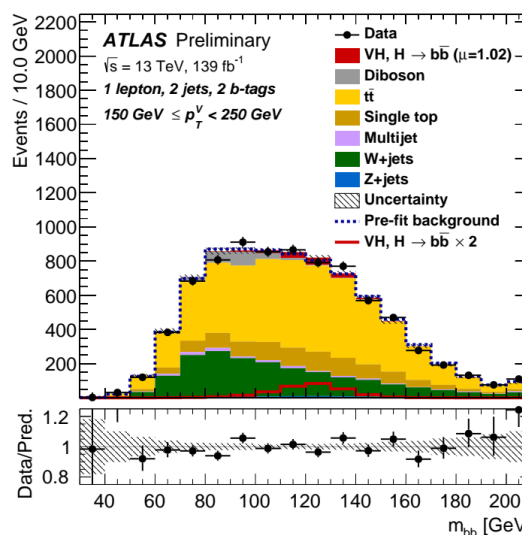
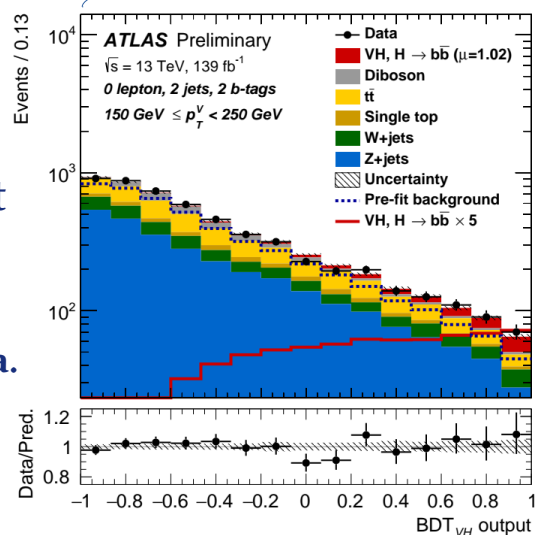
ATLAS-CONF-2020-007

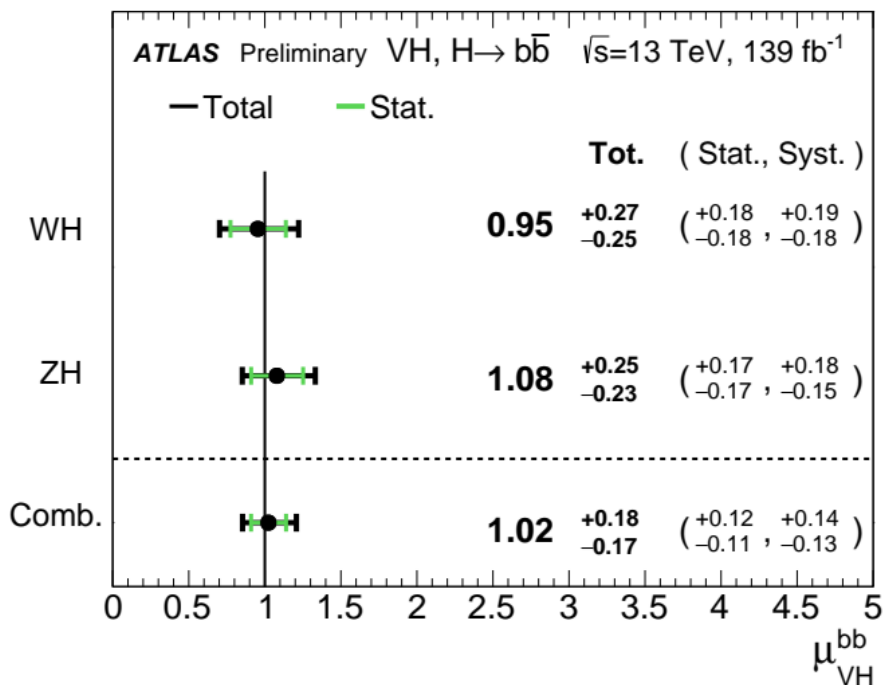
## Binned profile likelihood fit

$\mathcal{L}(\mathbf{x} | \mu_{VH}, \theta)$  where  $\mathbf{x}$  is:

→ BDT - MV analysis

→  $m_{bb}/m_J$  - (Di-)Jet Mass ana.





## Multivariate Analysis (MVA)

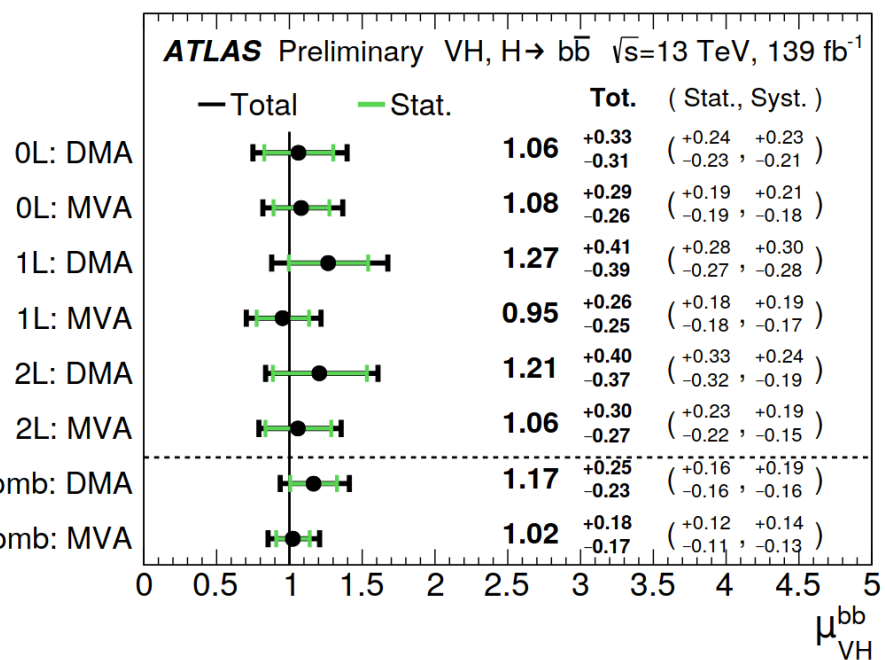
Obs. (exp.)

$Z_0 = 4.0$  (4.1)  $\sigma$  ← Evidence for WH production

$Z_0 = 5.3$  (5.1)  $\sigma$  ← Observation of ZH production

$Z_0 = 6.7$  (6.7)  $\sigma$  ← Combined WH + ZH observation

## Di-jet Mass Analysis (DMA)

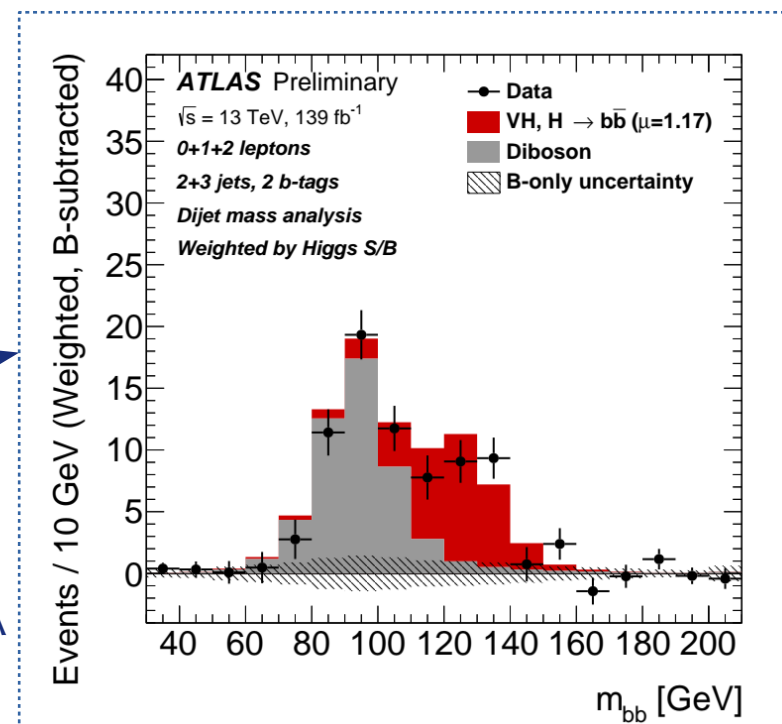


S/B Weighted combination of  $m_{bb}$  distributions from 0+1+2L channels

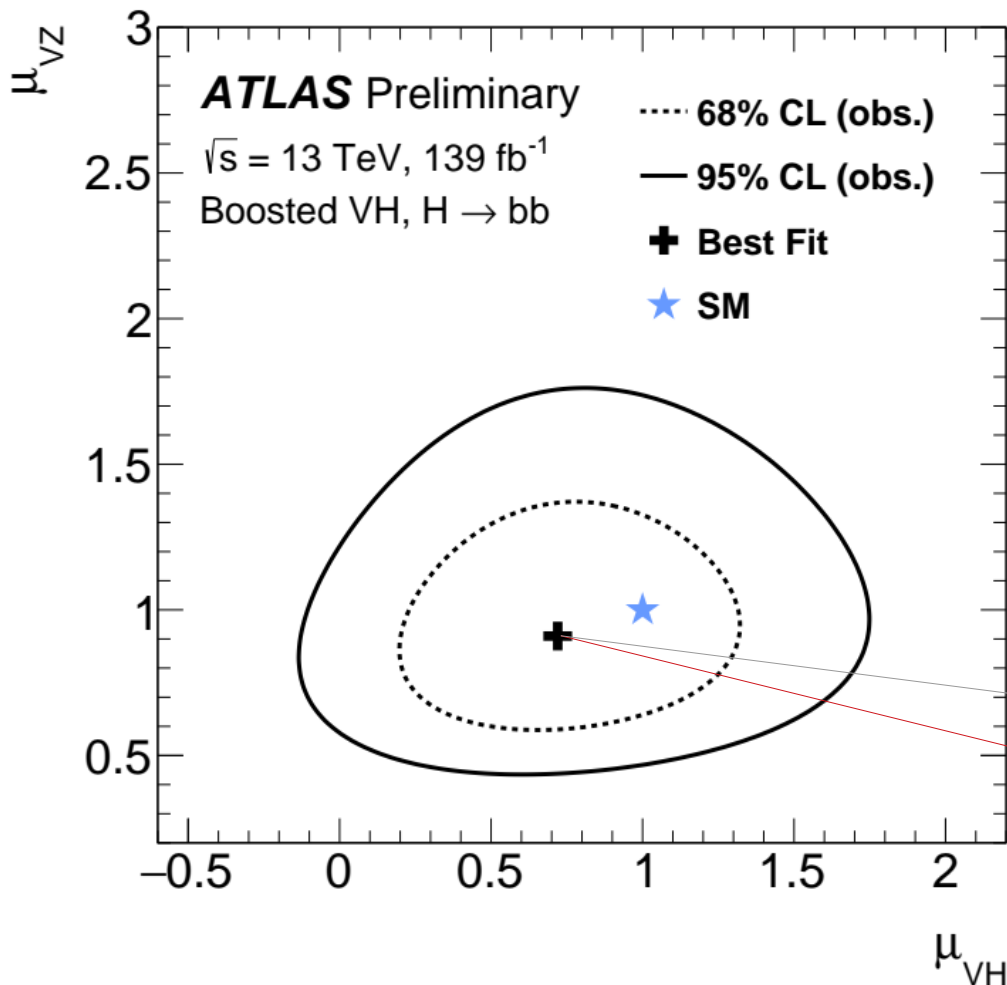
Obs. (exp.)  
 $Z_0 = 5.4$  (4.9)  $\sigma$

→ Good agreement between MVA & DMA

Stephen Jiggins



→ Simultaneous fit of VZ & VH signal strengths ( $[\mu_{VZ}, \mu_{VH}]$ ):

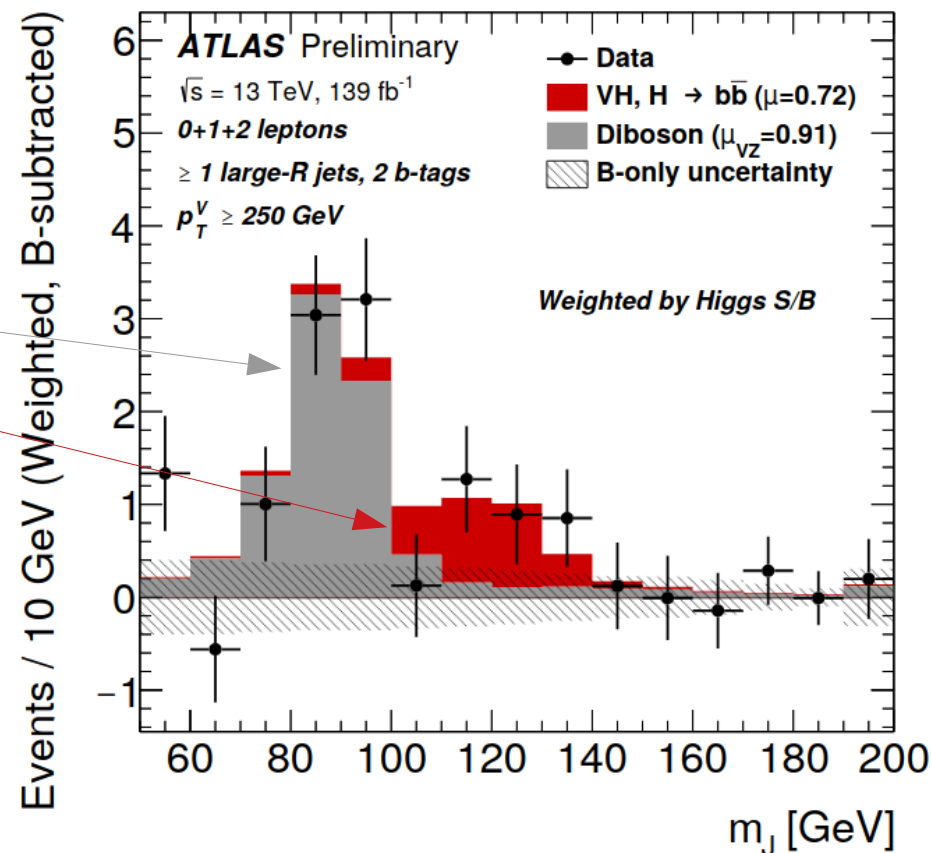


$$\mu_{VZ}^{bb} = 0.91_{-0.23}^{+0.29} = 0.91 \pm 0.15(\text{stat.})_{-0.17}^{+0.25}(\text{syst.})$$

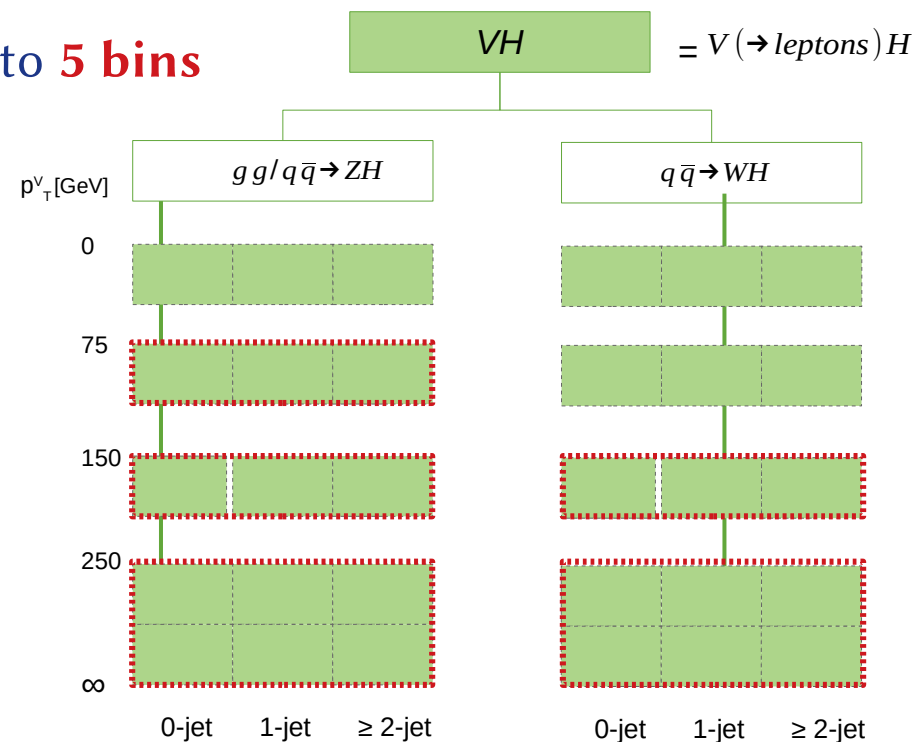
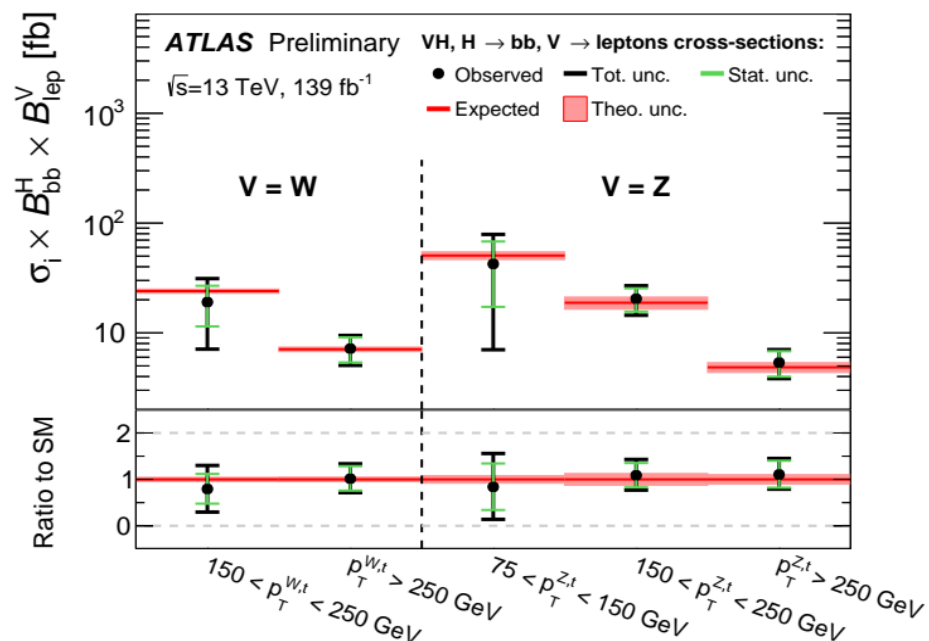
Obs. (exp.) significance  
 $Z_0 = 5.4 \quad (5.7) \sigma$

$$\mu_{VH}^{bb} = 0.72_{-0.36}^{+0.39} = 0.72_{-0.28}^{+0.29}(\text{stat.})_{-0.22}^{+0.26}(\text{syst.})$$

Obs. (exp.) significance  
 $Z_0 = 2.1 \quad (2.7) \sigma$



→ **VHbb resolved: Stage 1.2 STXS scheme merged down to 5 bins**

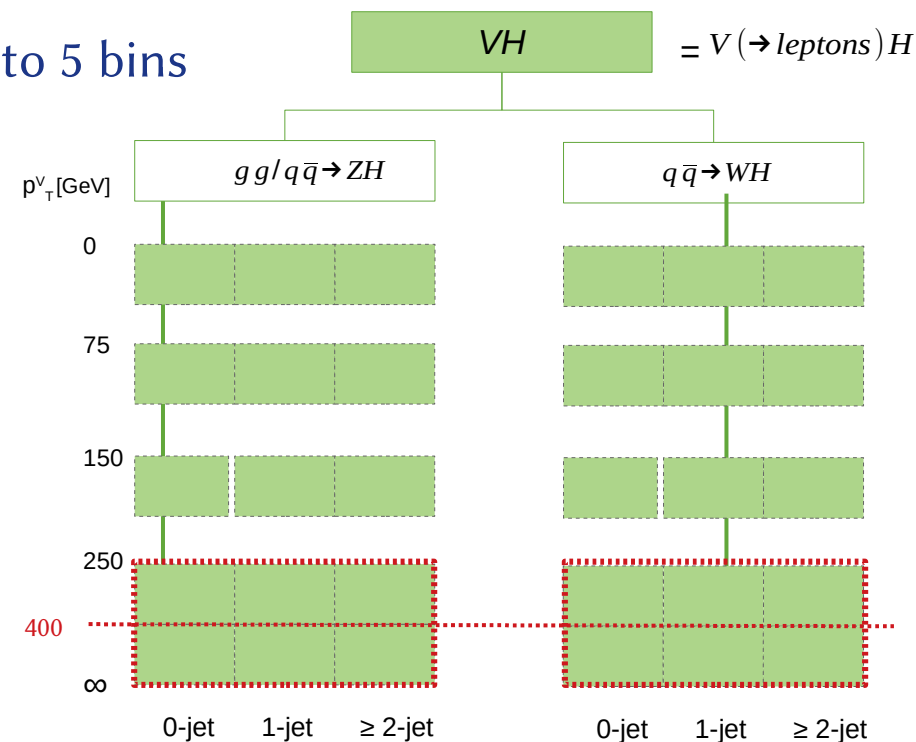
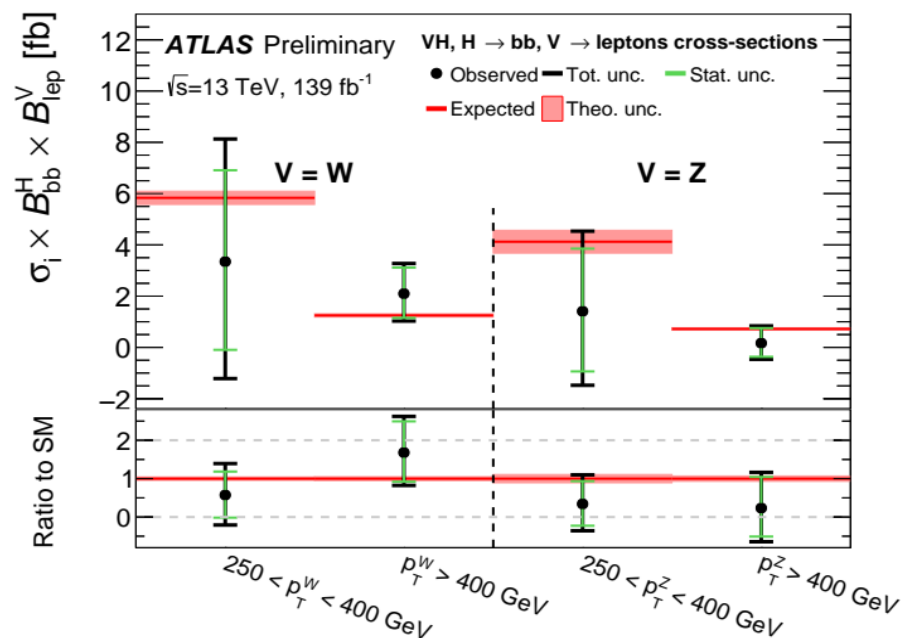
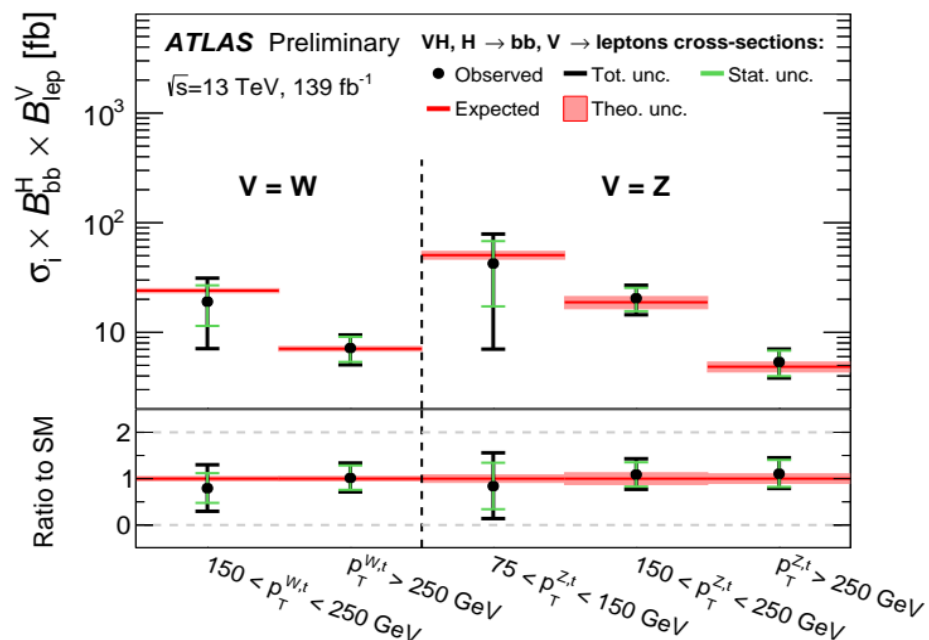


→ **VHbb Resolved: Increased precision of 5 POI  $\sigma^{W/ZH}$  results:**

**80fb<sup>-1</sup>:** 50%-125% uncertainty on  $\sigma^{W/ZH}$

**139fb<sup>-1</sup>:** 30%-85% uncertainty on  $\sigma^{W/ZH}$

→ **VHbb resolved**: Stage 1.2 STXS scheme merged down to 5 bins



→ **VHbb Resolved**: Increased precision of 5 POI  $\sigma^{W/ZH}$  results:

**80fb<sup>-1</sup>**: 50%-125% uncertainty on  $\sigma^{W/ZH}$

**139fb<sup>-1</sup>**: 30%-85% uncertainty on  $\sigma^{W/ZH}$

→ **VHbb boosted**: Stage 1.2 STXS scheme merged down to **4 bins**

- Measurement of  $p_T^V(\text{truth}) > 400$  GeV

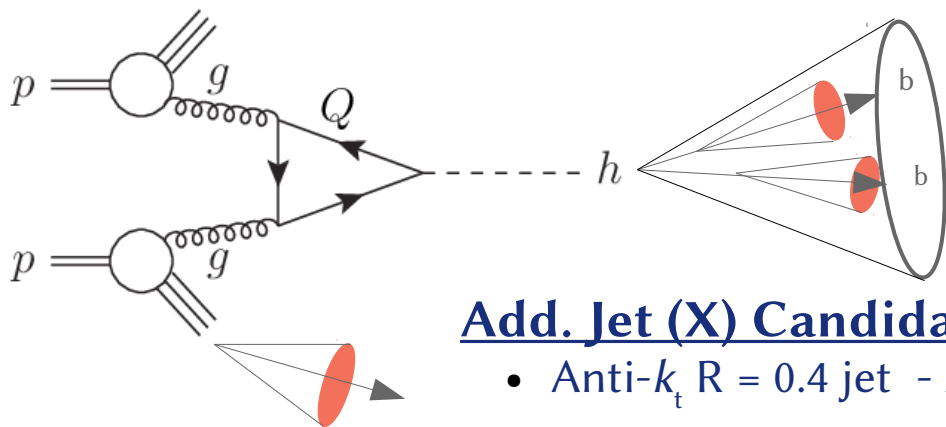
→ VHbb resolved + boosted **not orthogonal!**

→ See talk by [Nikita Belyaev](#) for more STXS/EFT results

→ Or backup for questions!



→ **Signal:** pp → H(→bb) + X, via ggF



**Higgs Candidate Reco.:** p<sub>T</sub><sup>H</sup> ~ p<sub>T</sub><sup>AK8</sup> > 450 GeV

- Anti-k<sub>t</sub> R = 0.8 jet - AK8 jet
- Soft-drop algorithm → m<sub>SD</sub>

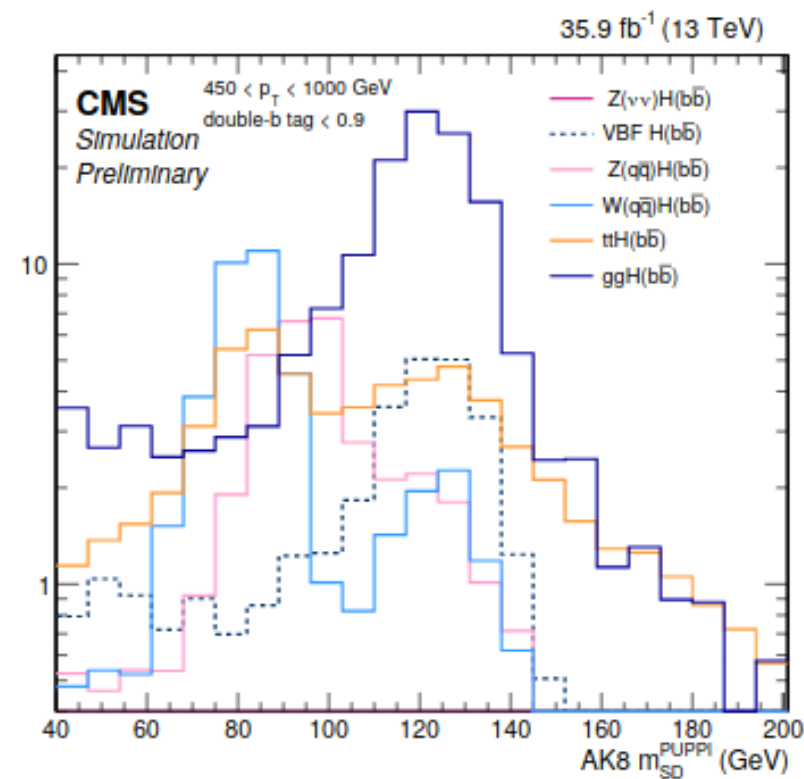
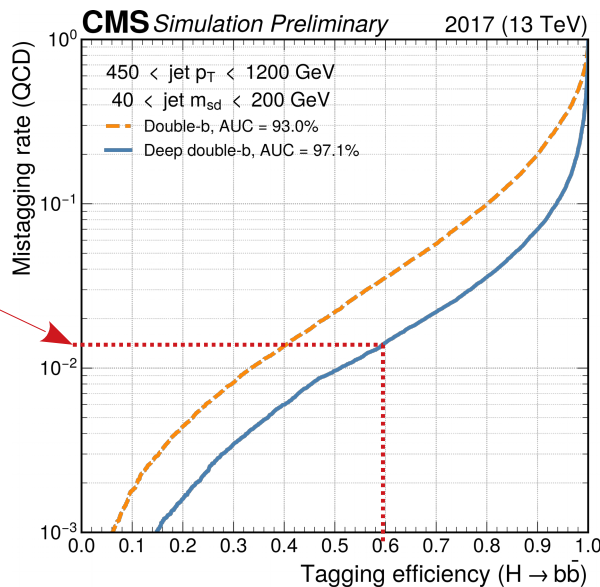
**Add. Jet (X) Candidate Reco.:**

- Anti-k<sub>t</sub> R = 0.4 jet - AK4 jet

Analysis fit discriminant!

## Double b-jet Identification:

- Double-b tagging algorithm using a new 'deep neural network'
- AK8 jet must contain two b-tags
  - **60% eff. for signal**
  - **1% misidentification rate for QCD**
- 'Passing' / 'Failing' double b-tag = 'Signal' / 'Control' region  
→ Used to constrain QCD background





# Inclusive ggF high $p_T^H$ : Analysis Strategy

→ Maximum likelihood fits of  $\mu_{H}^{ggF}$ :

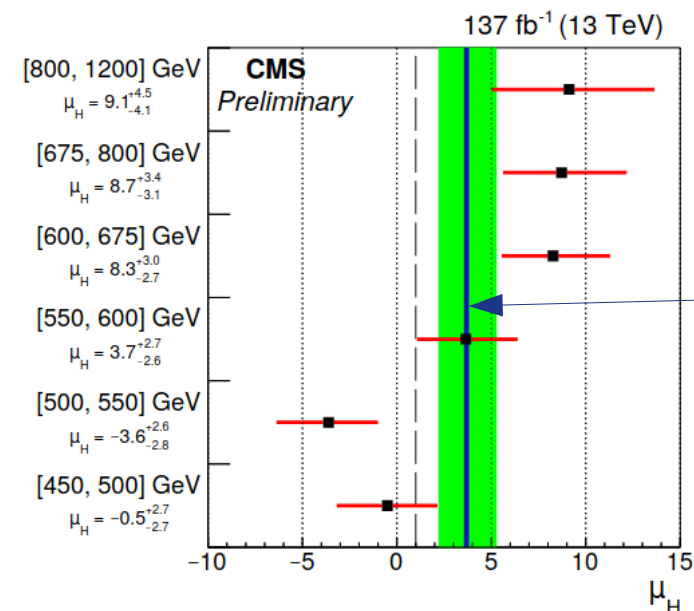
- $p_T$  AK8 binning:  $[\mu_{H}^{450}, \mu_{H}^{550}, \mu_{H}^{600}, \mu_{H}^{675}, \mu_{H}^{800}]$
- Combined:  $[\mu_{H}^{comb.}]$

→ Likelihood based unfolding to particle level comparing:

- LHC XS WG  $\sigma_{H \rightarrow bb}$ : LHCHXSWG-2019-002
- HF-MINLO  $\sigma_{H \rightarrow bb}$ : MC generator configurations

→  $\sigma_{H \rightarrow bb}^{300-1200}$  upward deviation of **1.91 $\sigma$**

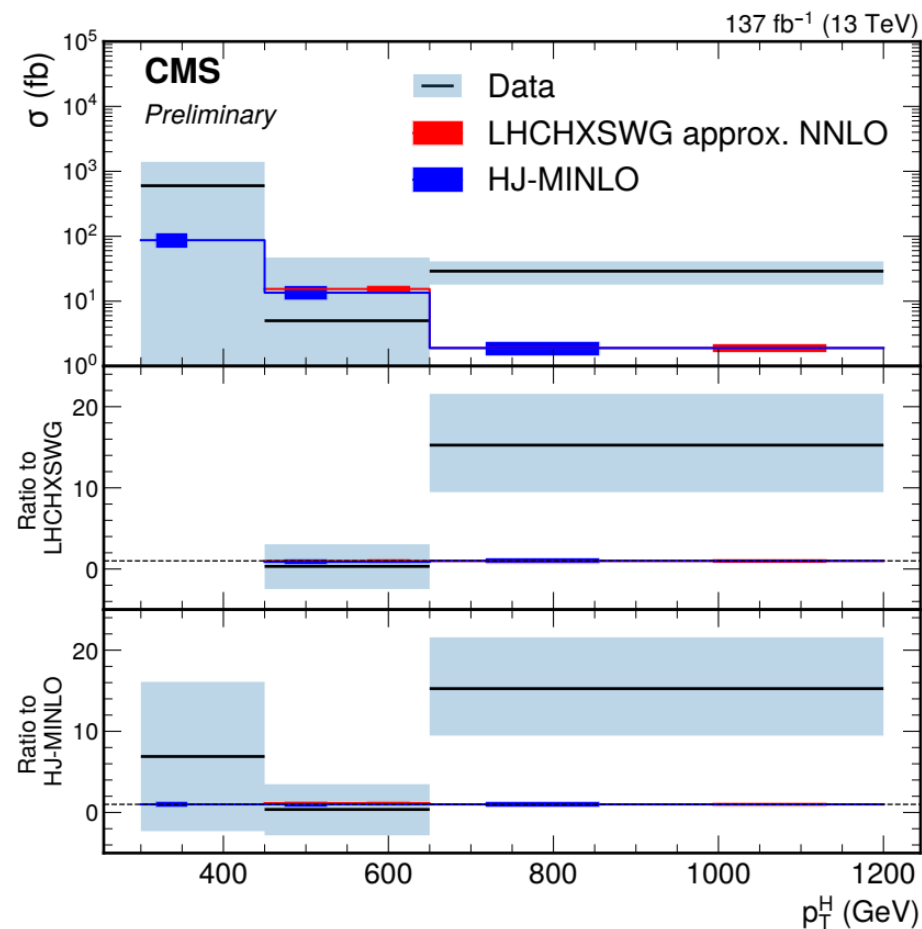
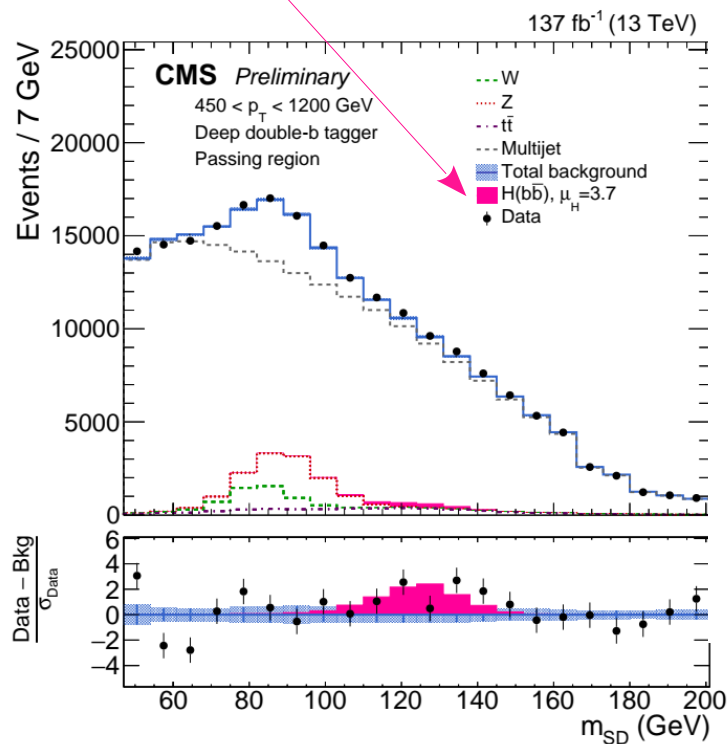
→  $\sigma_{H \rightarrow bb}^{650-1200}$  upward deviation of **2.65 $\sigma$**



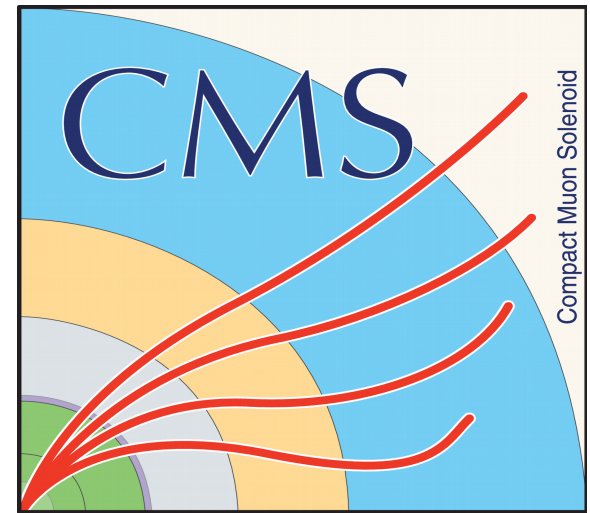
$\mu_{VH}^{comb.} = 3.68^{+1.58}_{-1.46}$

$Z^{obs(exp)}_{\mu=0} = 2.54(0.71)\sigma$

→ Excess exceeding  $\mu_{VH} = 1$  by **1.85 $\sigma$**



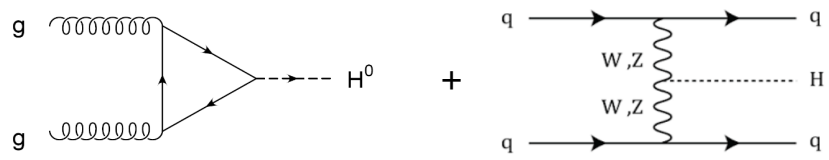
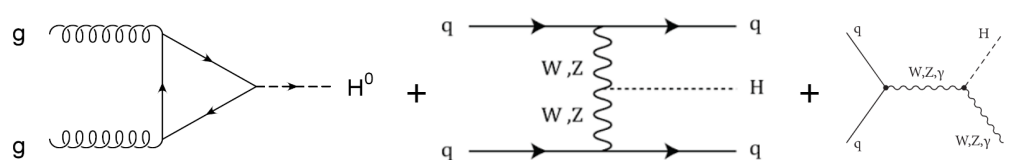




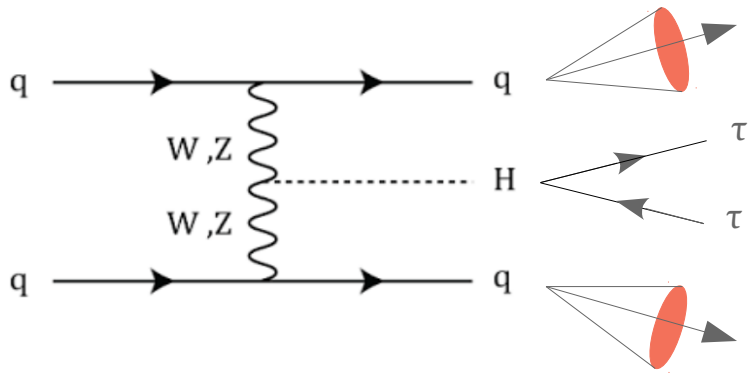
$$\underline{H} \rightarrow \underline{\tau\tau}$$

→ Only one **new** paper for H → ττ

→ ATLAS now published a CP invariance test of BSM using H → ττ - counterpart to CMS 2019 publication

ATLAS Publications			
Paper	Luminosity	Signal	Date
Phys. Lett. B 805 (2020) 135426	36.1fb <sup>-1</sup> <i>New</i>		Feb. 2020
PhysRevD. 99 072001	36.1fb <sup>-1</sup>		April 2019
CMS Publications			
PRD 100 (2019) 112002	Run 2: 35.9-80.2fb <sup>-1</sup> Run 1: 5.1+19.7fb <sup>-1</sup>		Dec. 2019
HIG-18-032	77.4fb <sup>-1</sup>		March 2019

Counterparts



## Higgs Candidate Reco.:

- $\tau_{\text{lep}} \tau_{\text{lep}}$  **SF**: Same flavour leptons
- $\tau_{\text{lep}} \tau_{\text{lep}}$  **DF**: Different flavour leptons
- $\tau_{\text{lep}} \tau_{\text{had}}$ : Semi-leptonic  $\tau$  decays
- $\tau_{\text{had}} \tau_{\text{had}}$ : Hadronic  $\tau$  decays

‘Missing Mass Calculator’  
 $\rightarrow m_{\tau\tau}^{\text{MMC}}$  (arXiv:1012.4686)

## Jet Reco.:

- Anti- $k_t$   $R = 0.4$  jet - AK4 jet

## Physics Interpretation:

$\rightarrow$  Effective lagrangian ( $\mathcal{L}_{\text{eff}}$ ) composed of:

- Standard Model:  $\mathcal{L}_{\text{SM}}$
- CP-odd mass dim. Six:  $\mathcal{L}_{\text{CP}}^6$

$$\mathcal{L}_{\text{eff}} = \mathcal{L}_{\text{SM}} + \sum_i \frac{f_i^{(5)}}{\Lambda} \mathcal{O}_i^{(5)} + \sum_i \frac{f_i^{(6)}}{\Lambda^2} \mathcal{O}_i^{(6)} + \mathcal{O}\left(\frac{1}{\Lambda^3}\right)$$

$\rightarrow \tilde{d}$  parameterises strength of CP-violation:

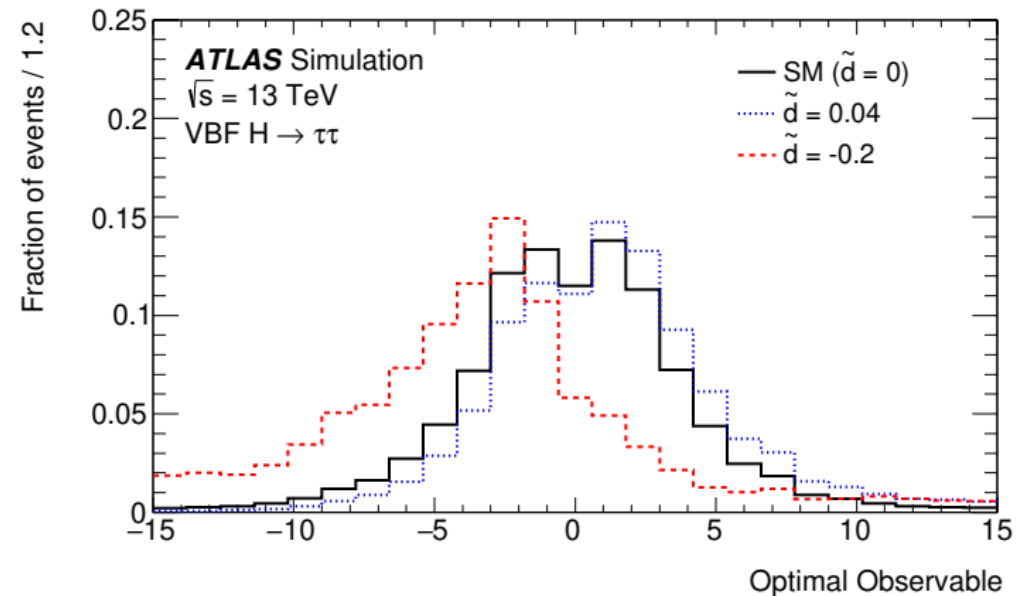
$$|\mathcal{M}|^2 = |\mathcal{M}_{\text{SM}}|^2 + 2\tilde{d} \cdot \text{Re}(\mathcal{M}_{\text{SM}}^* \mathcal{M}_{\text{CP-odd}}) + \tilde{d}^2 \cdot |\mathcal{M}_{\text{CP-odd}}|^2$$

## Fit Discriminant:

$\rightarrow$  Utilise matrix element calculated from HAWK [Link]

$\rightarrow$  **Optimal Observable:**

$$O_{\text{opt}} = \frac{2 \text{Re}(\mathcal{M}_{\text{SM}}^* \mathcal{M}_{\text{CP-odd}})}{|\mathcal{M}_{\text{SM}}|^2}$$



- Binned maximum likelihood  $\mathcal{L}(\mathbf{x}, \mu | \theta)$  as a function of each  $\tilde{d}$  hypothesis
- Unconstrained signal normalisation ‘ $\mu$ ’ - **shape only analysis**
- Summary of mean <Optimal Obs.> for each channel and combined result:

Channel	<Optimal Observable>
$\tau_{\text{lep}}\tau_{\text{lep}}$ SF	$-0.54 \pm 0.72$
$\tau_{\text{lep}}\tau_{\text{lep}}$ DF	$0.71 \pm 0.81$
$\tau_{\text{lep}}\tau_{\text{had}}$	$0.74 \pm 0.78$
$\tau_{\text{had}}\tau_{\text{had}}$	$-1.13 \pm 0.65$
Combined	$-0.19 \pm 0.37$

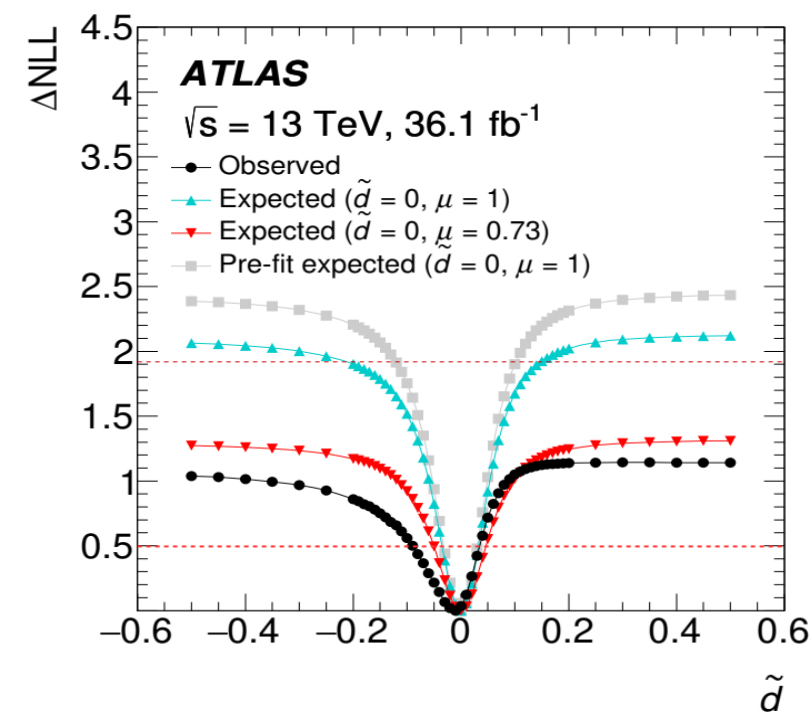
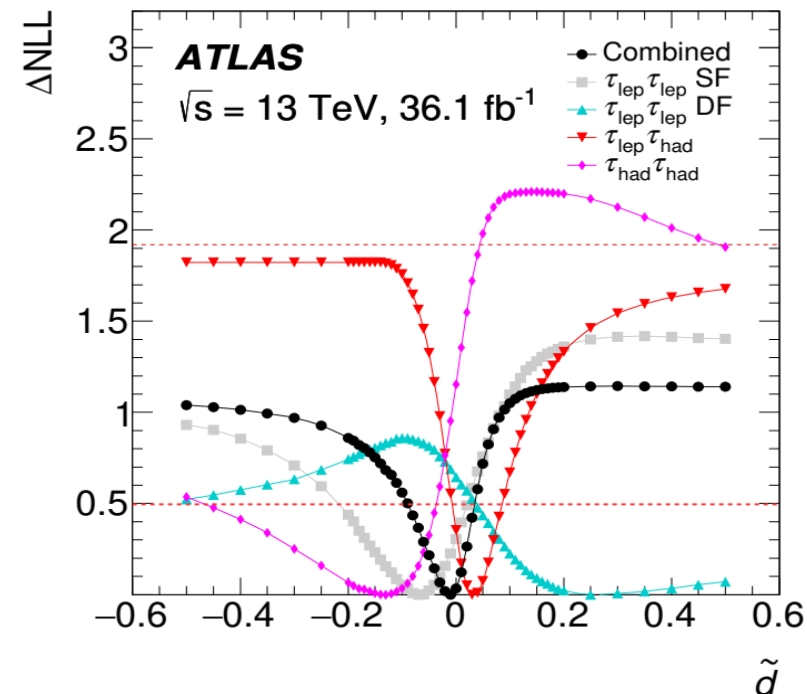
- *Expected results:* Asimov dataset from Np set to observed CR fit only values
- Pre-fit Expected:* Asimov dataset from Np set to SM expectation asimov fit.

- Conditional [ $\mu=1, \tilde{d}=0$ ] and [ $\mu=0.73, \tilde{d}=0$ ] asimov fits demonstrate loss of observed sensitivity due to lower than expected event yields

- 68%(95%) CL interval on  $\tilde{d}$  set for observed and expected:

**Obs. 68% CL:**  $\tilde{d} \in [-0.090, 0.035]$   
**Exp. 68% CL:**  $\tilde{d} \in [-0.035, 0.033]$   
**Obs. 95% CL:**  $\tilde{d} \in [N/A]$   
**Exp. 95% CL:**  $\tilde{d} \in [-0.21, 0.15]$

Asymmetry in CL due to  
 asymmetric Opt. Obs.  
 → See previous slide





# Constraints on anomalous HVV couplings: $H \rightarrow \tau\tau$

PRD 100 (2019) 112002

HIG-18-032

→ Anomalous HVV couplings in VBF/ggF/VH production using:

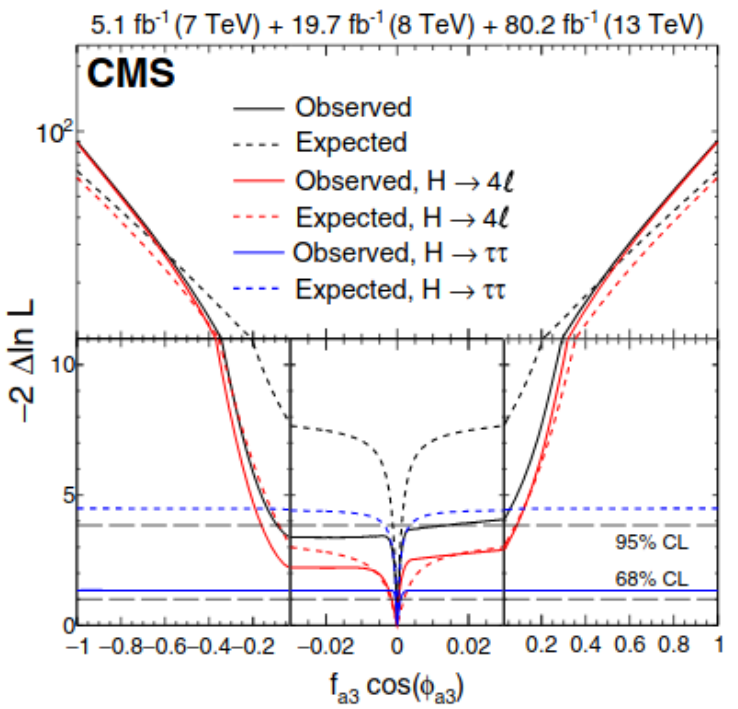
- $H \rightarrow \tau\tau$   $35.9\text{fb}^{-1}$  analysis (see PLB 779 (2018) 283)
- $H \rightarrow 4\ell$  Run 1+2 analyses (see PhysRevD. 99 112003)

→ Amplitude for spin-0 Higgs with two spin-1 gauge bosons VV:

$$A(HVV) \sim \left[ a_1^{VV} + \frac{\kappa_1^{VV} q_1^2 + \kappa_2^{VV} q_2^2}{(\Lambda_1^{VV})^2} \right] m_{V1}^2 \epsilon_{V1}^* \epsilon_{V2}^* + a_2^{VV} f_{\mu\nu}^{*(1)} f^{*(2)\mu\nu} + a_3^{VV} f_{\mu\nu}^{*(1)} \tilde{f}^{*(2)\mu\nu}$$

- $\Lambda_1$ : BSM scale
- $a_3^{VV}$  CP-odd interaction
- $a_2^{VV}$  CP-even interaction

→ HVV anomalous couplings measured using effective cross-section ratios  $f_{ai}$ , and relative phase  $\Phi$ :



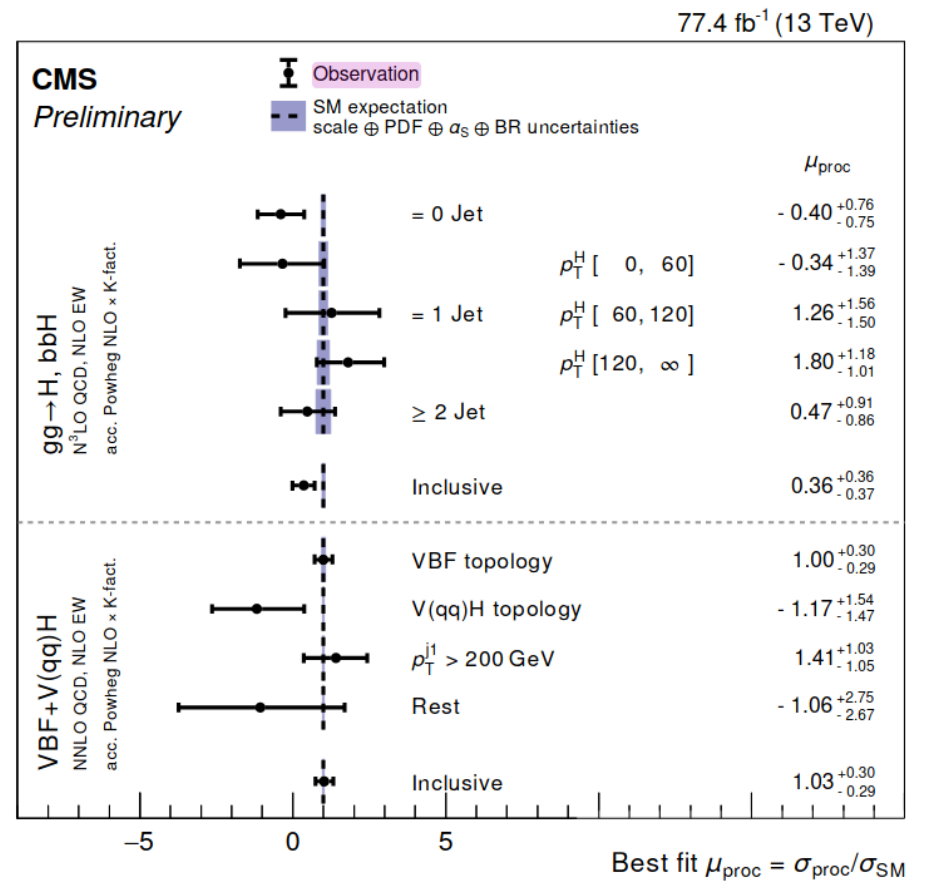
$$\phi_{a_i} = \arg\left[\frac{a_i}{a_1}\right]$$

$$f_{a_i} = \frac{a_i^2 \sigma_i}{\sum a_i^2 \sigma_i}$$

→ Measurement of  $H \rightarrow \tau\tau$  sensitive to VBF+ggF+VH production modes updated with  $77.4\text{fb}^{-1}$

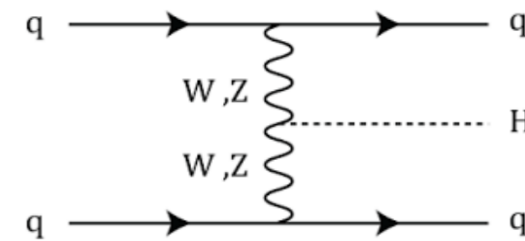
→ **Update 1:** Multiclass NN used to separate 9-classes  
- [ggF,VBF] signal + 7 bkg

→ **Update 2:** Included a STXS result for ggF and VBF production modes:



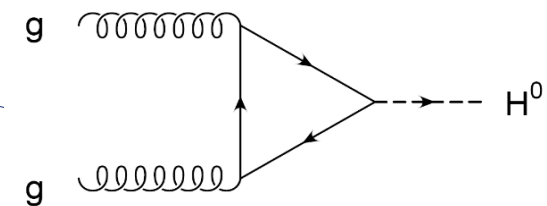
Stephen Jiggins

# Conclusions



VBF:  $\sigma(pp \rightarrow H+X) \sim 7\%$

→ Constraints on CP invariance via EFT Lagrangian extensions



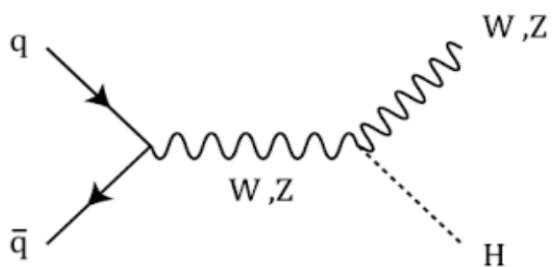
ggF:  $\sigma(pp \rightarrow H+X) \sim 87\%$

→ Intriguing excess beyond SM ggF  $H \rightarrow bb$  production

→ High  $p_T^H$  excess most dominant

→ Keep a close eye in the future!

Paper	Analysis	Date
Phys. Lett. B 805 (2020) 135426 	$H \rightarrow \tau\tau$ Tests of CP Invariance $36.1 \text{ fb}^{-1}$ <b>New</b>	Feb. 2020
HIG-19-003 	Highly boosted $H \rightarrow bb$ at $\sqrt{s} = 13 \text{ TeV}$ with CMS detector - $137 \text{ fb}^{-1}$ <b>New</b>	April 2020
ATLAS-CONF-2020-007 	Boosted $VH \rightarrow bb$ $\sqrt{s} = 13 \text{ TeV}$ with the ATLAS detector - $139.1 \text{ fb}^{-1}$ <b>New</b>	April 2020
ATLAS-CONF-2020-006 	$VH \rightarrow bb$ at $\sqrt{s} = 13 \text{ TeV}$ 13TeV with the ATLAS detector - $139.1 \text{ fb}^{-1}$ <b>New</b>	April 2020



VH:  $\sigma(pp \rightarrow H+X) \sim 5\%$

→ Observation of  $VH \rightarrow bb$

→ Observation of  $ZH \rightarrow bb$

→ Strong evidence of  $WH \rightarrow bb$

→ Proof of concept for boosted  $VH \rightarrow bb$  topology

**Not via combination!**

Stephen Jiggins

# Backup

---

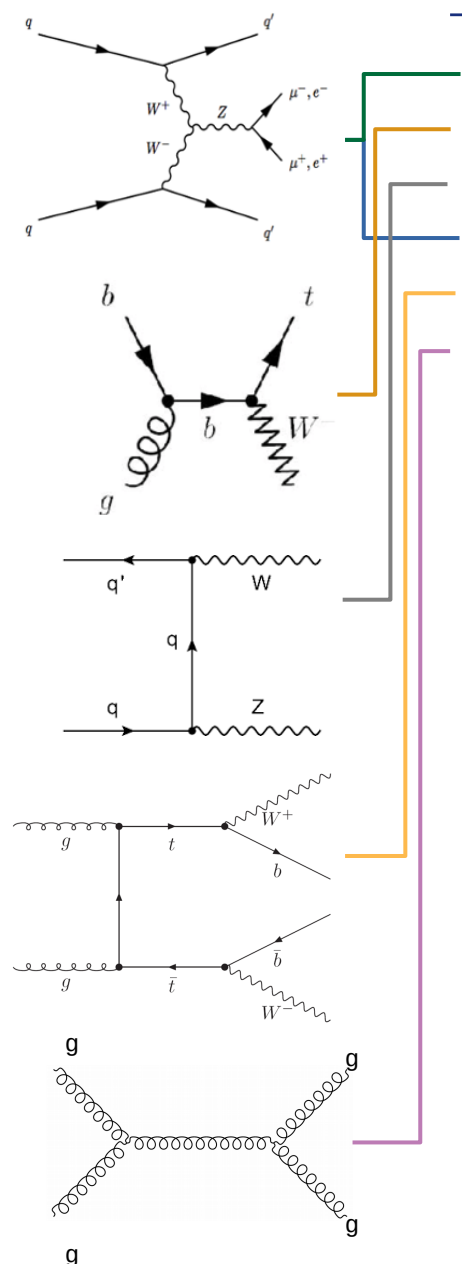




## Background Estimation

→ Common backgrounds in both resolved & boosted:

- **W+Jets**
  - **Wt**
  - **VV**
  - **Z+Jets**
  - **tt**
  - **QCD**
- Resolved+Boosted:** Purely Monte Carlo (MC) estimated  
**Resolved:** Mix of MC/Data-driven estimates/errors  
**Boosted:** Purely MC estimated  
**Resolved+Boosted:** Data-driven estimates/errors

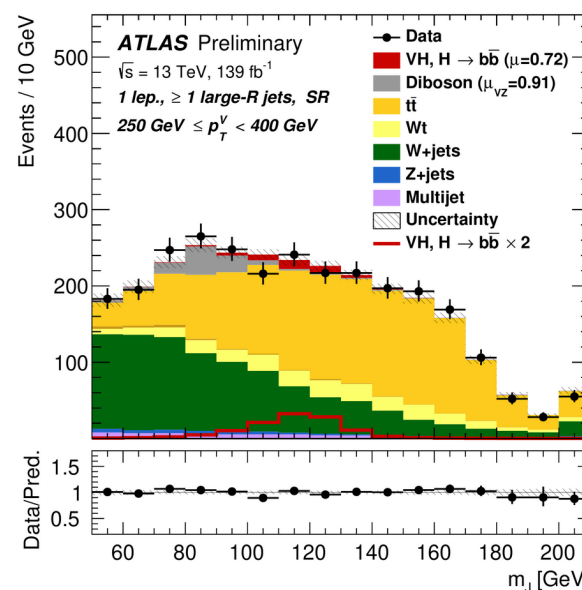
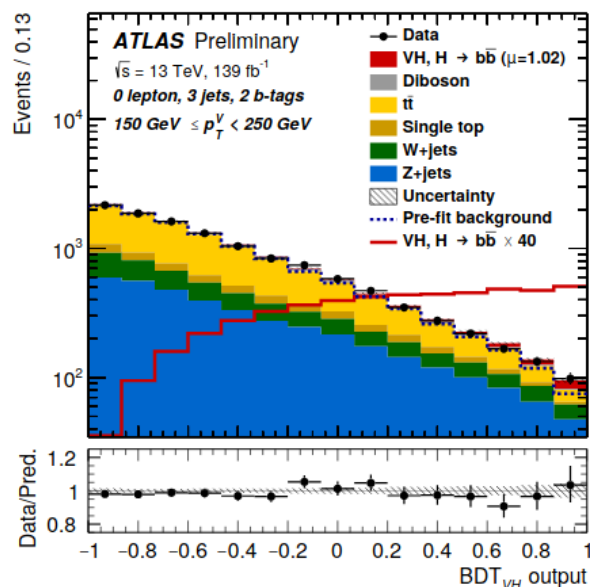


## Fit Strategy

→ Binned profile likelihood fit  $\mathcal{L}(\mathbf{x} | \mu_{VH}, \theta)$  where  $\mathbf{x}$  is:

$\mathbf{x} = \text{BDT}$ : Resolved only

$\mathbf{x} = m_{bb/J}$ : Resolved + Boosted



→ **Resolved:** 42 fit regions

→ **Boosted:** 14 fit regions

→ 3 signal results quoted:

→  $[\mu_{VH}, \mu_{WH}, \mu_{ZH}]$

→ **Multi-Variate Analysis (MVA)**

→ **(Di-)Jet Mass Analysis (DMA)**

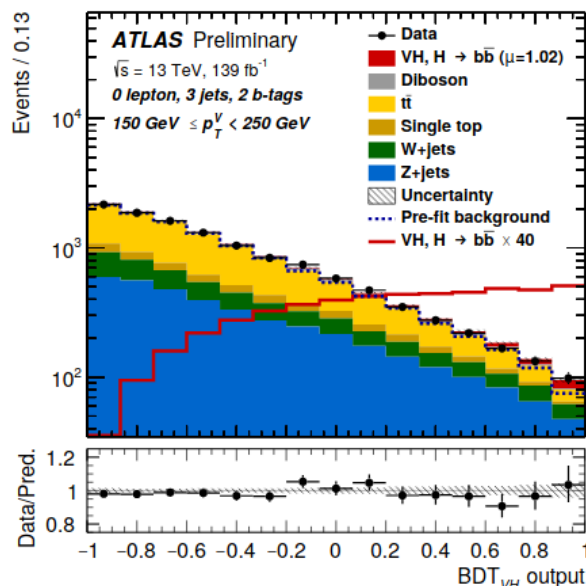


## Multi-Variate Analysis (MVA): Resolved only

→ Binned profile likelihood fit  $\mathcal{L}(\mathbf{x}, \mu_{VH} | \theta)$  using a  $BDT_{VH}$  fit discriminant in signal regions (SR)

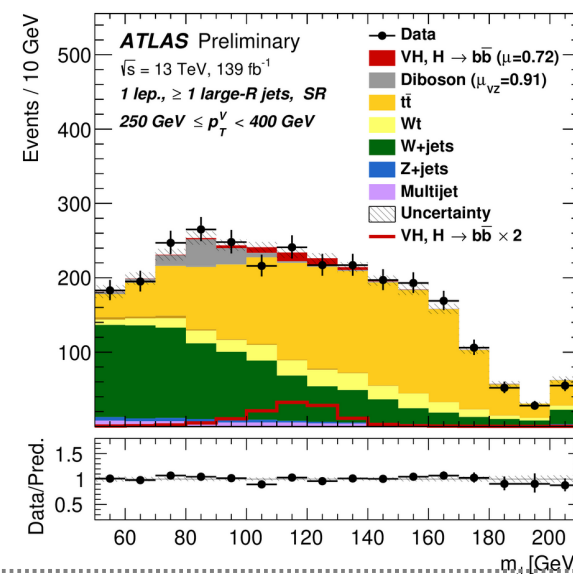
→ Analysis fit regions defined by  $[p_T^V, \Delta R(\mathbf{b}, \mathbf{b})]$  plane:

- [0, 1, 2]-lepton channels
- [2, 3(+)] jets
- [75, 150, 250+]  $p_T^V$  bins
- [ $CR_{Low}$ , SR,  $CR_{high}$ ]



## (Di-)Jet Mass Analysis (DMA): Resolved + Boosted

→ Binned profile likelihood fit  $\mathcal{L}(\mathbf{x}, \mu_{VH} | \theta)$  of  $m_{bb}/m_j$  (Res./Boosted):



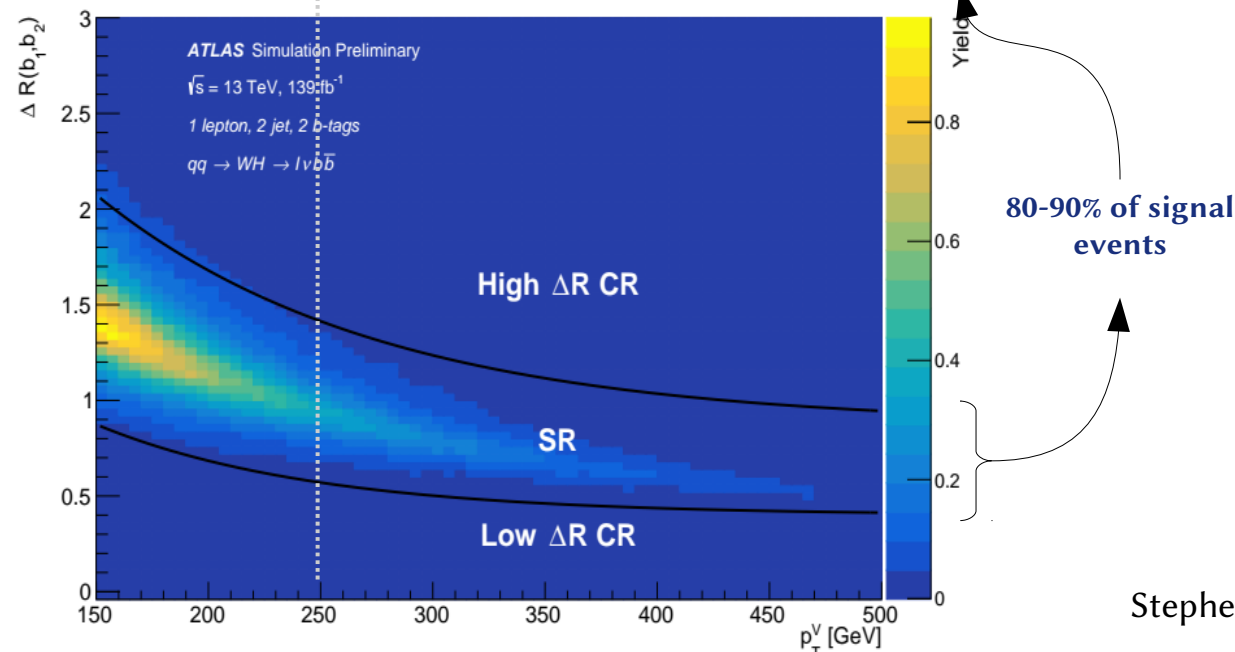
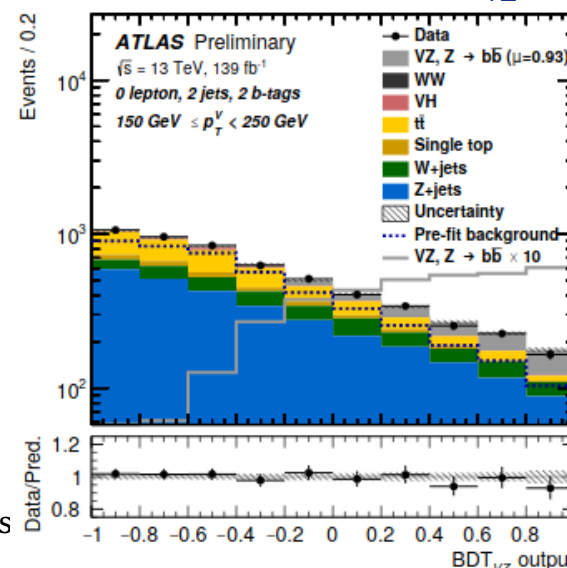
### Boosted: $m_j$

- Analysis fit regions by:
- [0, 1, 2]-lepton channels
  - [0, 1+] b-tag add. track jets
  - [250, 400+]  $p_T^V$  bins
  - [0, 1+] add. AK4 jets

14 fit regions

## VZ(→bb) Analysis (VZ): Resolved + Boosted

→ VZ(bb)  $\mathcal{L}(\mathbf{x}, \mu | \theta)$  fit using  $\mu_{VZ}$  instead fitting  $BDT_{VZ}$  or  $m_j$

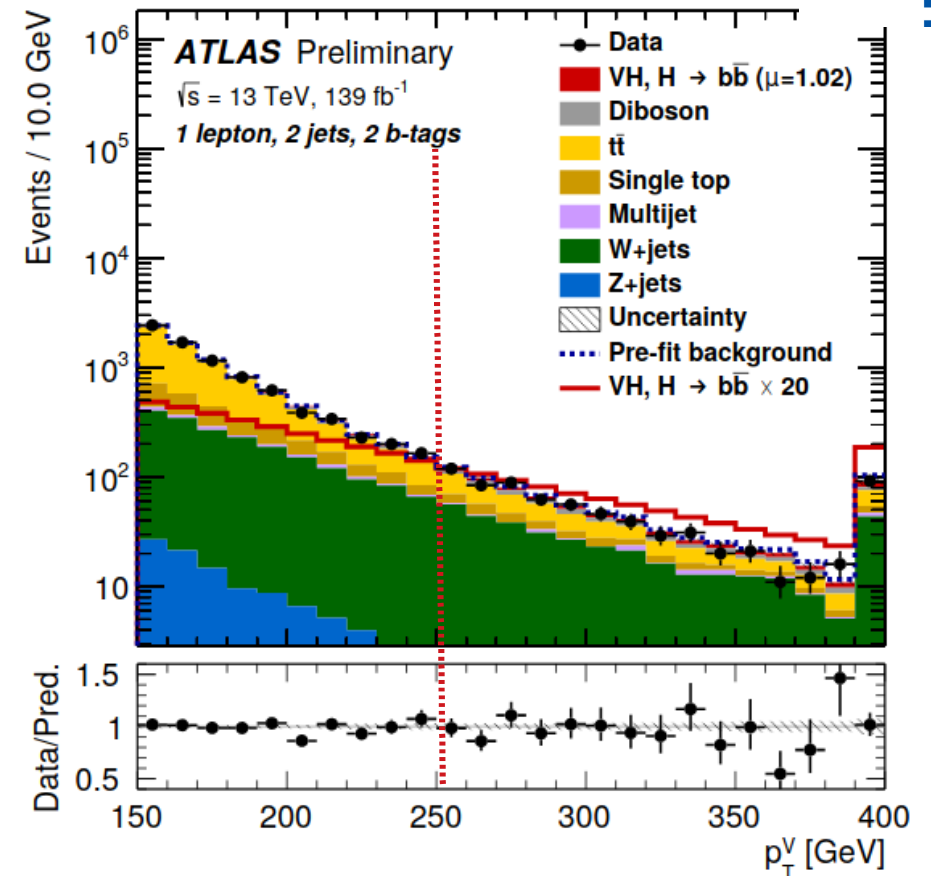
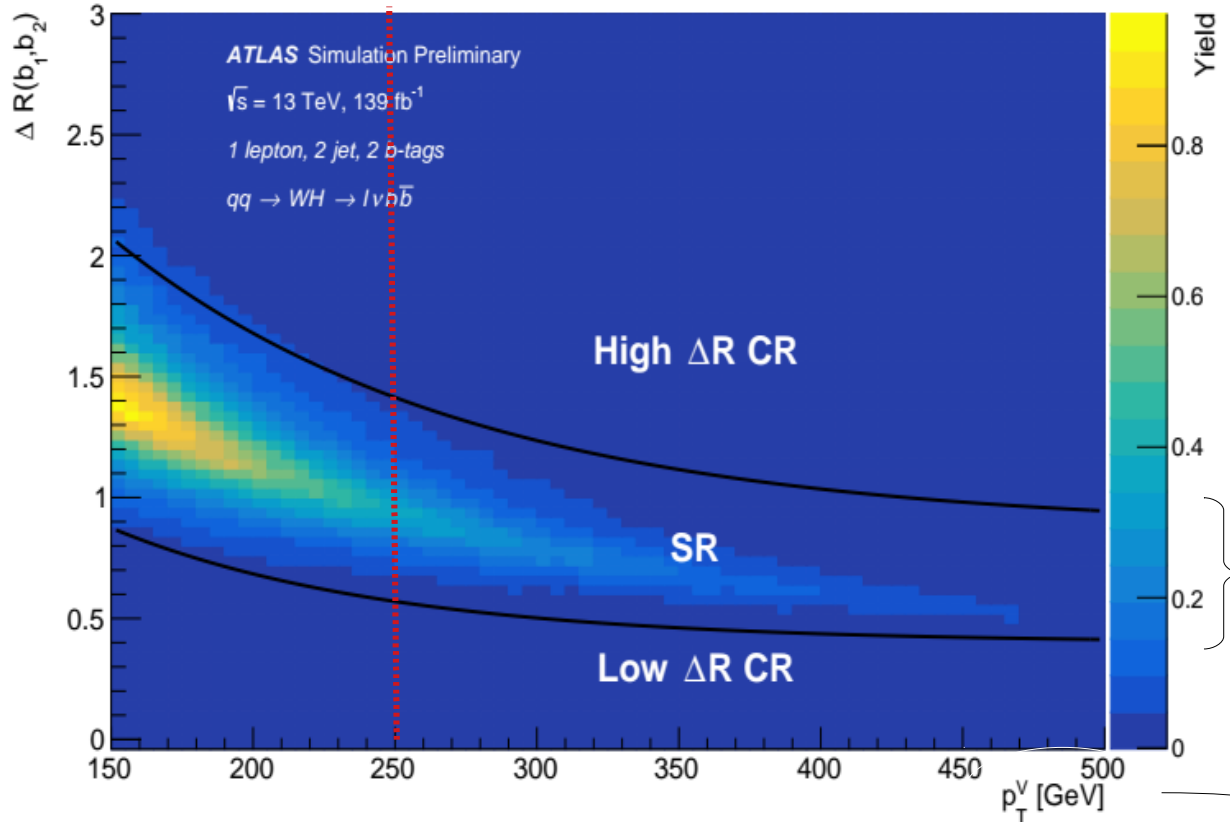


# VH → bb Resolved Event Categorisation

## Analysis Event Categorisation:

- $\Delta R(b_1, b_2)$  and  $p_T^V$  define analysis fit regions

80-90% of signal events



## Analysis fit regions:

- [0, 1, 2]-lepton channels
  - [2, 3(+)] jets
  - [75, 150, 250+]  $p_T^V$  bins
  - [CR<sub>Low</sub>, SR, CR<sub>high</sub>]
- } = 42 fit regions

→ Slice  $p_T^V$  axis in 2(3)  $p_T^V$  bins:  
[(75,)150,250+]

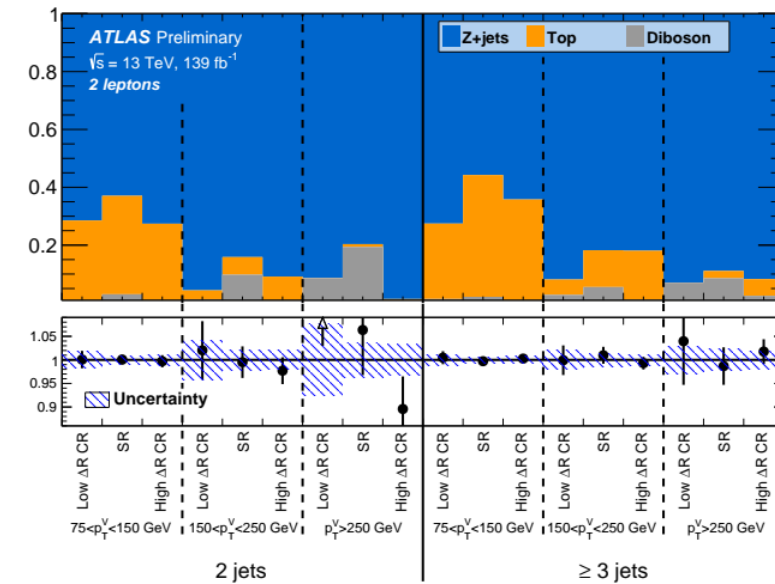
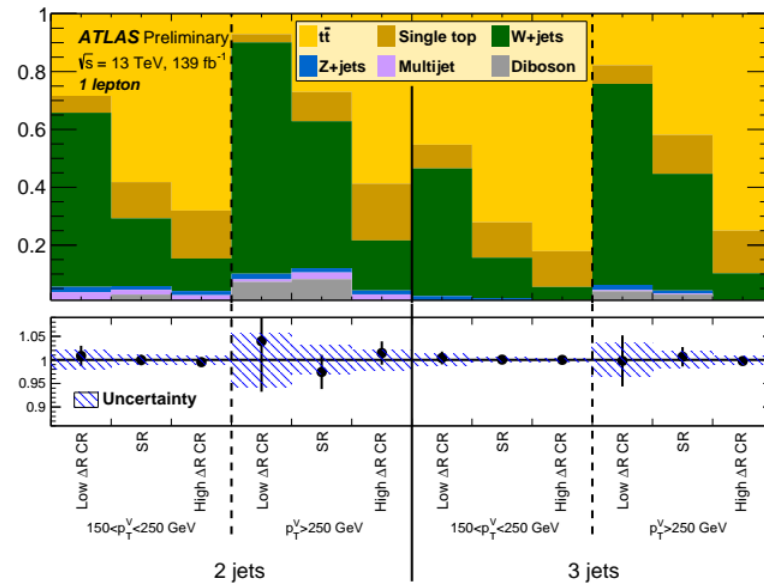
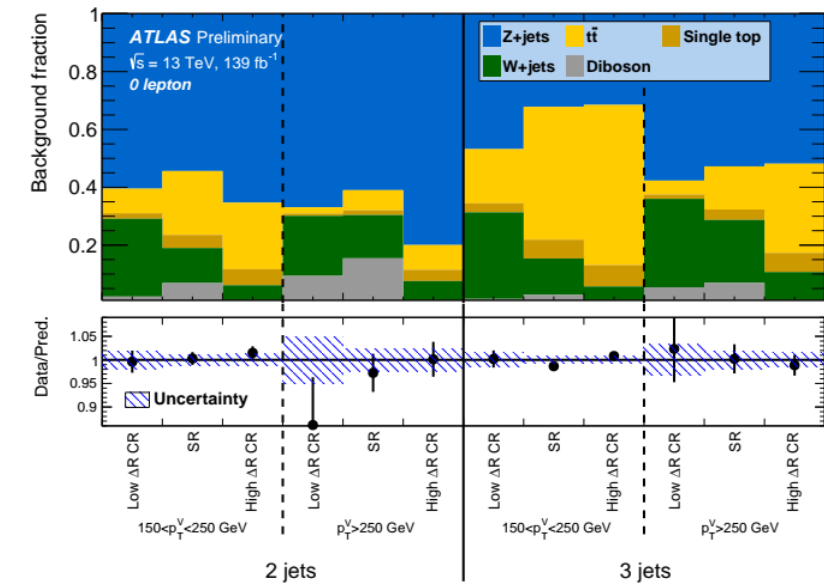
→ For 0/1-(2-) lepton channels

# VH → bb Resolved Event Categorisation – Fit Regions



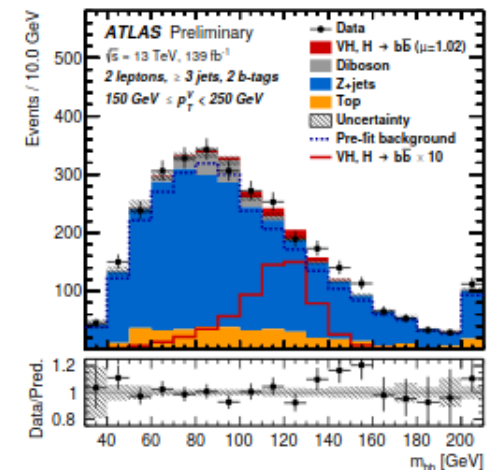
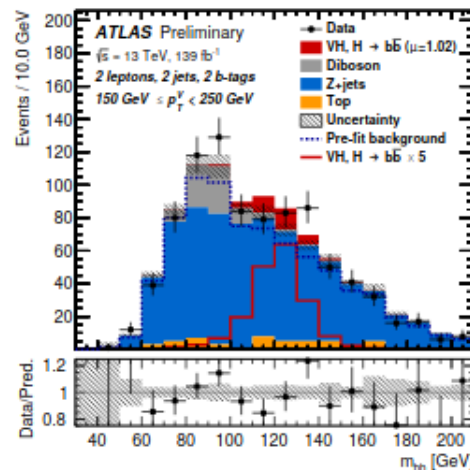
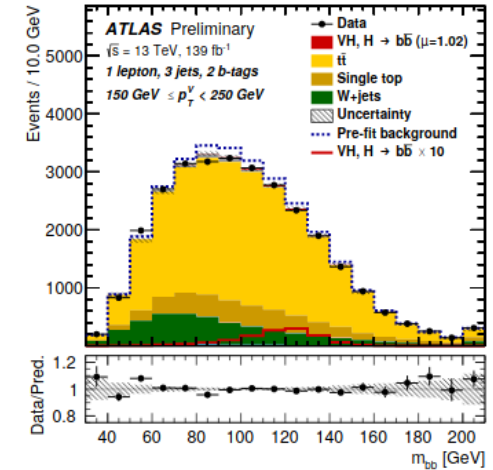
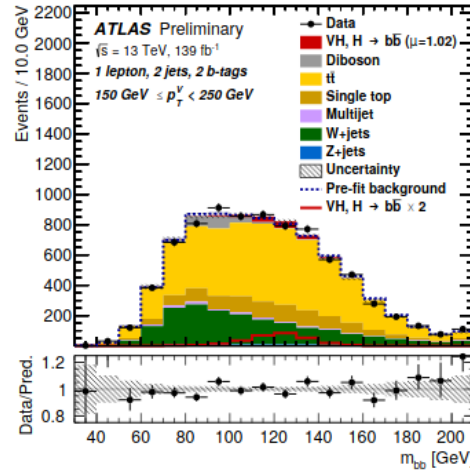
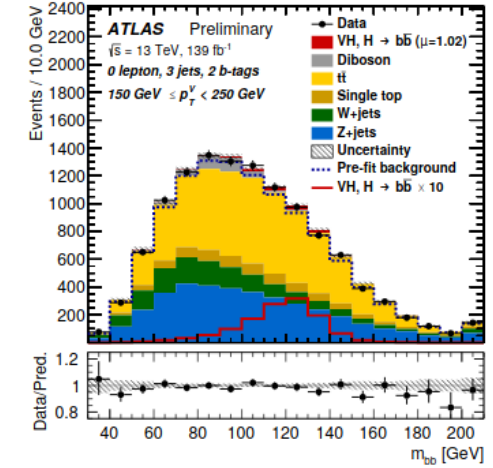
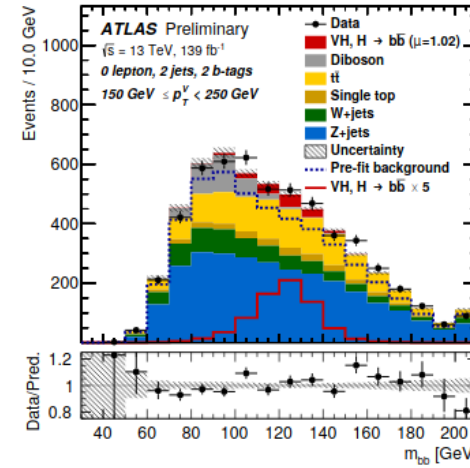
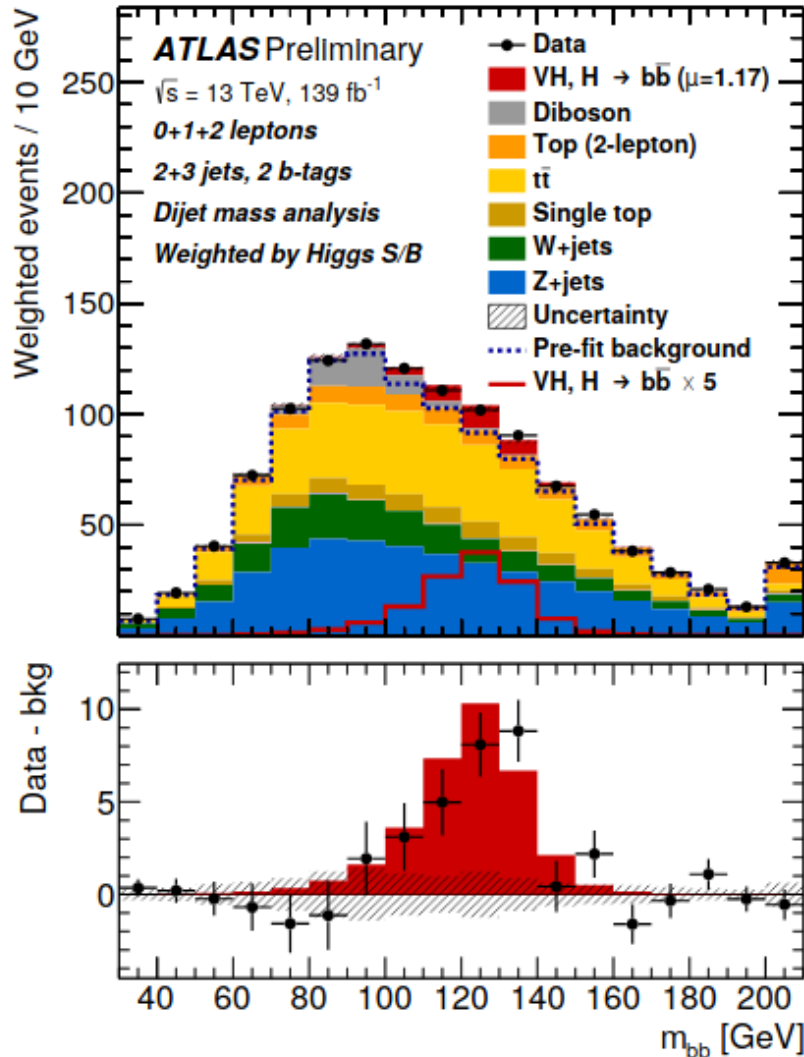
- $BDT_{score}$  used as fit discriminant in SR's
- $CR_{Low/High}$  used only to constrain normalisation – single bin
- Across  $p_T^V$  regions CR single bins provide differential shape information

Channel	Region	Categories					
		$75 \text{ GeV} < p_T^V < 150 \text{ GeV}$		$150 \text{ GeV} < p_T^V < 250 \text{ GeV}$		$p_T^V > 250 \text{ GeV}$	
		2-jets	3-jets	2-jets	3-jets	2-jets	3-jets
0-lepton	Low- $\Delta R$ -CR	–	–	Yields	Yield	Yield	Yield
	Signal region	–	–	BDT	BDT	BDT	BDT
	High- $\Delta R$ -CR	–	–	Yield	Yield	Yield	Yield
1-lepton	Low- $\Delta R$ -CR	–	–	Yield	Yield	Yield	Yield
	Signal region	–	–	BDT	BDT	BDT	BDT
	High- $\Delta R$ -CR	–	–	Yield	Yield	Yield	Yield
2-lepton	Low- $\Delta R$ -CR	Yield	Yield	Yield	Yield	Yield	Yield
	Signal region	BDT	BDT	BDT	BDT	BDT	BDT
	High- $\Delta R$ -CR	Yield	Yield	Yield	Yield	Yield	Yield



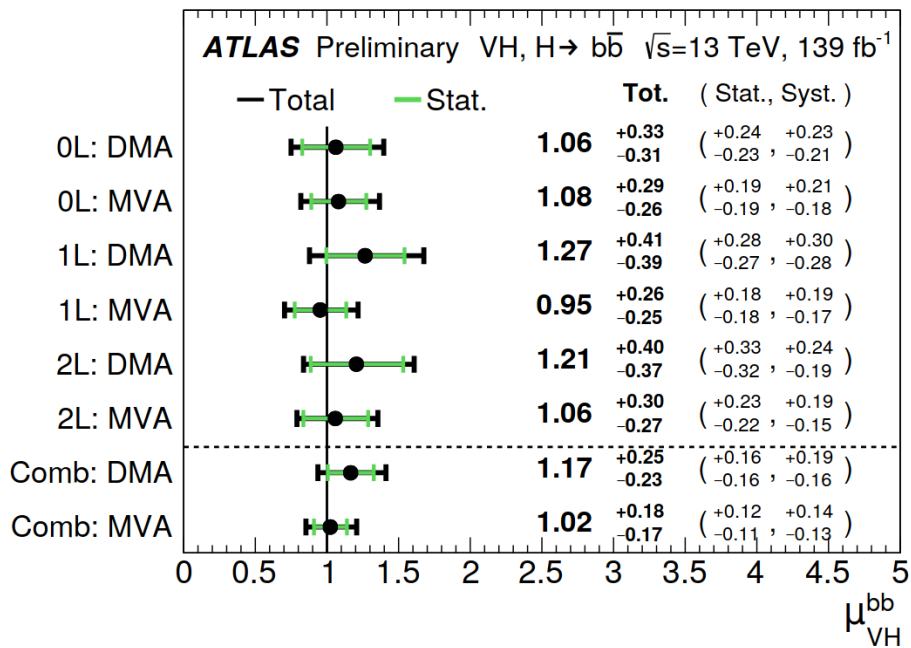
# VH $\rightarrow$ bb Resolved Di-jet Mass Analysis

- $\rightarrow$  Identical fit regions as MVA following new 2D  $[p_T^V, \Delta R(b,b)]$  plane definitions:
- $\rightarrow$  Binned profile likelihood fit  $\mathcal{L}(\mathbf{x}, \mu | \theta)$  with **total of 42 fit regions**





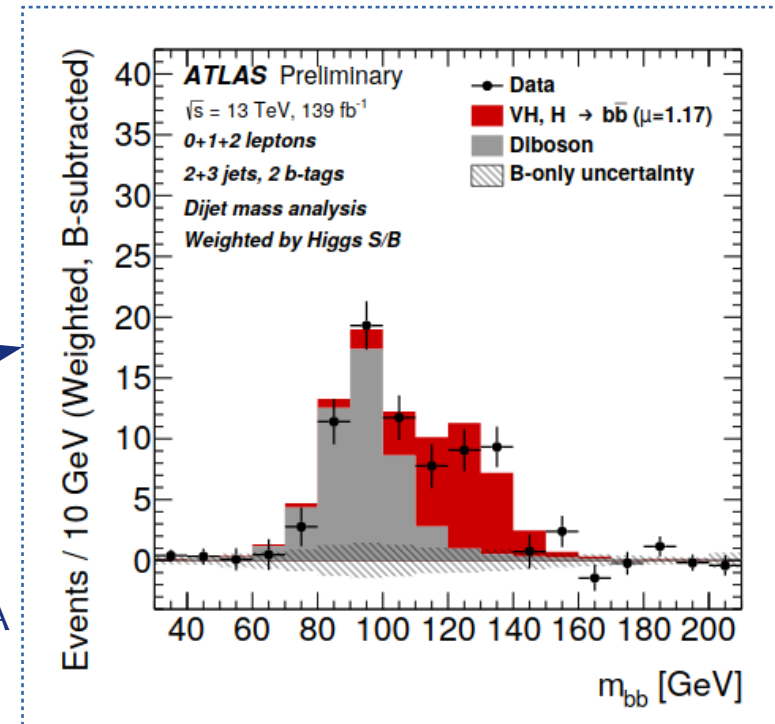
## Di-jet Mass Analysis (DMA)



S/B Weighted combination of  $m_{bb}$  distributions from 0+1+2L channels

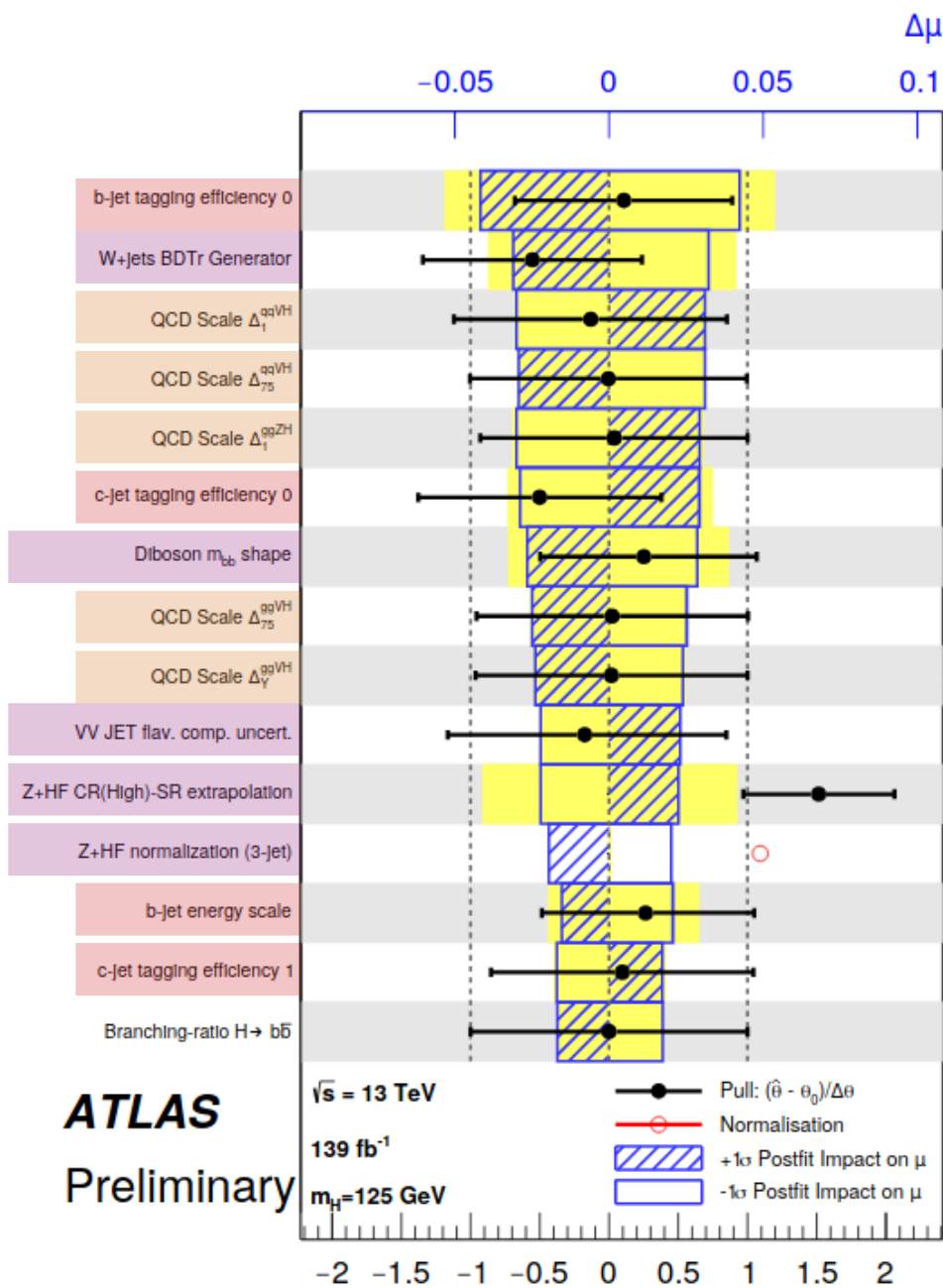
$$Z_0 = \frac{\text{Obs.}}{\text{(exp.)}} = \frac{5.4}{(4.9) \sigma}$$

→ Good agreement between MVA & DMA



# VH → bb Resolved: Systematics

- Statistical and systematics approximately the same!
- Modelling/signal MC uncertainties and b-tagging dominant!



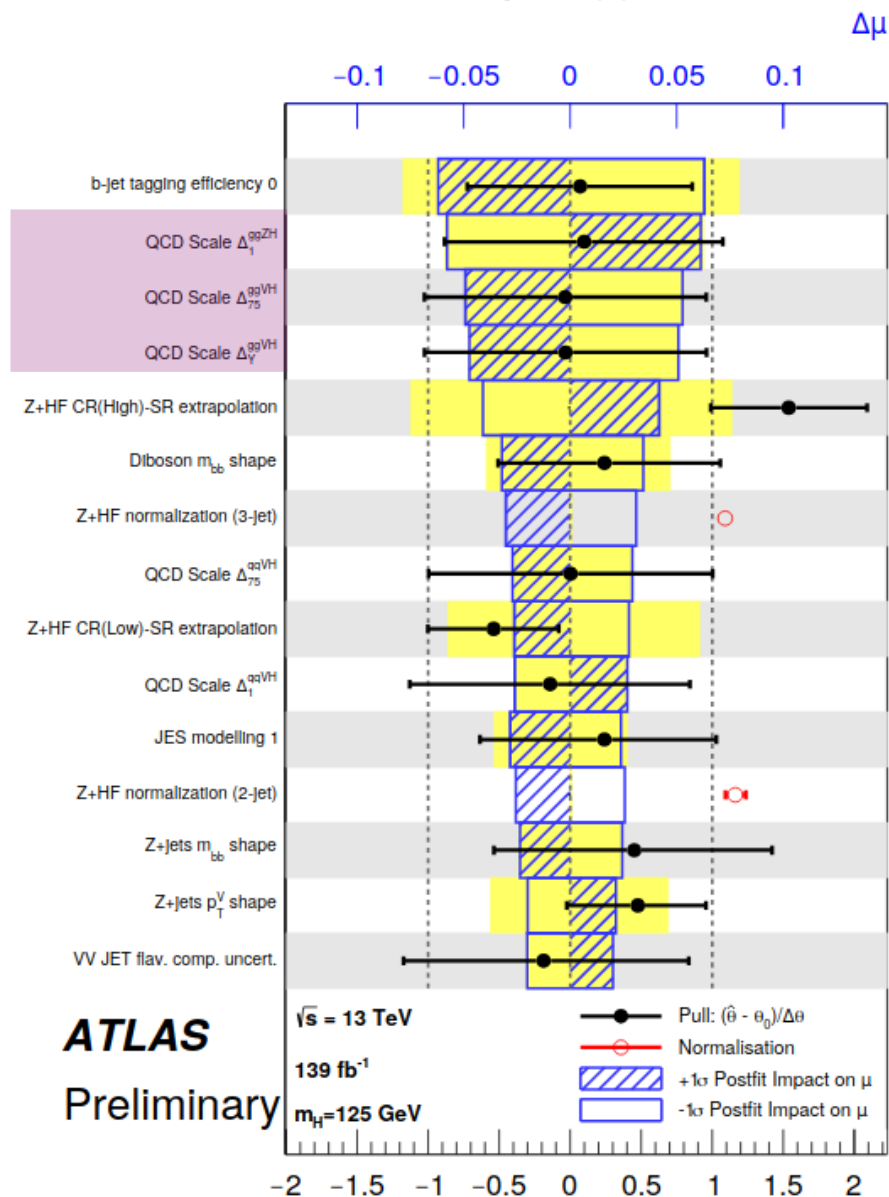
Source of uncertainty	$\sigma_\mu$			
	VH	WH	ZH	
<b>Total</b>	<b>0.177</b>	<b>0.260</b>	<b>0.240</b>	
Statistical	0.115	0.182	0.171	
Systematic	0.134	0.186	0.168	
<b>Statistical uncertainties</b>				
Data statistical	0.108	0.171	0.157	
$t\bar{t} e\mu$ control region	0.014	0.003	0.026	
Floating normalisations	0.034	0.061	0.045	
<b>Experimental uncertainties</b>				
Jets	0.043	0.050	0.057	
$E_T^{\text{miss}}$	0.015	0.045	0.013	
Leptons	0.004	0.015	0.005	
<b>b-tagging</b>	<i>b</i> -jets	0.045	0.025	0.064
	<i>c</i> -jets	0.035	0.068	0.010
	light-flavour jets	0.009	0.004	0.014
Pile-up	0.003	0.002	0.007	
Luminosity	0.016	0.016	0.016	
<b>Theoretical and modelling uncertainties</b>				
<b>Signal</b>	<b>0.052</b>	<b>0.048</b>	<b>0.072</b>	
Z + jets	0.032	0.013	0.059	
W + jets	0.040	0.079	0.009	
$t\bar{t}$	0.021	0.046	0.029	
Single top quark	0.019	0.048	0.015	
Diboson	0.033	0.033	0.039	
Multi-jet	0.005	0.017	0.005	
MC statistical	0.031	0.055	0.038	

Stat. ~ Syst uncert.

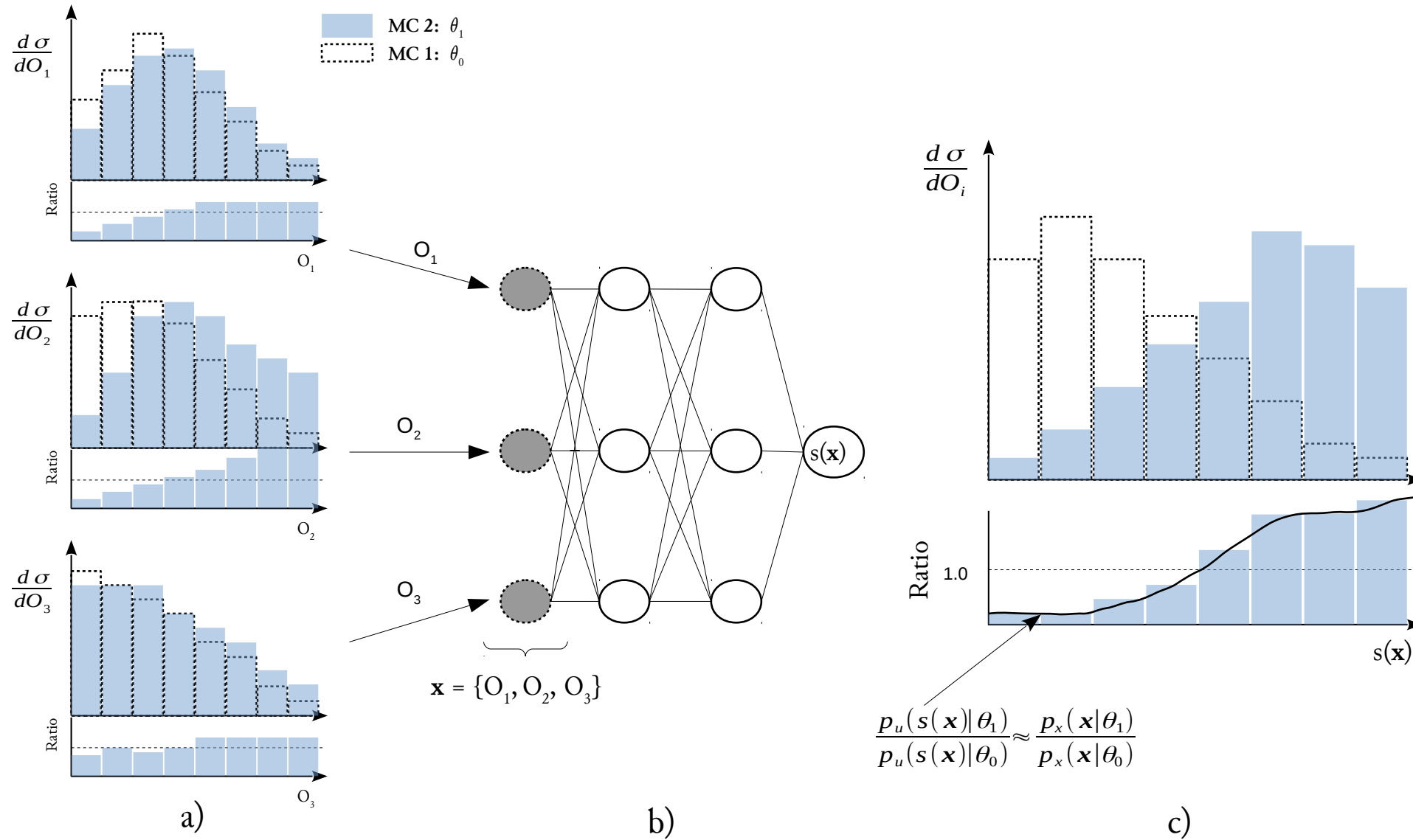
# VH → bb: Systematics (ZH)

→ **Special statement:** For ZH NLO corrections for  $gg \rightarrow ZH$  production that are missing dominant the measurement precision

→ Limits the  $H \rightarrow bb$  sensitivity to  $ggF$ !

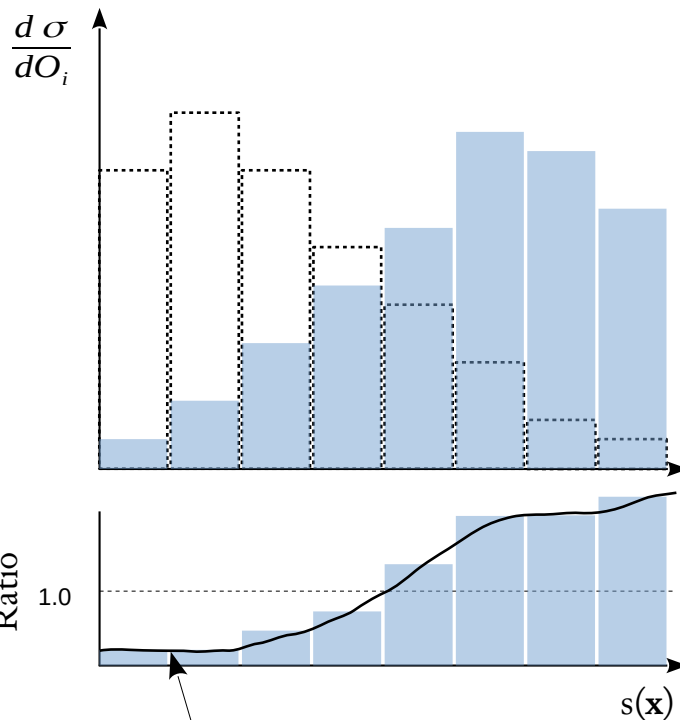
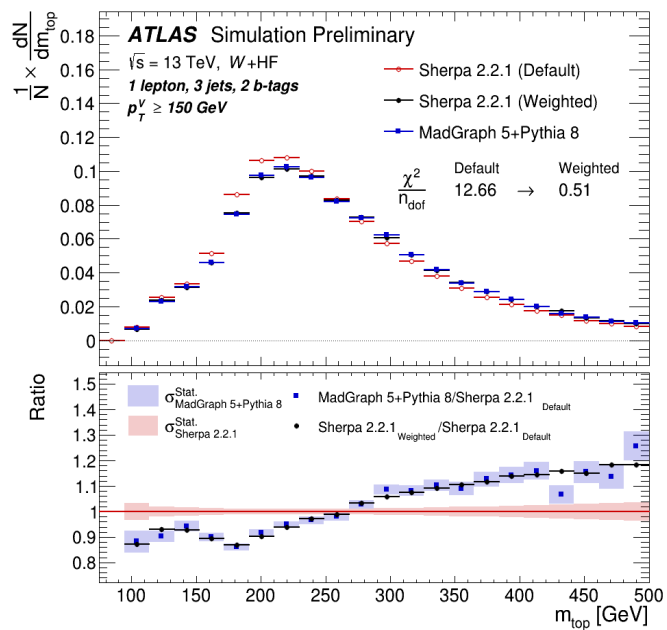
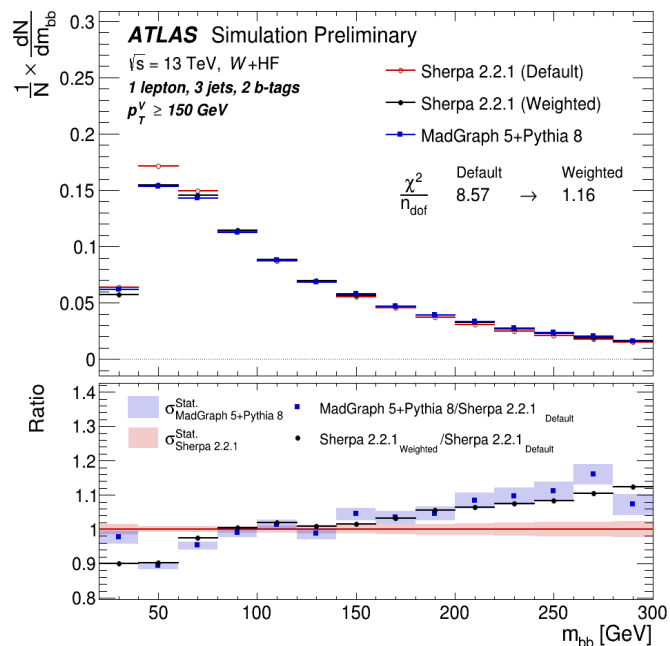


Source of uncertainty	$\sigma_\mu$		
	VH	WH	ZH
<b>Total</b>	<b>0.177</b>	<b>0.260</b>	<b>0.240</b>
Statistical	0.115	0.182	0.171
Systematic	0.134	0.186	0.168
<b>Statistical uncertainties</b>			
Data statistical	0.108	0.171	0.157
$t\bar{t} e\mu$ control region	0.014	0.003	0.026
Floating normalisations	0.034	0.061	0.045
<b>Experimental uncertainties</b>			
Jets	0.043	0.050	0.057
$E_T^{\text{miss}}$	0.015	0.045	0.013
Leptons	0.004	0.015	0.005
$b$ -tagging	$b$ -jets	0.045	0.025
	$c$ -jets	0.035	0.068
	light-flavour jets	0.009	0.004
Pile-up	0.003	0.002	0.007
Luminosity	0.016	0.016	0.016
<b>Theoretical and modelling uncertainties</b>			
<b>Signal</b>	<b>0.052</b>	<b>0.048</b>	<b>0.072</b>
Z + jets	0.032	0.013	0.059
W + jets	0.040	0.079	0.009
$t\bar{t}$	0.021	0.046	0.029
Single top quark	0.019	0.048	0.015
Diboson	0.033	0.033	0.039
Multi-jet	0.005	0.017	0.005
MC statistical	0.031	0.055	0.038





## Input Space:

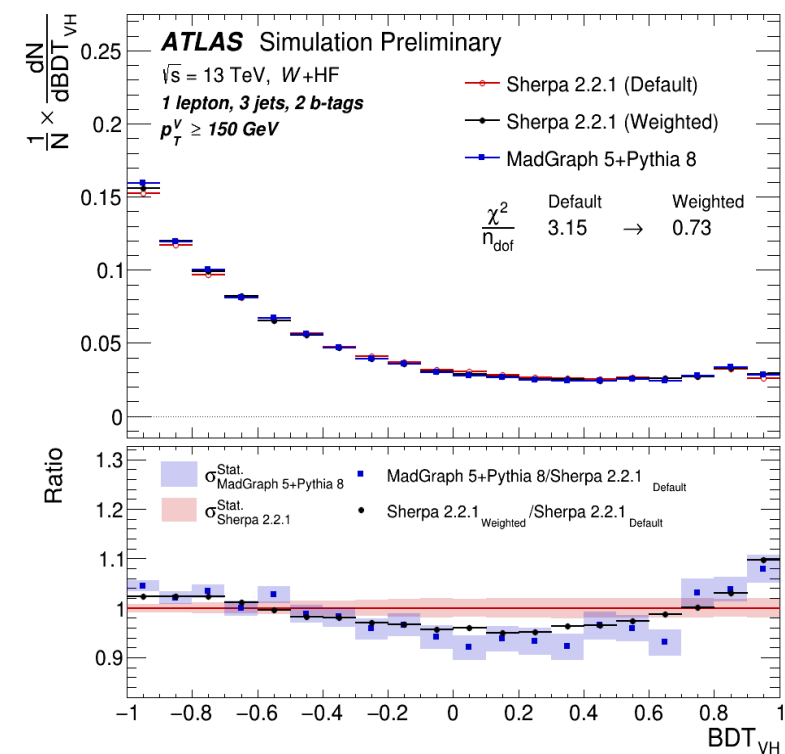


$$\frac{p_u(s(\mathbf{x})|\theta_1)}{p_u(s(\mathbf{x})|\theta_0)} \approx \frac{p_x(\mathbf{x}|\theta_1)}{p_x(\mathbf{x}|\theta_0)}$$

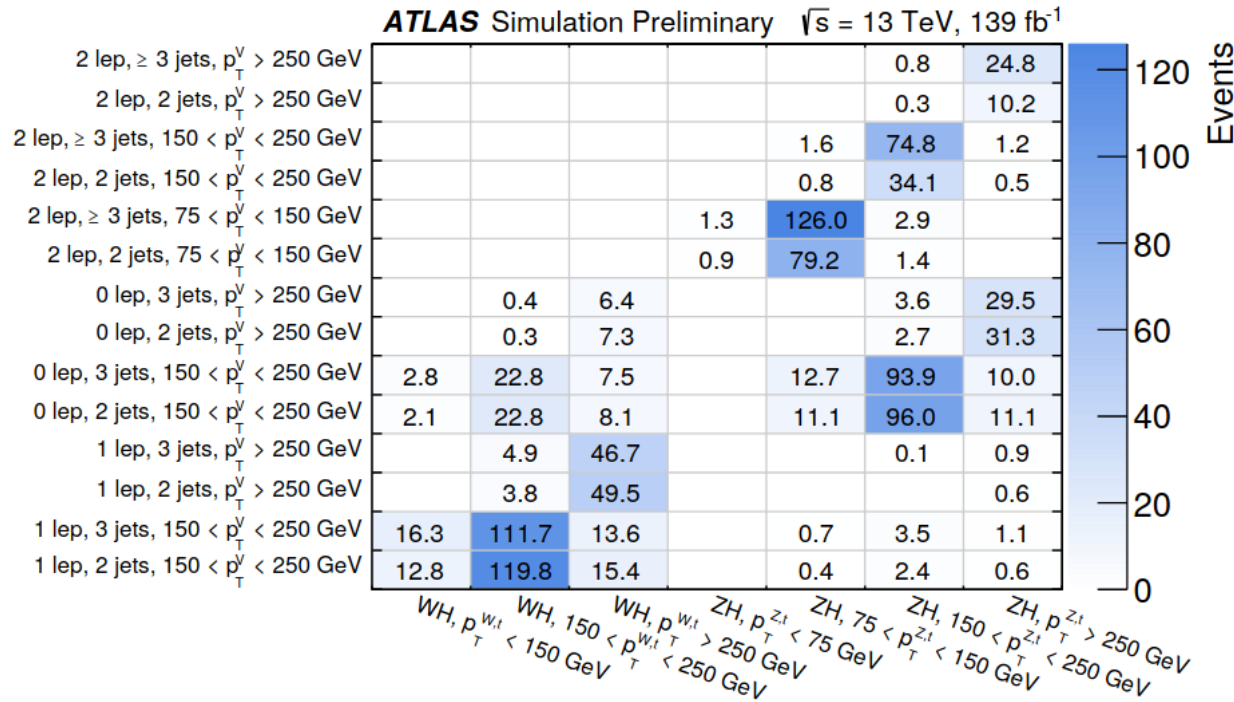


Re-weight using MVA calibrated density ratio estimator and pass to analysis BDT

## Fit Discriminant Space:

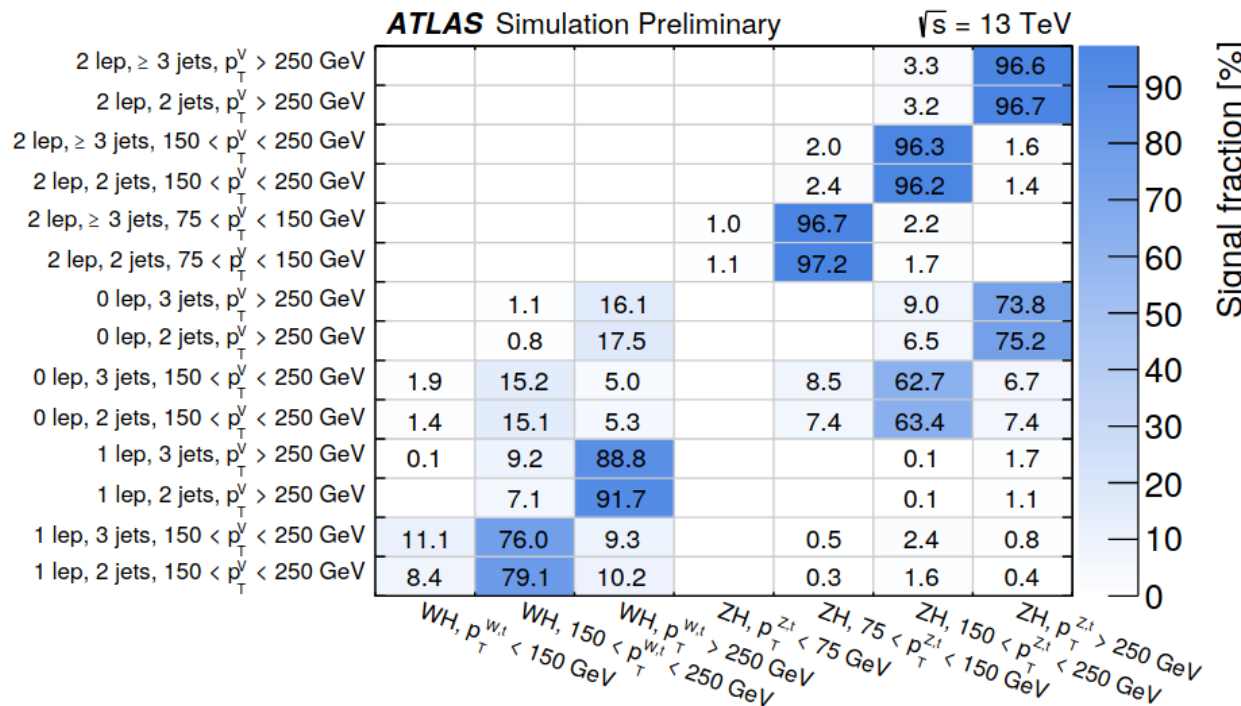


# VHbb Resolved: STXS Bin Signal Division



→ Expected signal yields per:

- Reconstruction category (y-axis)
- Truth category (x-axis)

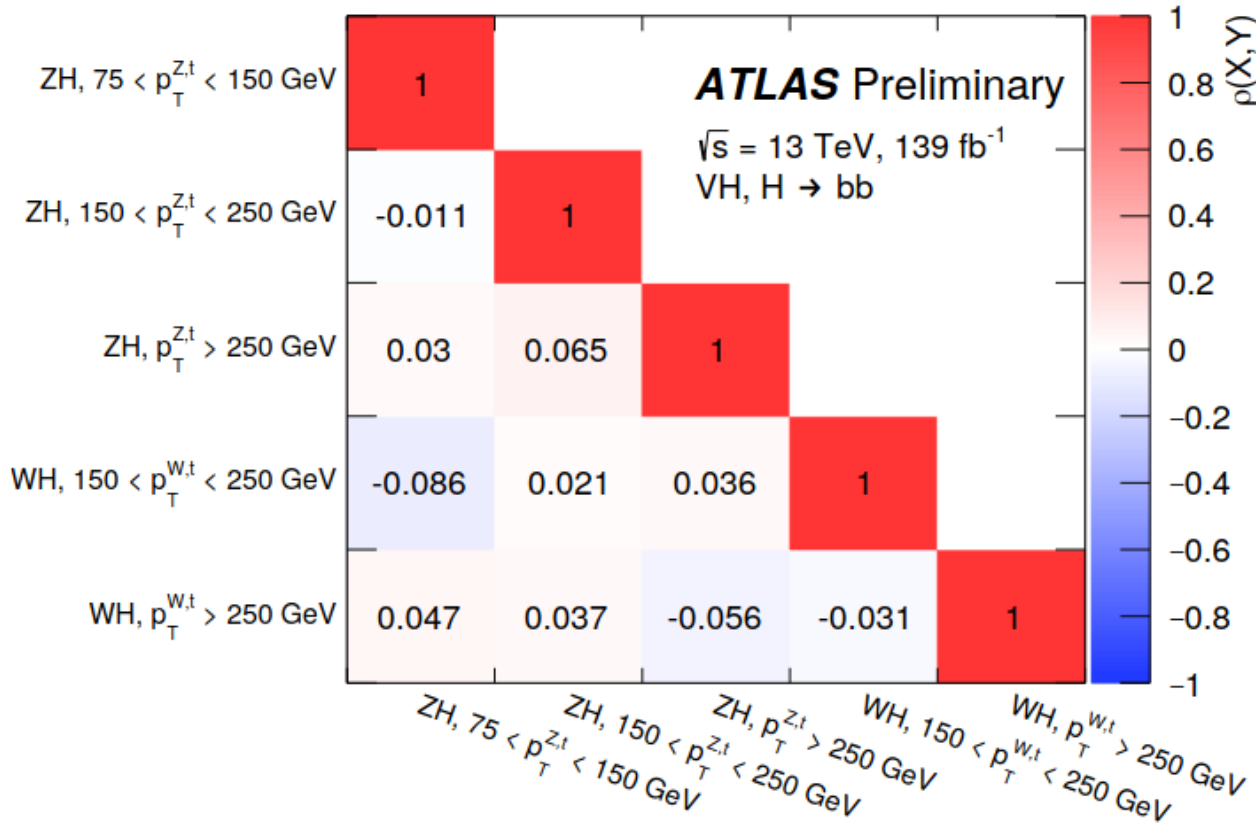


→ Fraction of expected signal yields per:

- Reconstruction category (y-axis)
- Truth category (x-axis)

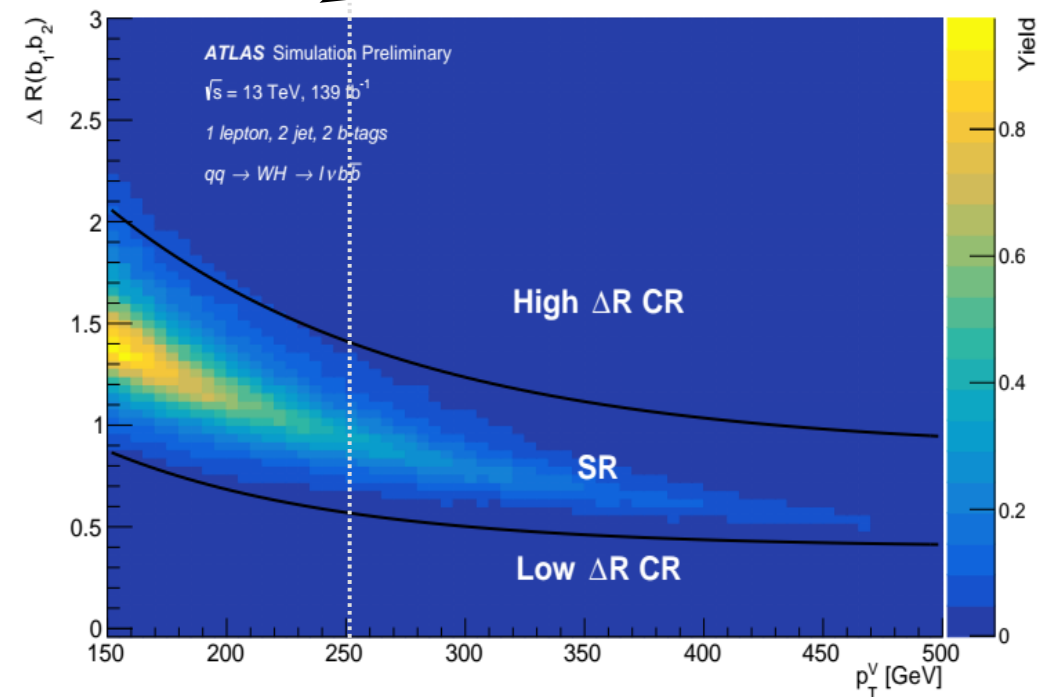
Normalised according to the total fiducial phase space yield.

# VHbb Resolved: STXS Bin Correlations



→ Observed correlations between reduced stage 1.2 STXS scheme for 5-POI scheme  
 - Statistical & Systematics included

→ Expansion of STXS scheme to include an exclusive  $150 \text{ GeV} < p_T^V(\text{truth}) < 250 \text{ GeV}$  bin reduces cross-correlation



# VHbb Resolved: EFT

→ Effective lagrangian approach using the Warsaw basis:

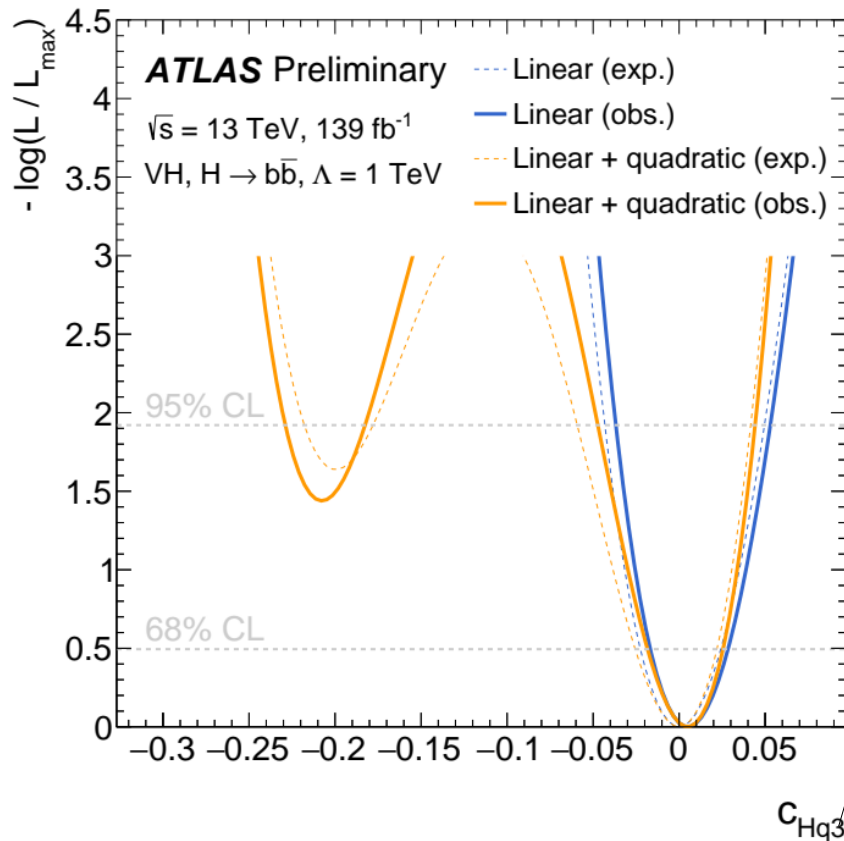
$$\mathcal{L}_{\text{SMEFT}} = \mathcal{L}_{\text{SM}} + \sum_i \frac{c_i^{(D)}}{\Lambda^{D-4}} \mathcal{O}_i^{(D)},$$

→ Only dimension D=6 operators are considered:

→ D=5 violate lepton/baryon number

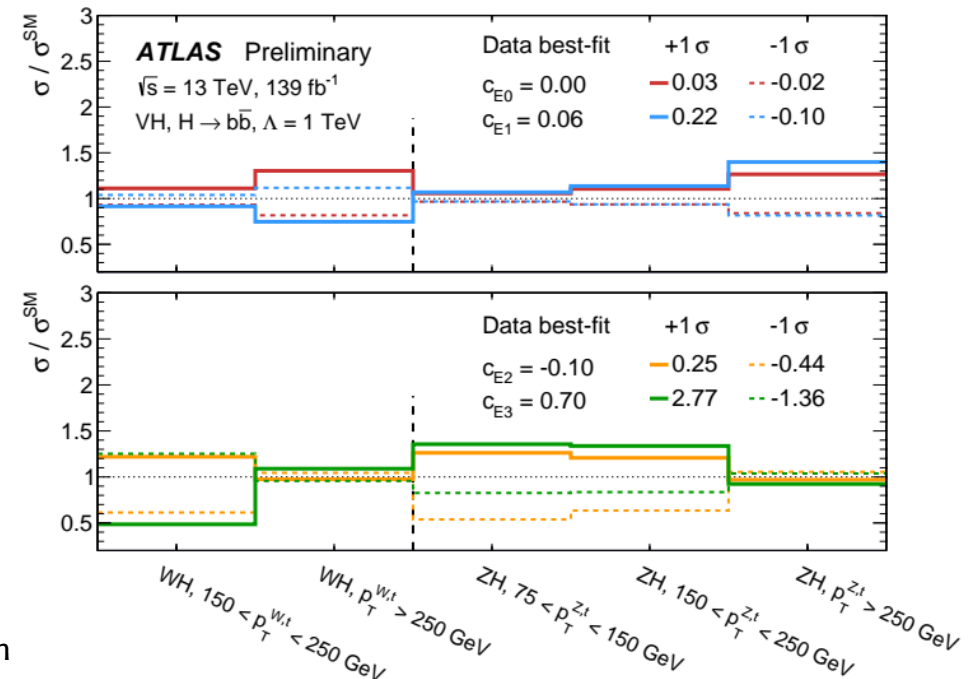
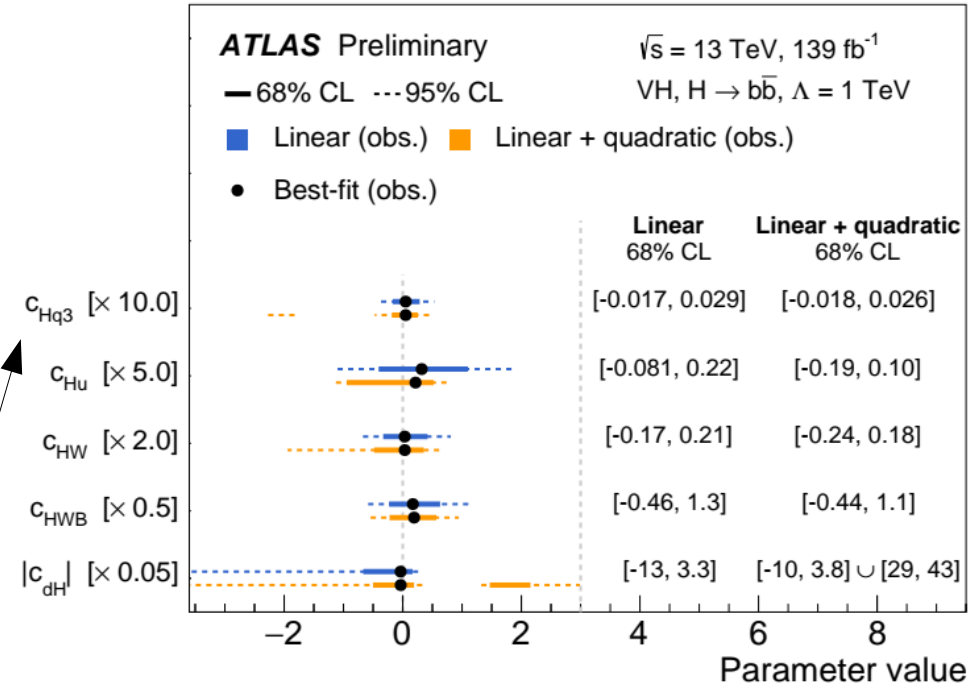
→ D=7+ suppressed by further powers of 1/Λ beyond Λ<sup>4</sup>

→ Linear (interference) and quadratic (D=6)<sup>2</sup> parameterised in each STXS bin:

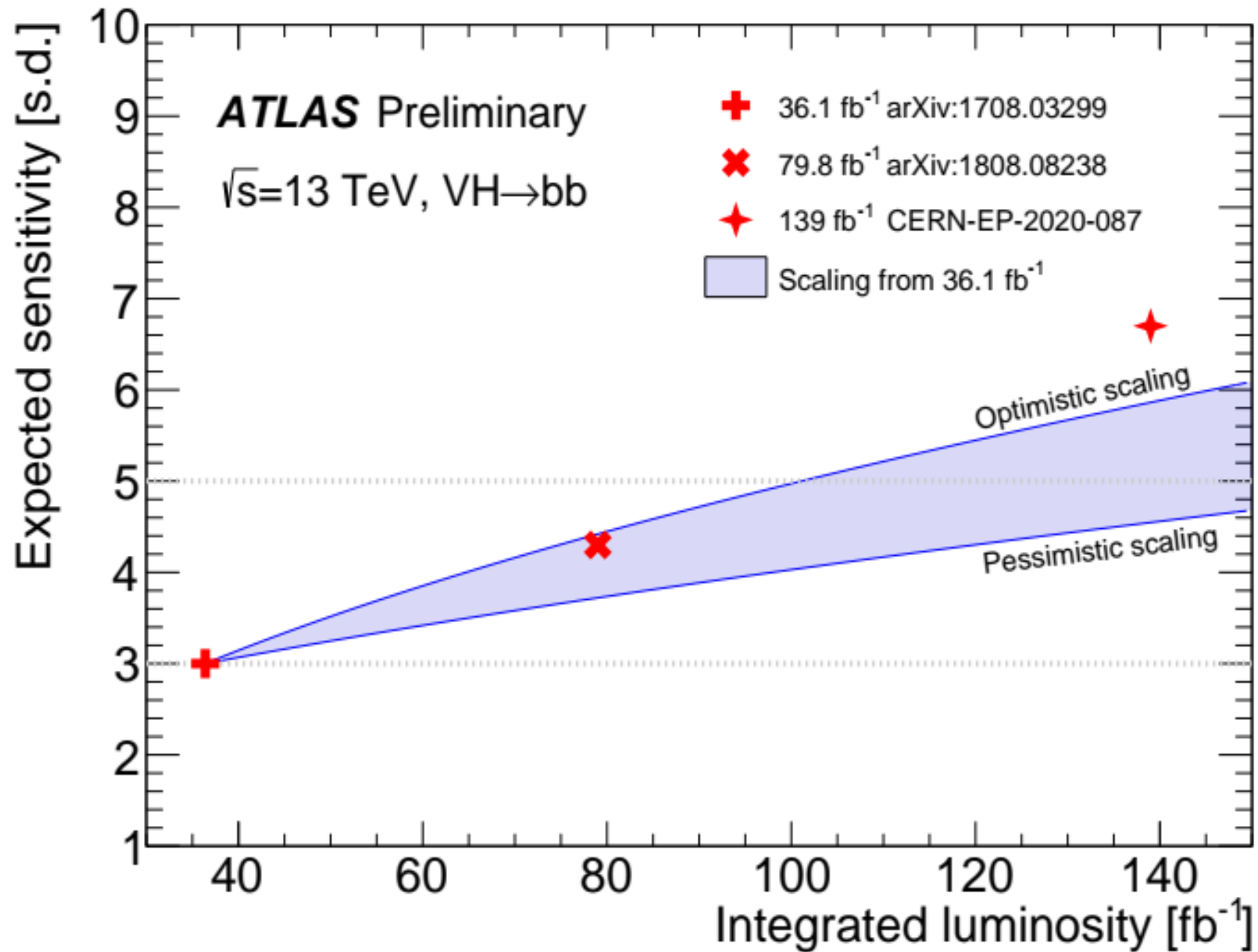


Apply constrained on Wilson co-efficients

Stephen Jiggin



# VHbb Resolved: Analysis Sensitivity over the years!

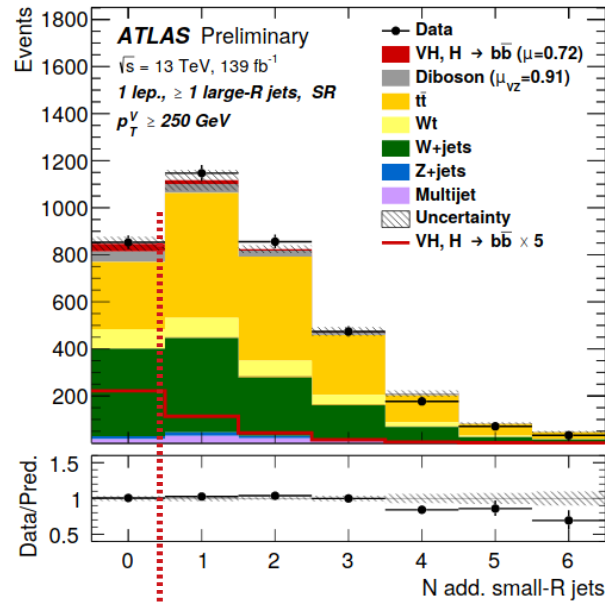




# VH → bb Boosted Event Categorisation – Fit Regions



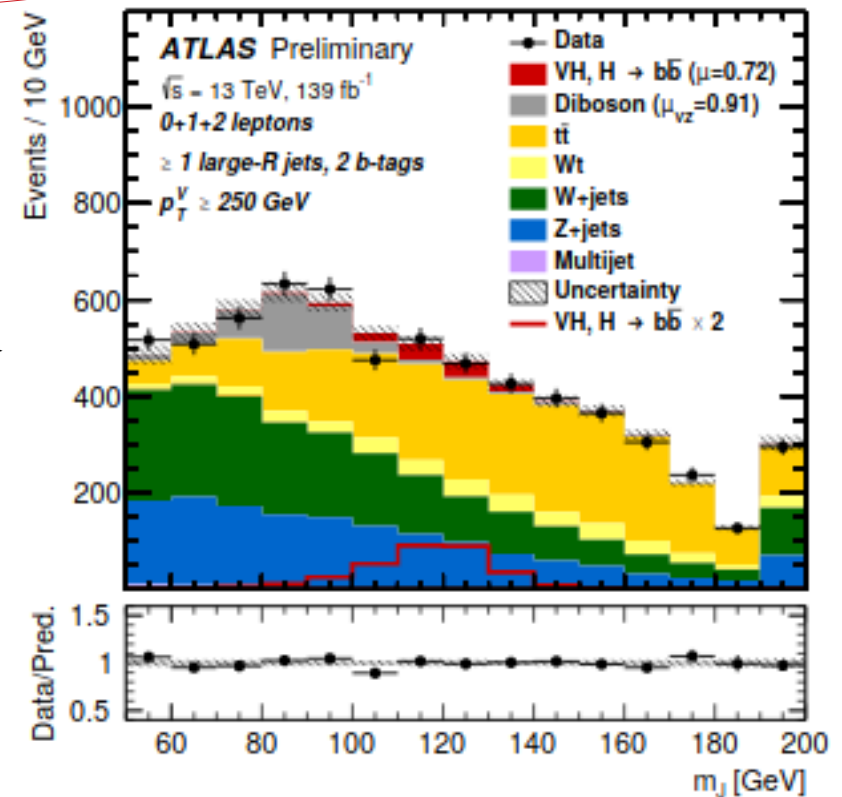
→ Low(High) purity SR's defined by additional AK4 jets:



Channel	Categories					
	$250 < p_T^V < 400 \text{ GeV}$			$p_T^V \geq 400 \text{ GeV}$		
	0 add. $b$ -track-jets		$\geq 1$ add. $b$ -track-jets	0 add. $b$ -track-jets		$\geq 1$ add. $b$ -track-jets
	0 add. small- $R$ jets	$\geq 1$ add. small- $R$ jets	0 add. small- $R$ jets	$\geq 1$ add. small- $R$ jets	$\geq 1$ add. $b$ -track-jets	
0-lepton	HP SR	LP SR	CR	HP SR	LP SR	CR
1-lepton	HP SR	LP SR	CR	HP SR	LP SR	CR
2-lepton		SR			SR	

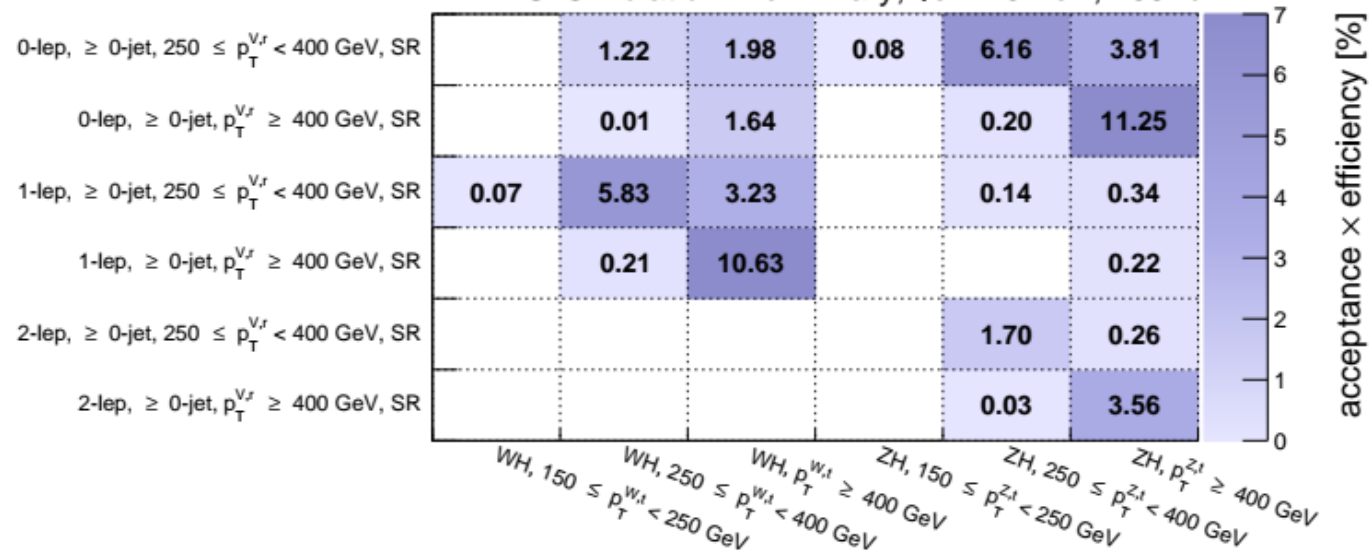
→ tt CR's defined by additional AK2 VR track jets

→  $m_j$  used as fit discriminant in CR/SR's - showing sum of lepton channel SRs:



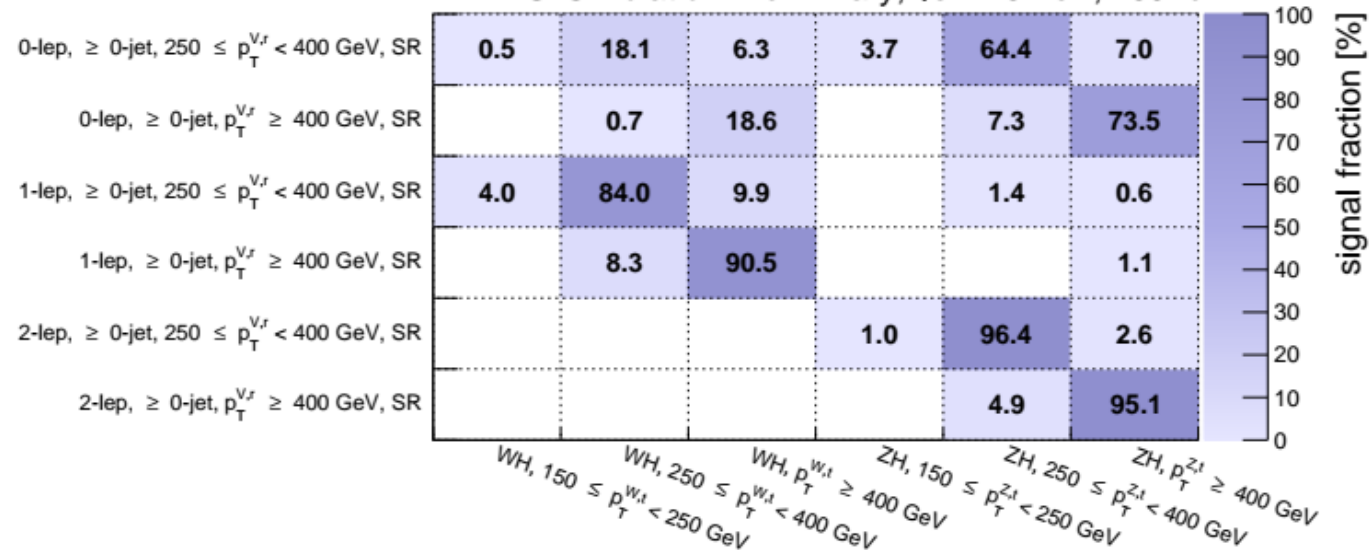
# VHbb Boosted: STXS Bin Signal Division

ATLAS Simulation Preliminary,  $\sqrt{s} = 13$  TeV,  $139 \text{ fb}^{-1}$



→ Signal acceptance x eff. per:  
 - Reconstruction category (y-axis)  
 - Truth category (x-axis)

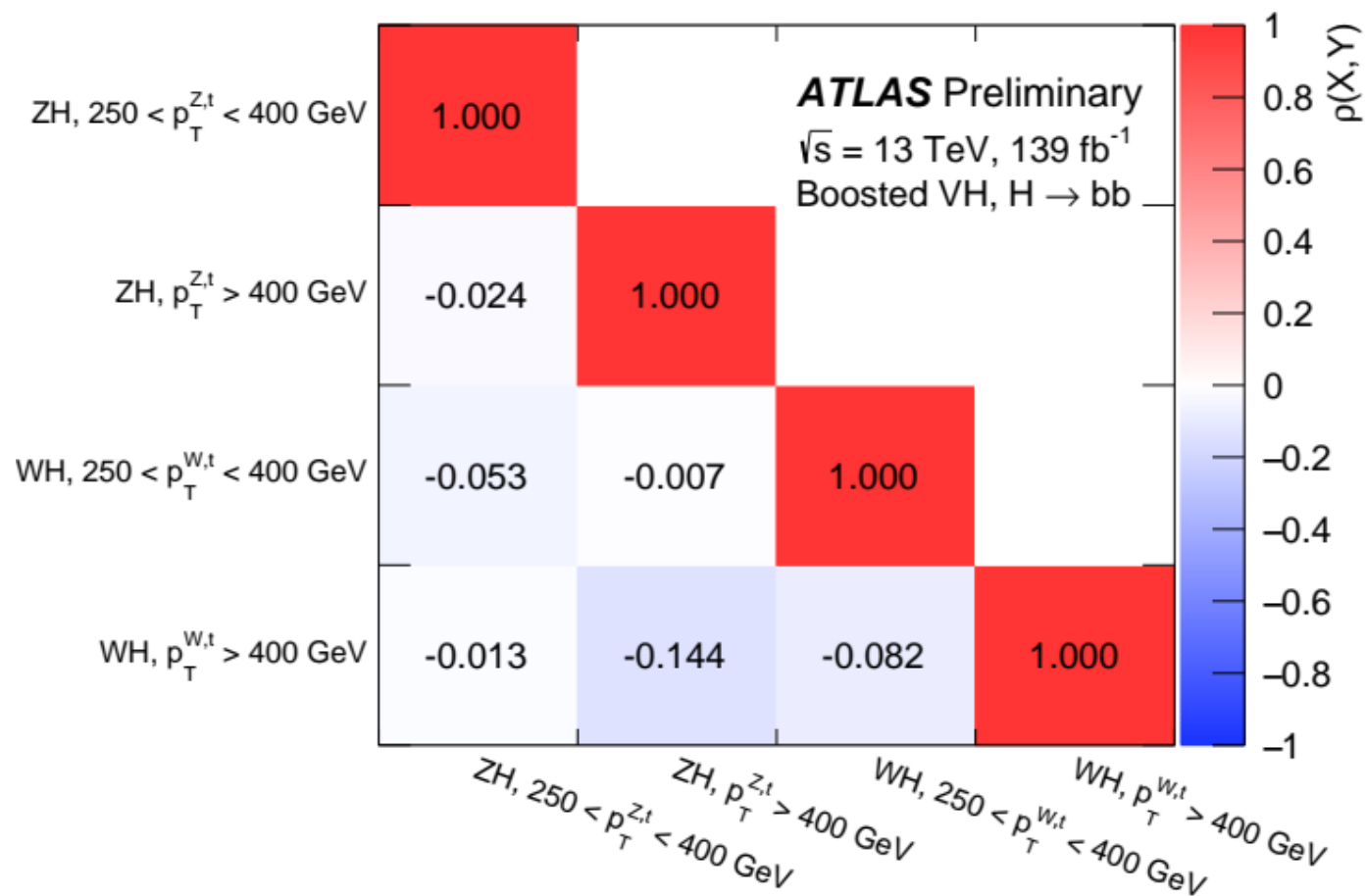
ATLAS Simulation Preliminary,  $\sqrt{s} = 13$  TeV,  $139 \text{ fb}^{-1}$



→ Signal purity:  
 - Reconstruction category (y-axis)  
 - Truth category (x-axis)

Normalised according to the total fiducial phase space yield.

# VHbb Boosted: STXS Bin Correlations



→ Observed correlations between reduced stage 1.2 STXS scheme for 4-POI scheme  
 - Statistical & Systematics included



→ Effective lagrangian approach use the Warsaw basis:

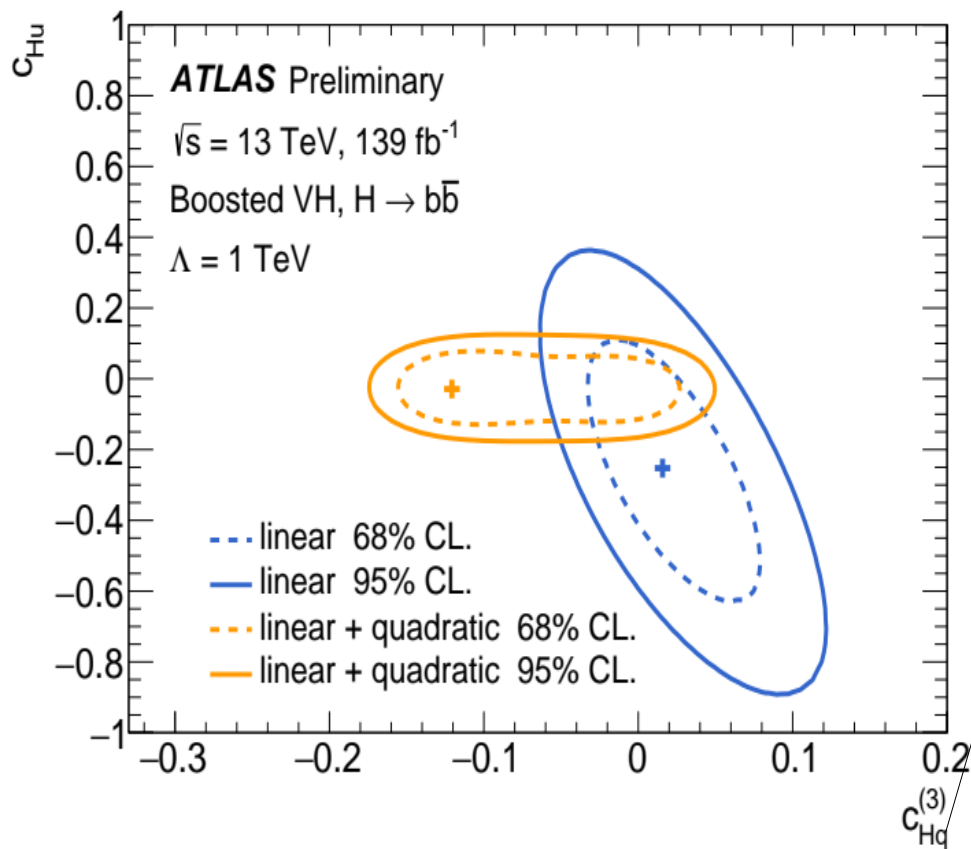
$$\mathcal{L}_{\text{SMEFT}} = \mathcal{L}_{\text{SM}} + \sum_i \frac{c_i^{(D)}}{\Lambda^{D-4}} \mathcal{O}_i^{(D)},$$

→ Only dimension D=6 operators are considered:

→ D=5 violate lepton/baryon number

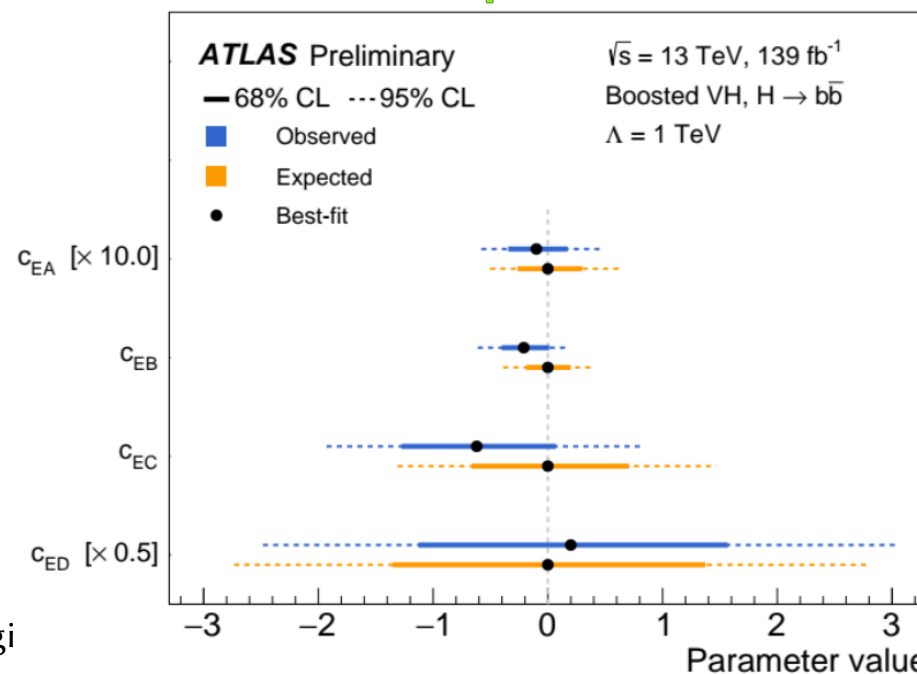
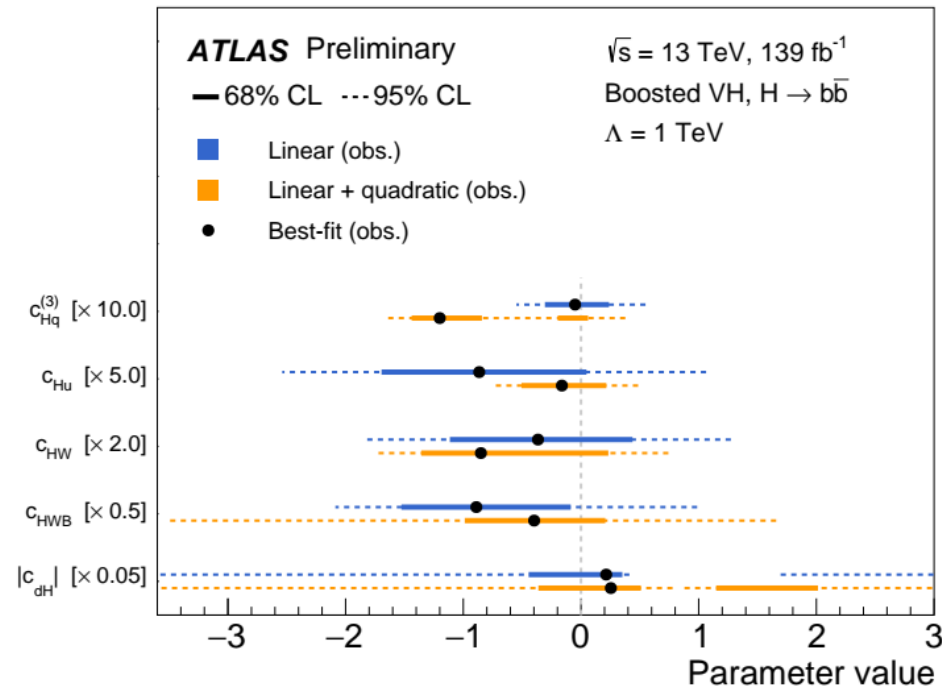
→ D=7+ suppressed by further powers of  $1/\Lambda$  beyond  $\Lambda^4$

→ Linear (interference) and quadratic (D=6)<sup>2</sup> parameterised in each STXS bin:

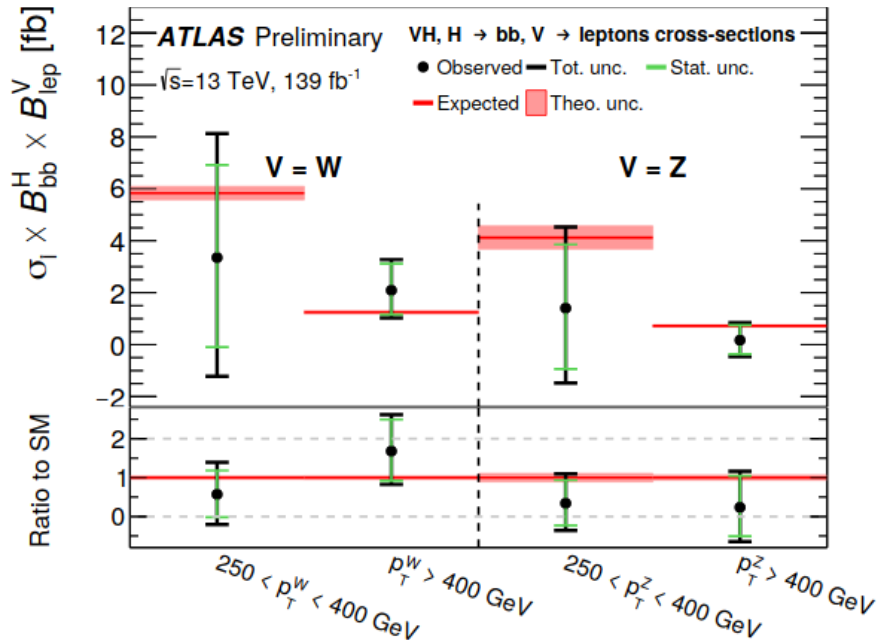
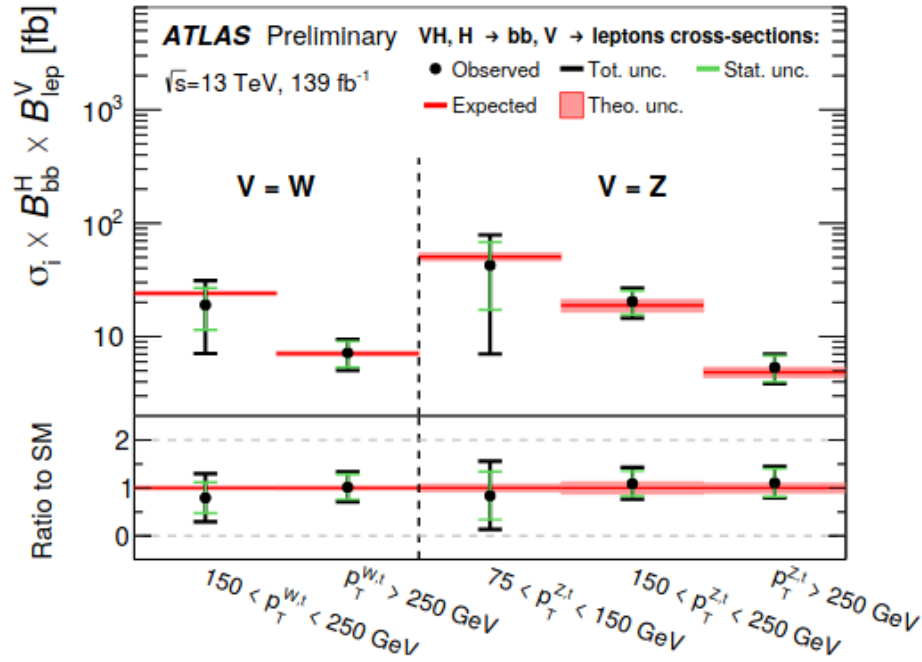


Apply constrained on Wilson co-efficients

Stephen Jiggi



→ **VHbb resolved**: Stage 1.2 STXS scheme merged down to 5/4 bins



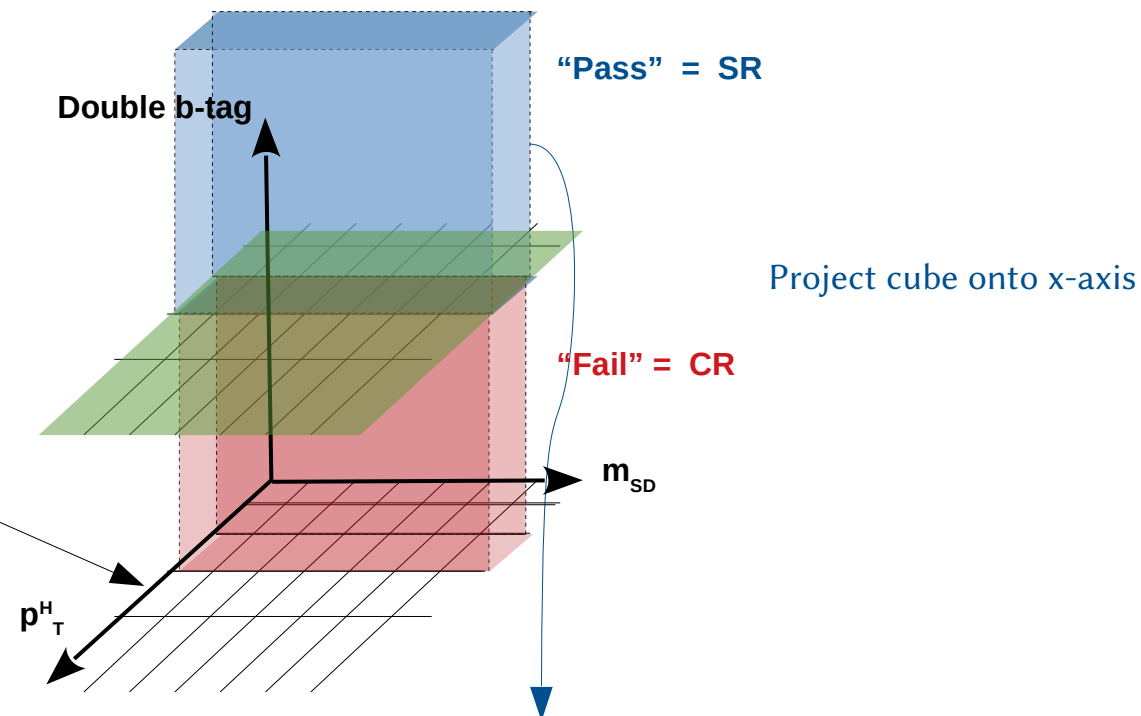
Measurement region ( $ y_H  < 2.5, H \rightarrow b\bar{b}$ )	SM prediction [fb]	Result [fb]	Stat. unc. [fb]	Syst. unc. [fb]		
				Th. sig.	Th. bkg.	Exp.
5-POI scheme						
$W \rightarrow \ell\nu; 150 < p_T^V < 250 \text{ GeV}$	$24.0 \pm 1.1$	$20 \pm 25$	$\pm 17$	$\pm 2$	$\pm 13$	$\pm 9$
$W \rightarrow \ell\nu; p_T^V > 250 \text{ GeV}$	$7.1 \pm 0.3$	$8.8 \pm 5.2$	$\pm 4.4$	$\pm 0.5$	$\pm 2.5$	$\pm 0.9$
$Z \rightarrow \ell\ell, \nu\nu; 75 < p_T^V < 150 \text{ GeV}$	$50.6 \pm 4.1$	$81 \pm 45$	$\pm 35$	$\pm 10$	$\pm 21$	$\pm 19$
$Z \rightarrow \ell\ell, \nu\nu; 150 < p_T^V < 250 \text{ GeV}$	$18.8 \pm 2.4$	$14 \pm 13$	$\pm 11$	$\pm 1$	$\pm 6$	$\pm 3$
$Z \rightarrow \ell\ell, \nu\nu; p_T^V > 250 \text{ GeV}$	$4.9 \pm 0.5$	$8.5 \pm 4.0$	$\pm 3.7$	$\pm 0.8$	$\pm 1.2$	$\pm 0.6$
3-POI scheme						
$W \rightarrow \ell\nu; p_T^V > 150 \text{ GeV}$	$31.1 \pm 1.4$	$35 \pm 14$	$\pm 9$	$\pm 2$	$\pm 9$	$\pm 4$
$Z \rightarrow \ell\ell, \nu\nu; 75 < p_T^V < 150 \text{ GeV}$	$50.6 \pm 4.1$	$81 \pm 45$	$\pm 35$	$\pm 10$	$\pm 21$	$\pm 19$
$Z \rightarrow \ell\ell, \nu\nu; p_T^V > 150 \text{ GeV}$	$23.7 \pm 3.0$	$28.4 \pm 8.1$	$\pm 6.4$	$\pm 2.4$	$\pm 3.6$	$\pm 2.3$

Measurement region ( $ y_H  < 2.5, H \rightarrow b\bar{b}$ )	SM prediction [fb]	Result [fb]	Stat. unc. [fb]	Syst. unc. [fb]	
				+	-
$W \rightarrow \ell\nu; p_T^W \in [250, 400[ \text{ GeV}$	$5.83 \pm 0.26$	$3.3$	$+ 4.8$ $- 4.6$	$+ 3.6$ $- 3.4$	$+ 3.2$ $- 3.0$
$W \rightarrow \ell\nu; p_T^W \in [400, \infty[ \text{ GeV}$	$1.25 \pm 0.06$	$2.1$	$+ 1.2$ $- 1.1$	$+ 1.0$ $- 0.9$	$+ 0.6$ $- 0.5$
$Z \rightarrow \ell\ell, \nu\nu; p_T^Z \in [250, 400[ \text{ GeV}$	$4.12 \pm 0.45$	$1.4$	$+ 3.1$ $- 2.9$	$+ 2.4$ $- 2.3$	$+ 1.9$ $- 1.7$
$Z \rightarrow \ell\ell, \nu\nu; p_T^Z \in [400, \infty[ \text{ GeV}$	$0.72 \pm 0.05$	$0.2$	$+ 0.7$ $- 0.6$	$+ 0.6$ $- 0.5$	$+ 0.3$ $- 0.3$

**Ultra high  $p_T^H$  environment!**

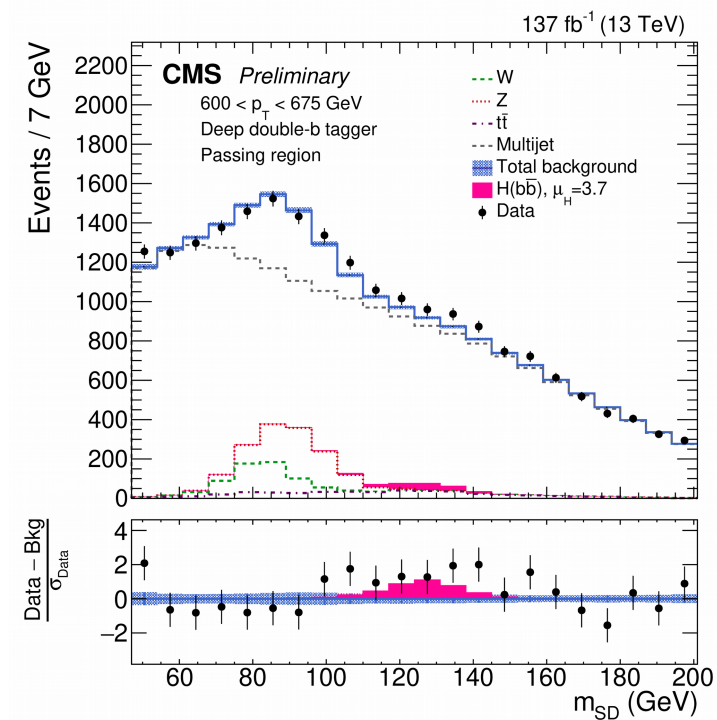
→ Parameterically fit QCD yield within  $(m_{SD,i}, p_{T,j})$  bins:

$$N_{\text{pass}}^{\text{QCD}}(m_{SDi}, p_{Tj}) = \epsilon^{\text{QCD}} \cdot \left( \sum_{k,\ell} a_{k\ell} \rho_{ij}^k p_{Tj}^\ell \right) \cdot N_{\text{fail}}^{\text{QCD}}(m_{SDi}, p_{Tj}),$$



→ **W/Z+jets** & **tt** estimated from Monte Carlo (MC)

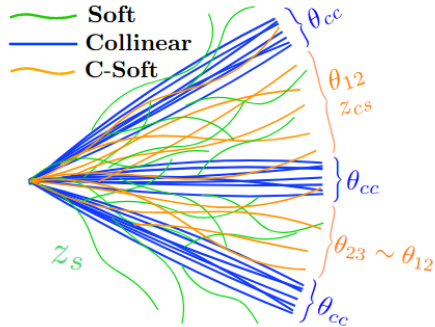
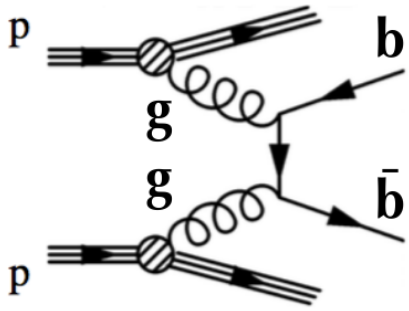
→ **W+Jets/Z+Jets/tt** control regions used to constrain normalisations/uncertainties



→ QCD  $\sim 10^7$  times greater than signal:

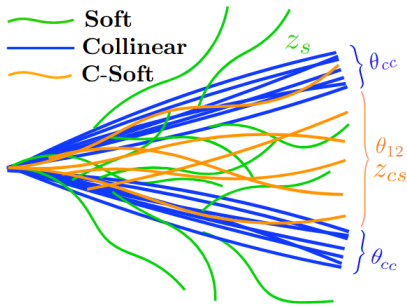
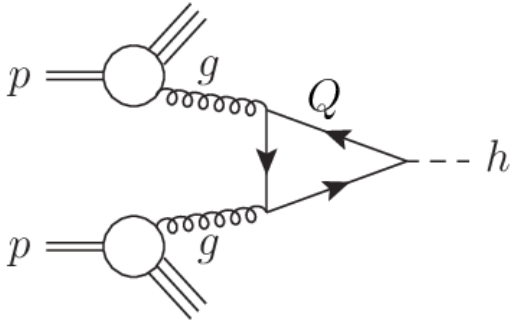
### 3-prong

QCD:  $pp \rightarrow bb+X$



### 2-prong

ggF:  $pp \rightarrow H+X$



Source: [arXiv:1609.07483](https://arxiv.org/abs/1609.07483)

→ Topological handle on QCD vs signal using:

- Ratio of 3-point/2-point energy correlation co-efficients:

$$N_2^1 = \frac{2e_3}{(1e_2)^2}$$

- Use transformed  $N_2^{1,DDT} = N_2^1 - X_{(26\%)}$  to discriminate QCD/signal (see here):

$$N_2^{1,DDT} < 0 \text{ for 26\% QCD accep. across } [\rho, p_T] \text{-plane}$$

→ QCD Bkg Estimation:

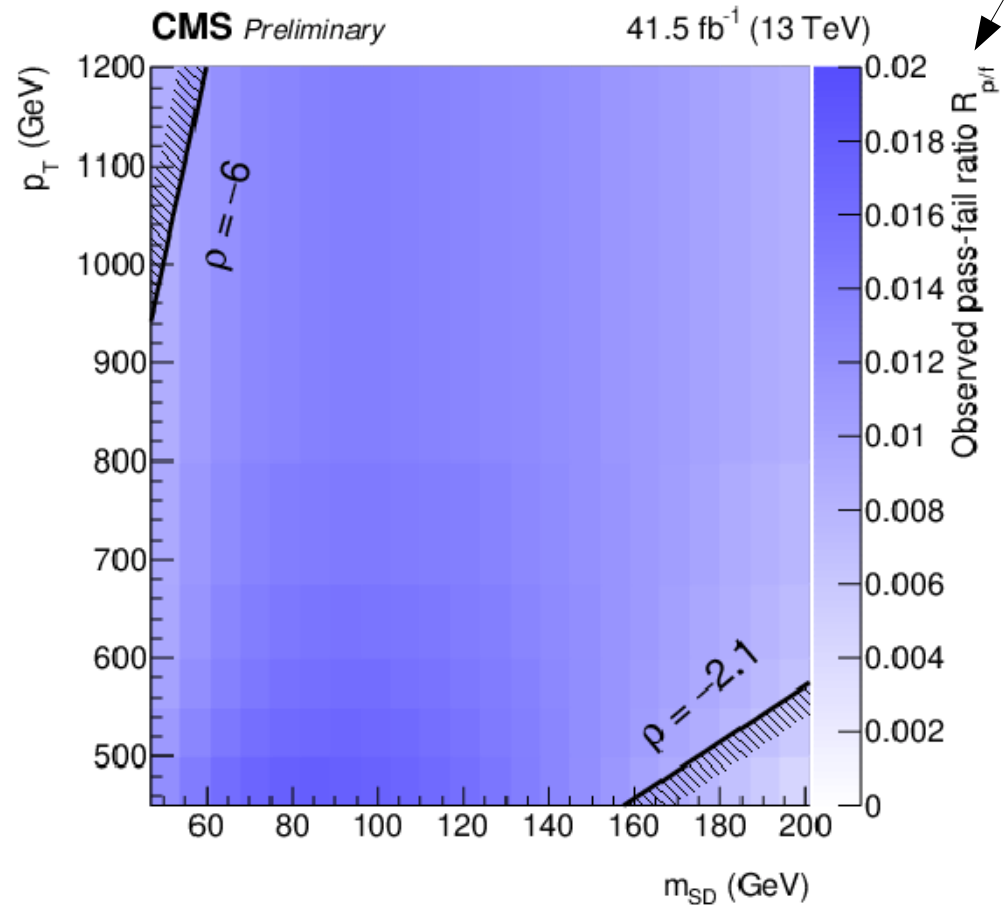
- Parameterically fit QCD yield within  $(m_{SD,i}, p_{T,j})$  bins:

$$N_{\text{pass}}^{\text{QCD}}(m_{SDi}, p_{Tj}) = \epsilon^{\text{QCD}} \cdot \left( \sum_{k,l} a_{kl} \rho_{ij}^k p_{Tj}^l \right) \cdot N_{\text{fail}}^{\text{QCD}}(m_{SDi}, p_{Tj}),$$

- Account for:

- 'double b-tag' mass dependence
- 'Residual' data/MC tagger performance

$$R_{p/f}(\rho, p_T)$$



# H → bb: Inclusive ggF high $p_T^H - N_{2,1}^{DDT,1}$

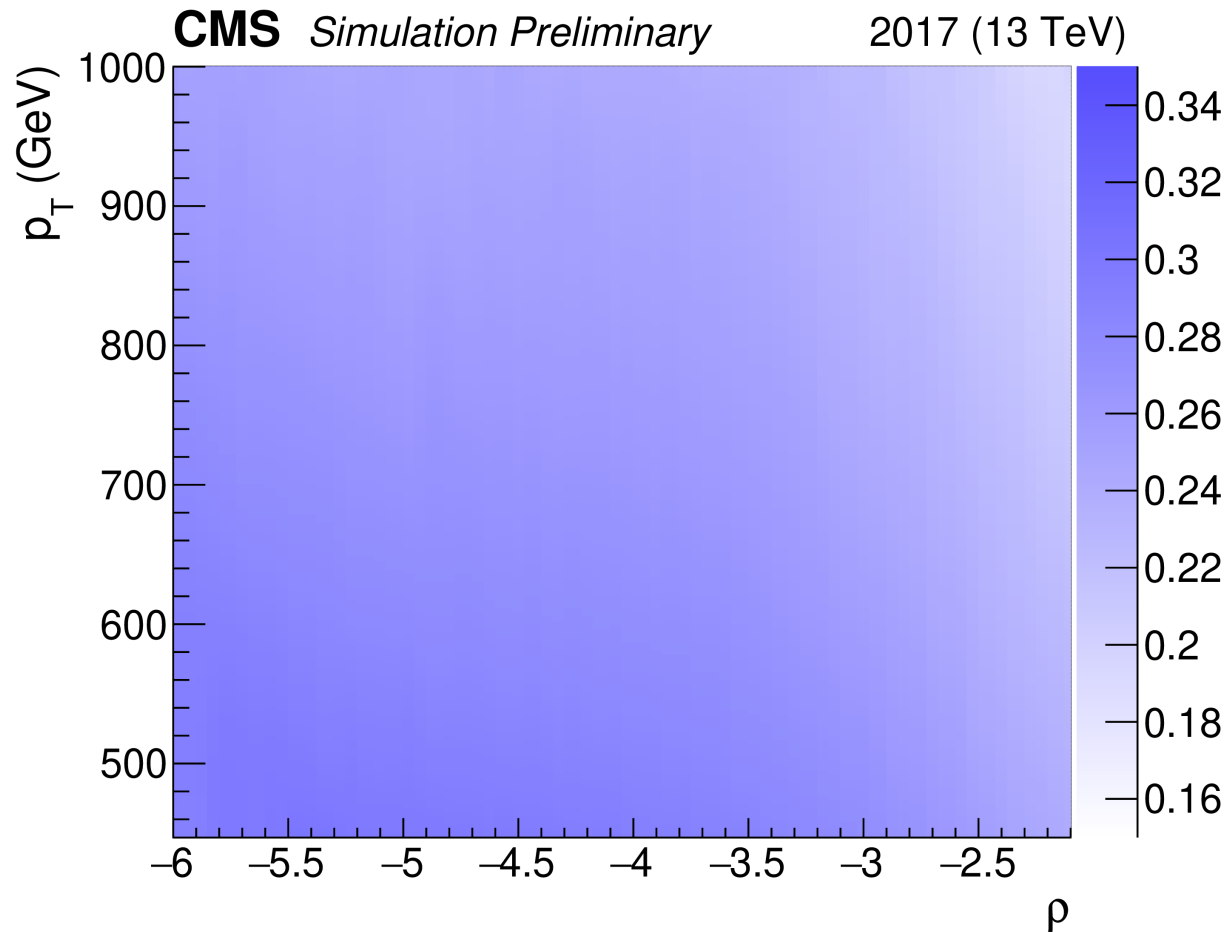


→ Ratio of 3-point/2-point energy correlation co-efficient:  $N_2^1 = \frac{2e_3}{(1e_2)^2}$ .

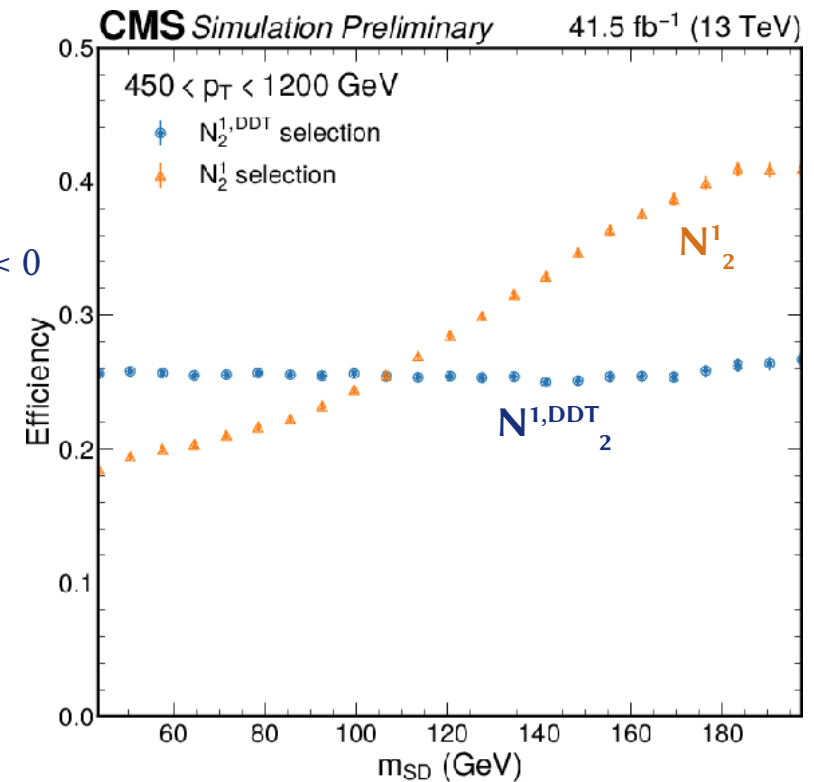
→  $N_2^1$  is transformed linearly to remove  $m_{SD}$  sculpting via subtracting the  $N_2^1$  value at which **26% of the simulated QCD** events are found:

$$N_{2,1}^{1,DDT} = N_2^1 - X_{(26\%)}$$

→  $X_{(26\%)}$  determined as function of  $(\rho, p_T)$ :



Apply:  
 $N_{2,1}^{1,DDT} = N_2^1 - X_{(26\%)}$ 
 $< 0$

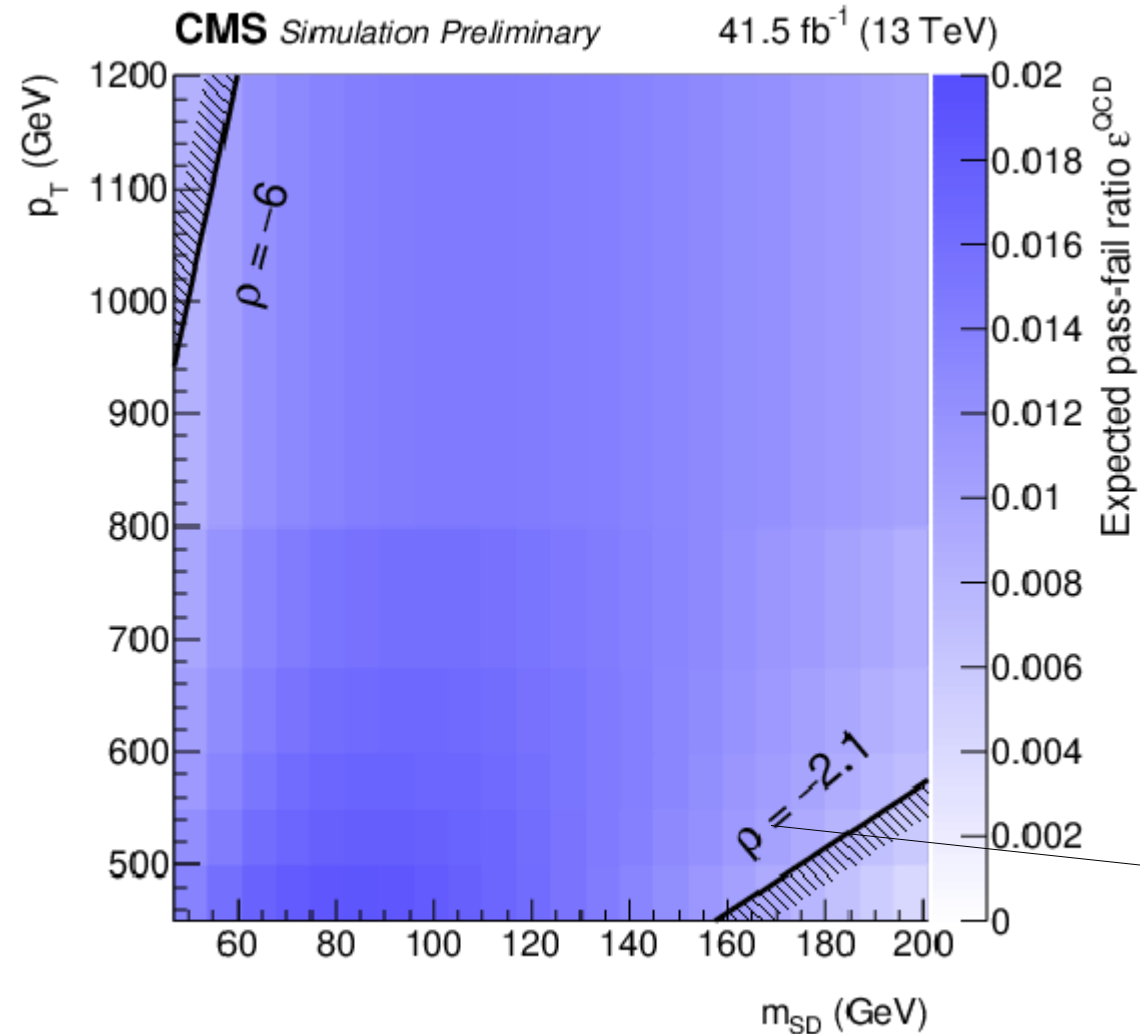




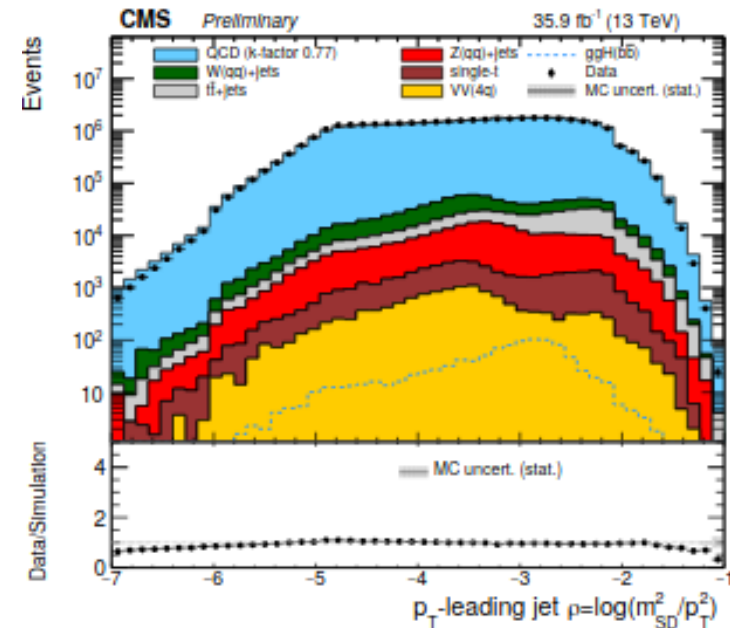
# H → bb: Inclusive ggF high $p_T^H$ - $\epsilon^{\text{QCD}}$ from QCD MC

→ Double b-tagger is designed to be jet mass independent – loss function contains penalty term for differences in jet mass distribution between pass/fail regions.

→ Some residual difference exists therefore 2D Bernstein polynomial fitted,  $\epsilon^{\text{QCD}}(\rho, p_T)$ , that characterises QCD simulated pass-fail ratio of events.



→ Dimensionless quantity that is approx. invariant as a function of jet  $p_T$ :



→  $\rho \sim -2$  corresponds to AK8 instability from finite cone effects  
 →  $\rho \sim -6$  corresponds to the non-perturbative regime of the soft-drop alg.

$$\rho = 2 \ln(m_{\text{SD}} / p_T)$$

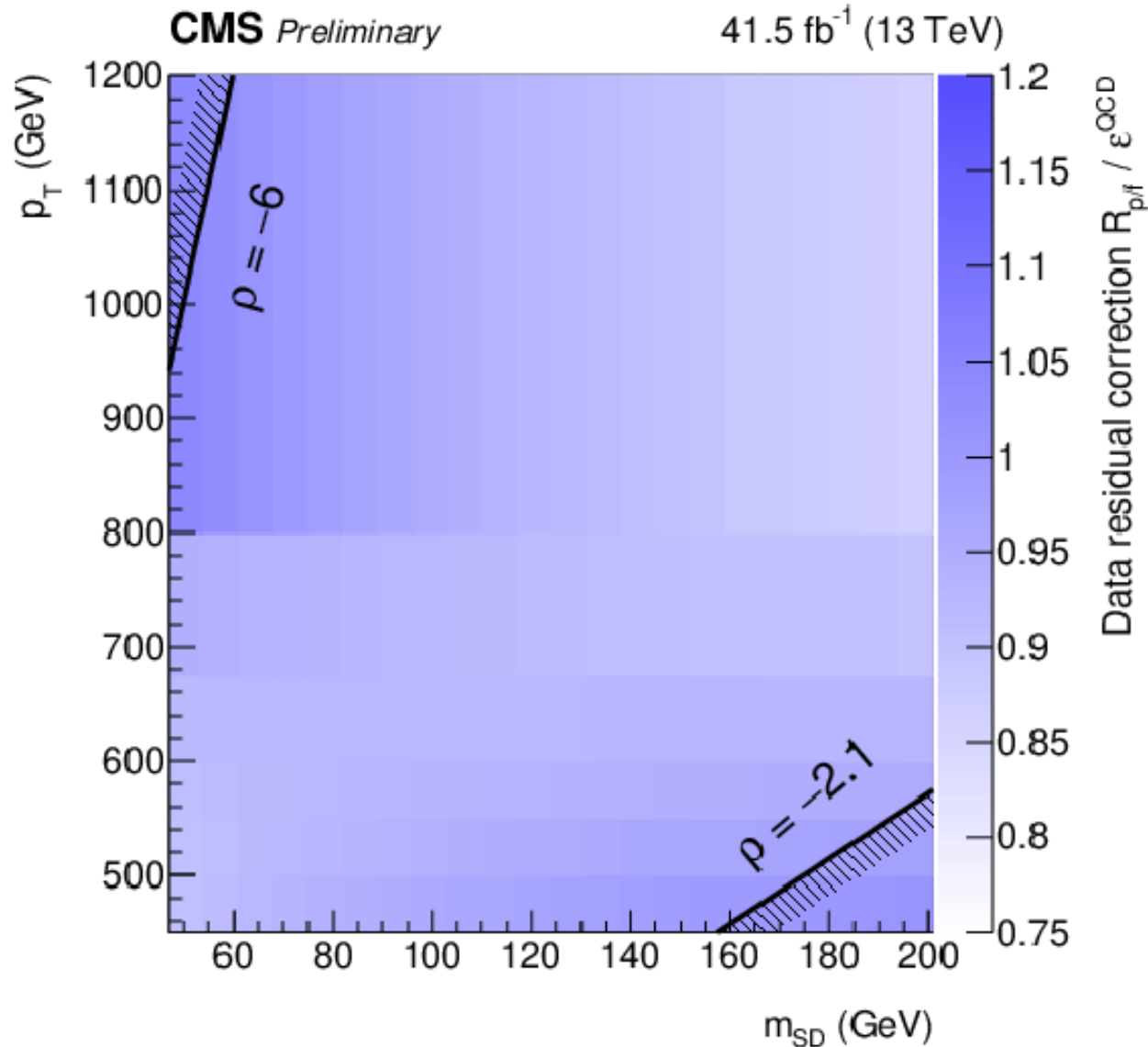
Source: [arXiv:1307.0007](https://arxiv.org/abs/1307.0007)

# H → bb: Inclusive ggF high p<sub>T</sub><sup>H</sup>

→ Double b-tagger performance differs in MC and data.

→ Fit simulation to data to extract residual differences – Bernstein polynomial as a function of (ρ, p<sub>T</sub>):

$$\left( \sum_{k,l} a_{kl} \rho_{ij}^k p_{Tj}^l \right)$$



$H \rightarrow \tau\tau$ :

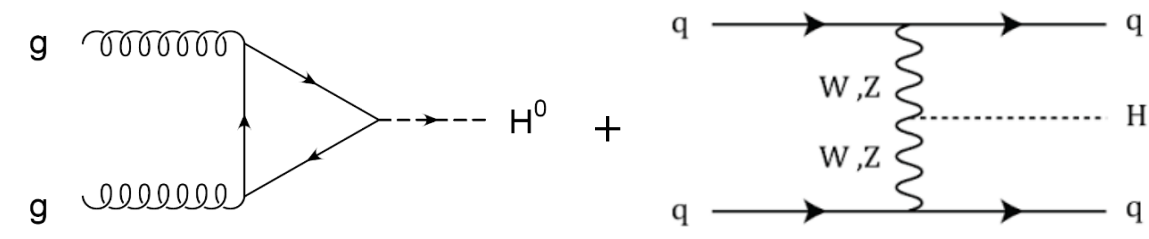
---



$H \rightarrow \tau\tau$

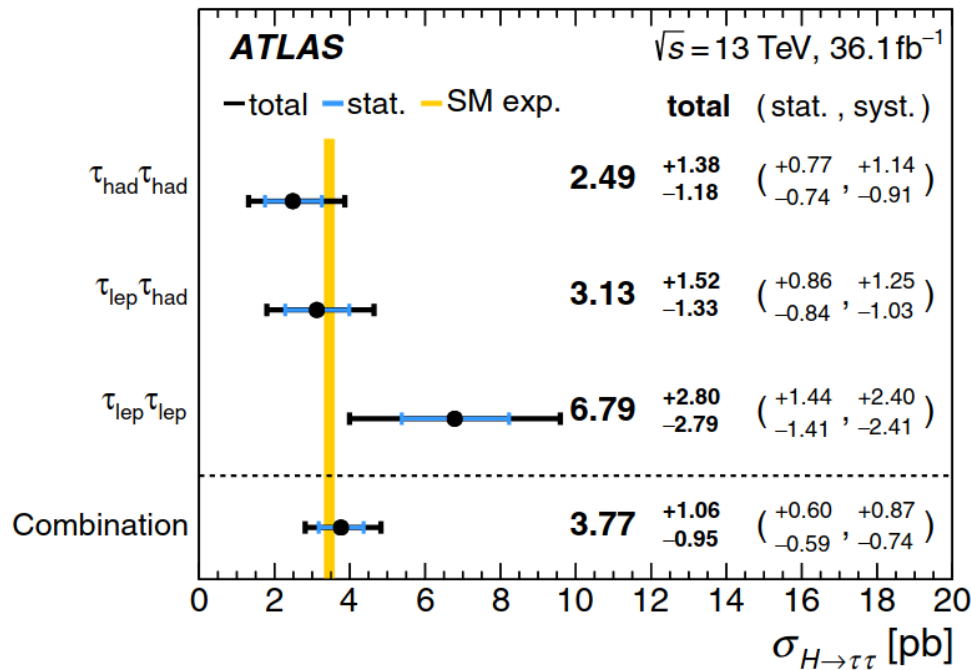
# Test of CP Invariance in VBF $H \rightarrow \tau\tau$

## ATLAS Publications

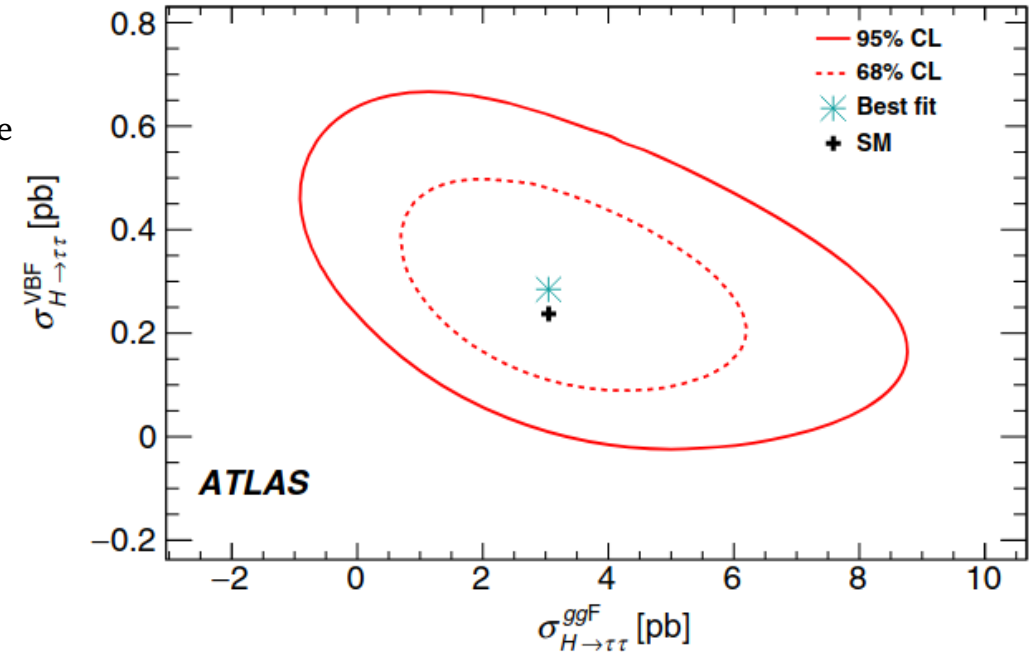
Paper	Luminosity	Date	Signal
Phys. Lett. B 805 (2020) 135426	36.1fb <sup>-1</sup>	Feb. 2020	

→ Uses same dataset as  $H \rightarrow \tau\tau$  observation paper:

Source: Phys Rev. D. 99.072001 (2019)



Analysis sensitive to both ggF and VBF production modes



## Physics Interpretation:

→ Effective Lagrangian ( $\mathcal{L}_{\text{eff}}$ ) composed of:

- Standard Model:  $\mathcal{L}_{\text{SM}}$
- CP-odd mass dim. Six:  $\mathcal{L}_{\text{CP}}^6$

$$\mathcal{L}_{\text{eff}} = \mathcal{L}_{\text{SM}} + \sum_i \frac{f_i^{(5)}}{\Lambda} \mathcal{O}_i^{(5)} + \sum_i \frac{f_i^{(6)}}{\Lambda^2} \mathcal{O}_i^{(6)} + \mathcal{O}\left(\frac{1}{\Lambda^3}\right)$$

$$\mathcal{L}_{\text{eff}} = \mathcal{L}_{\text{SM}} + \tilde{g}_{HAA} H \tilde{A}_{\mu\nu} A^{\mu\nu} + \tilde{g}_{HAZ} H \tilde{A}_{\mu\nu} Z^{\mu\nu} + g_{HZZ} H \tilde{Z}_{\mu\nu} Z^{\mu\nu} + \tilde{g}_{HWW} H \tilde{W}_{\mu\nu}^+ W^{-,\mu\nu}$$

→ CP-violation of VBF production parameterised by:

$$\begin{aligned} \tilde{g}_{HAA} &= \frac{g}{2m_W} (\tilde{d} \sin^2 \theta_W + \tilde{d}_B \cos^2 \theta_W) & \tilde{g}_{HAZ} &= \frac{g}{2m_W} \sin 2\theta_W (\tilde{d} - \tilde{d}_B) \\ \tilde{g}_{HZZ} &= \frac{g}{2m_W} (\tilde{d} \cos^2 \theta_W + \tilde{d}_B \sin^2 \theta_W) & \tilde{g}_{HWW} &= \frac{g}{m_W} \tilde{d}, \end{aligned}$$

→ Under arbitrary choice that  $\tilde{d} = \tilde{d}_B$ , one can parameterise the strength of CP-violation via:

$$|\mathcal{M}|^2 = |\mathcal{M}_{\text{SM}}|^2 + \tilde{d} \cdot 2 \text{Re}(\mathcal{M}_{\text{SM}}^* \mathcal{M}_{\text{CP-odd}}) + \tilde{d}^2 \cdot |\mathcal{M}_{\text{CP-odd}}|^2$$

→ The choice  $\tilde{d} = \tilde{d}_B$ , whilst arbitrary is motivated as it yields  $\kappa_W = \kappa_Z$  as and VBF HWW vs HZZ not separable:

$$\tilde{d} = -\hat{\kappa}_W = -(\tilde{\kappa}_W / \kappa_{\text{SM}}) \tan \alpha$$

→ This is the same assumption used in the  $H \rightarrow WW$  and  $H \rightarrow ZZ$  combination.

→ VBF sensitive to CP violation due to momentum dependence of CP-violating terms:

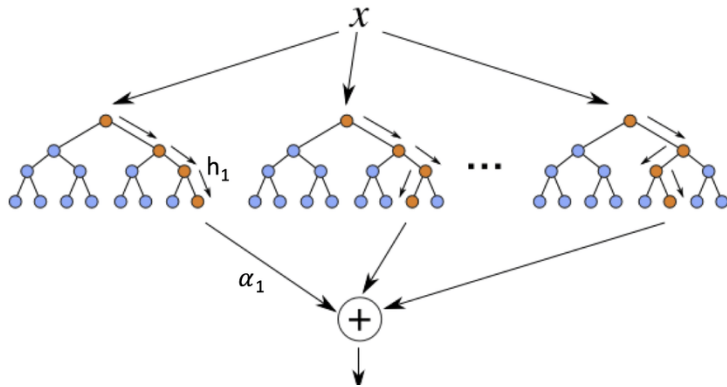
$$T^{\mu\nu}(p_1, p_2) = \sum_{V=W,Z} \frac{2m_V^2}{v} g^{\mu\nu} + \sum_{V=W,Z,\gamma} \tilde{d} \frac{2g}{m_W} \epsilon^{\mu\nu\rho\sigma} p_{1\rho} p_{2\sigma}$$

H → VV tensor structure

→  $H \rightarrow VV$  limited by  $m_H = (p_1 + p_2)^2$ , but VBF production is not.

→ Boosted Decision Tree (BDT) to define enriched VBF signal against SM bkg's:

- **H Properties:**  $[m_{\tau\tau}^{\text{MMC}}, \dots]$
- **$\tau\tau$  System:**  $[\Delta R(\tau\tau), \dots]$
- **VBF Topo.:**  $[m_{jj}, \dots]$



→ Cut on BDT:

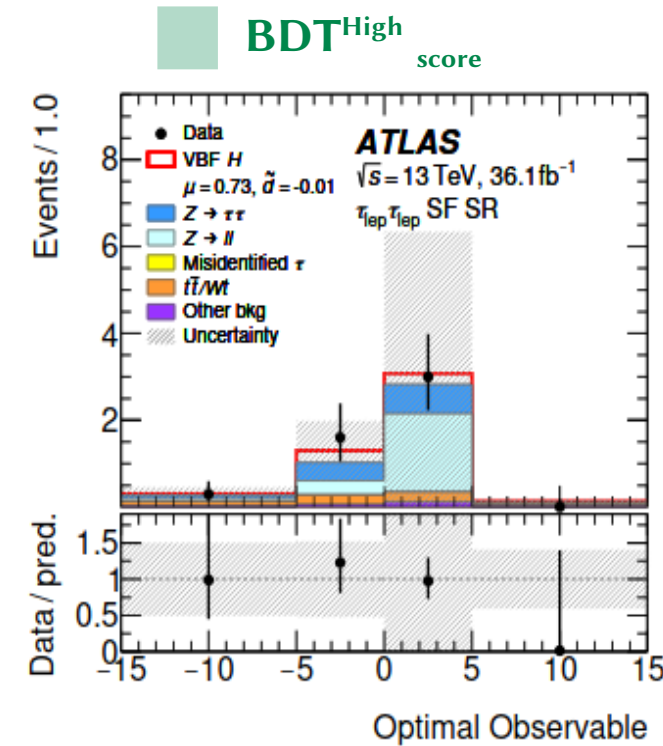
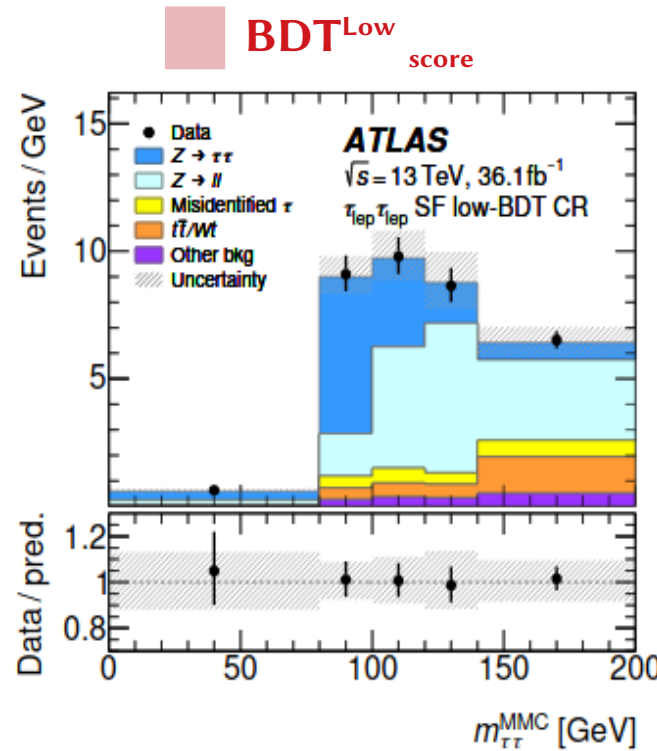
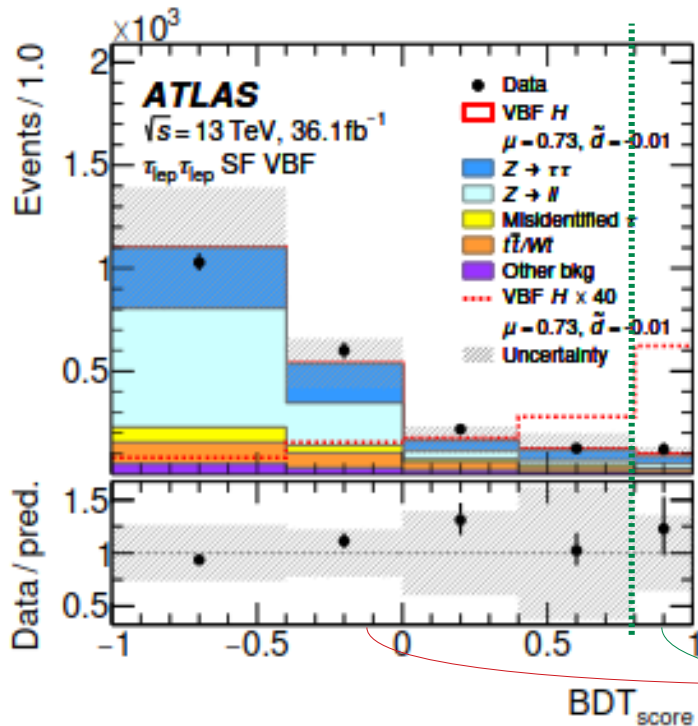
BDT<sub>High</sub> = Signal pure  
BDT<sub>Low</sub> = Bkg enriched

## Fit Model:

→ Total of 11 fit regions:

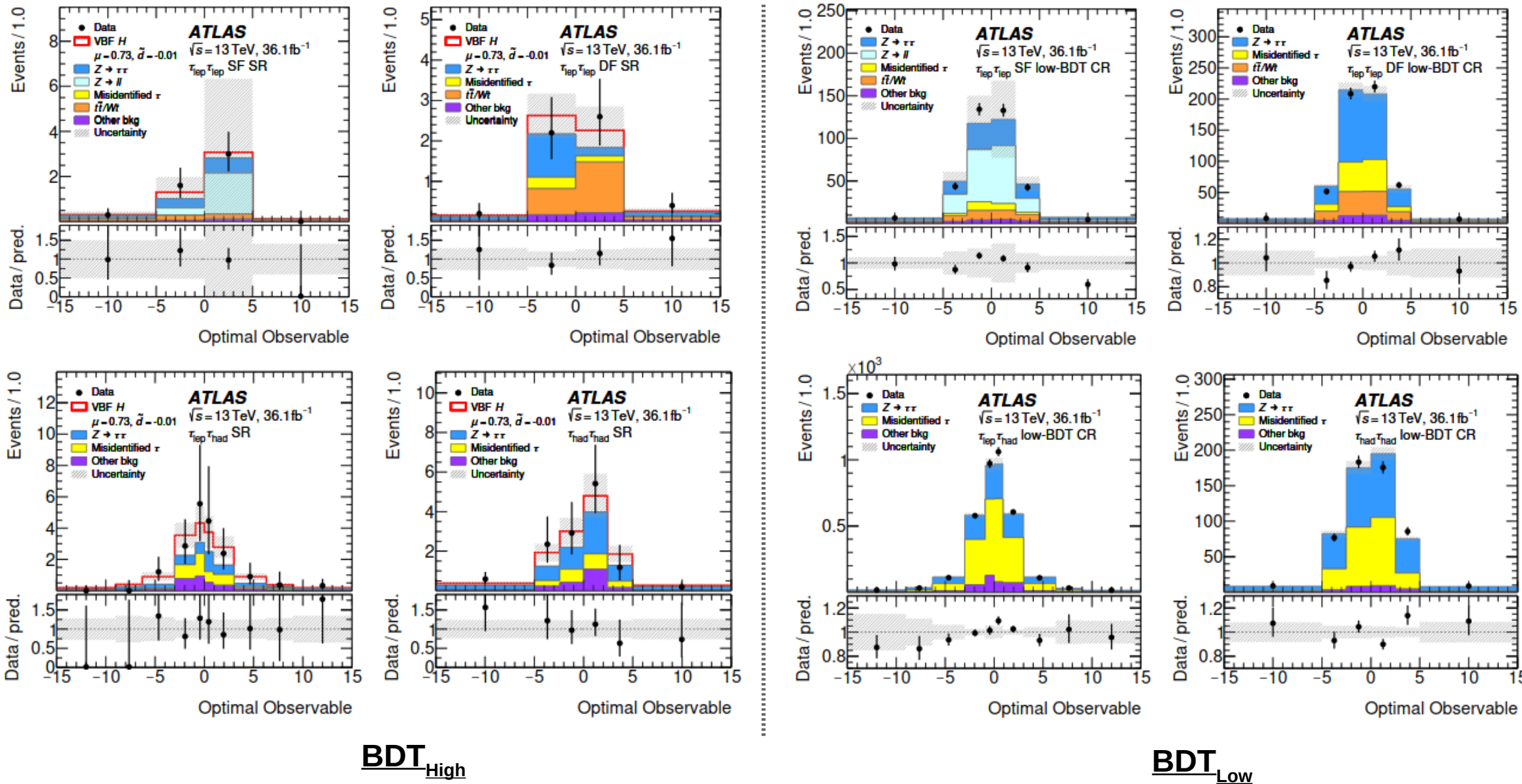
	$\tau_{\text{lep}} \tau_{\text{lep}}$ SF	$\tau_{\text{lep}} \tau_{\text{lep}}$ DF	$\tau_{\text{lep}} \tau_{\text{had}}$	$\tau_{\text{had}} \tau_{\text{had}}$
BDT <sup>High</sup> <sub>Score</sub>	Opt. Obs.	Opt. Obs.	Opt. Obs.	Opt. Obs.
BDT <sup>Low</sup> <sub>Score</sub>	$m_{\tau\tau}^{\text{MMC}}$	$m_{\tau\tau}^{\text{MMC}}$	$m_{\tau\tau}^{\text{MMC}}$	$m_{\tau\tau}^{\text{MMC}}$
Z → ll CR	Yield			
Top CR	Yield	Yield		

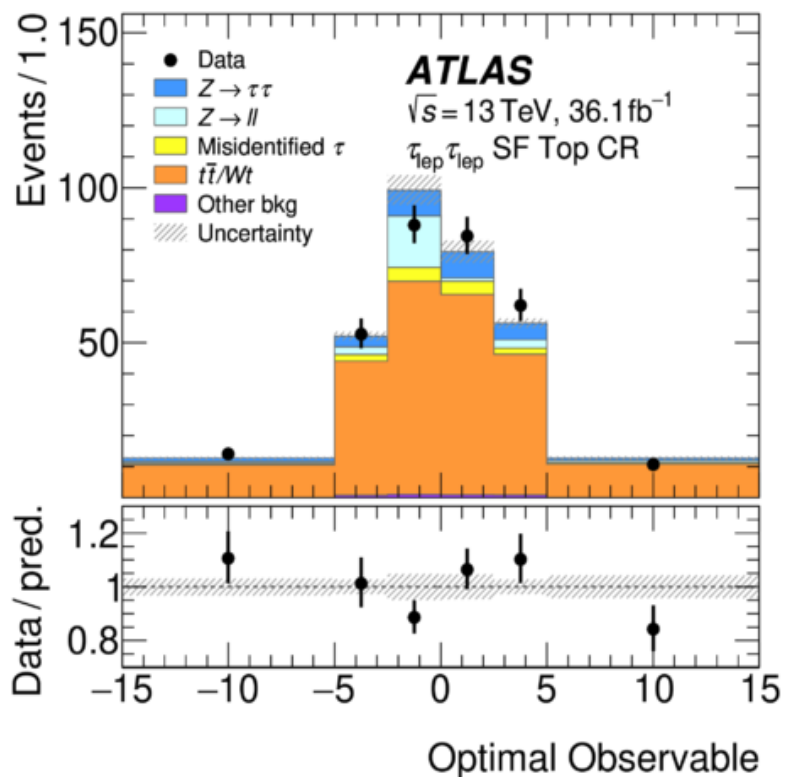
→ Example of Data/MC for  $\tau_{\text{lep}} \tau_{\text{lep}}$  SF



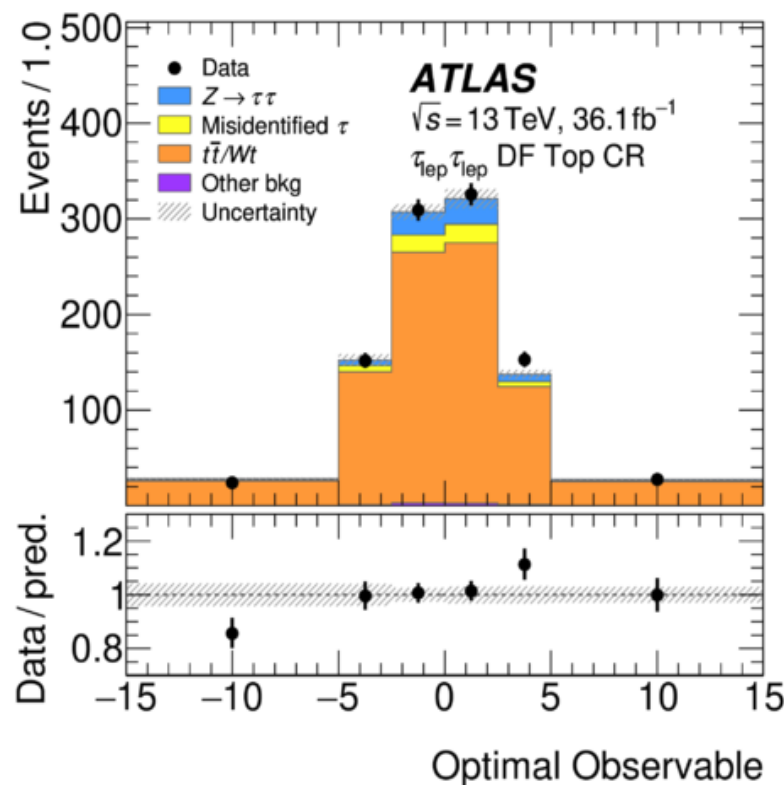
Stephen Jiggins



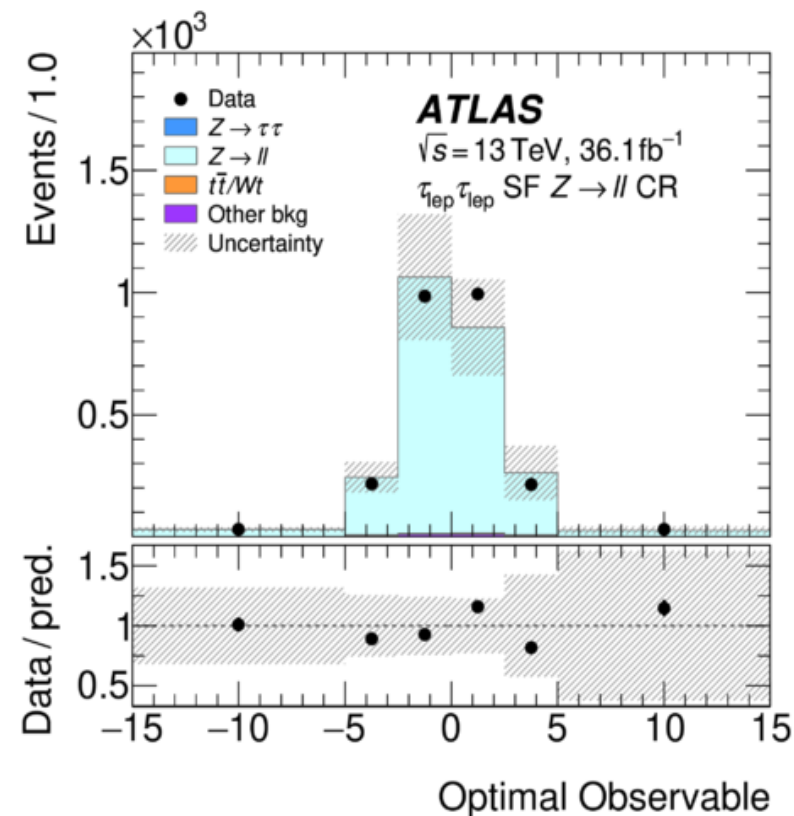




Top CR (SF)



Top CR (DF)



Z->ll CR

→ 77.4 fb<sup>-1</sup> measurement of H → ττ sensitive to VBF+ggF+VH production modes

→ Utilises [eμ, eτ<sub>h</sub>, μτ<sub>h</sub>, τ<sub>h</sub>τ<sub>h</sub>] leptonic channels:

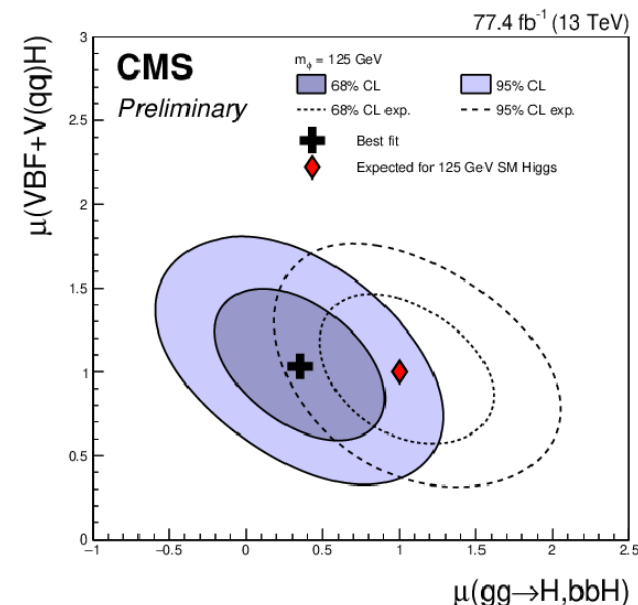
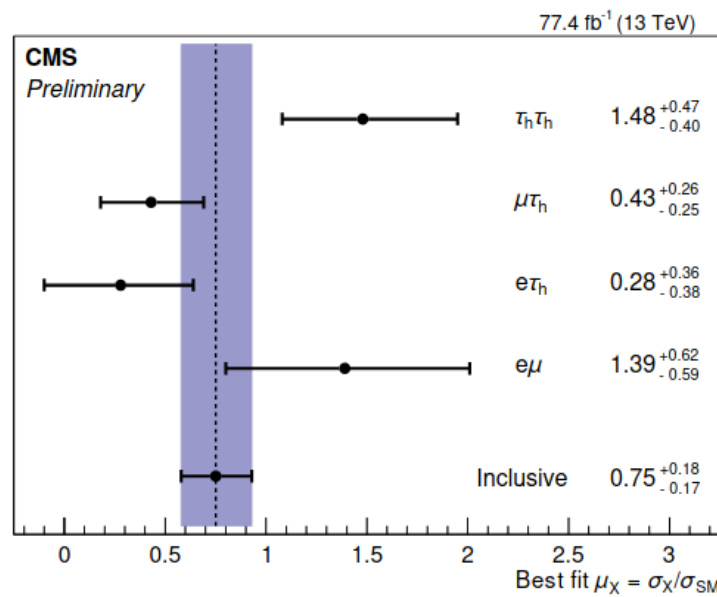
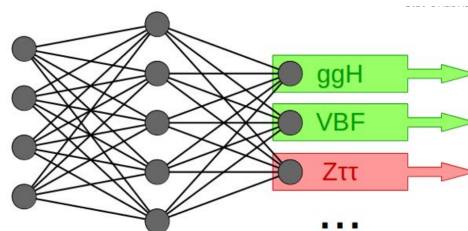
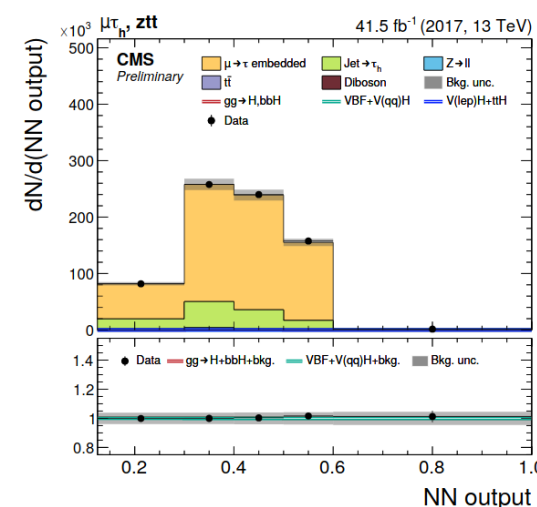
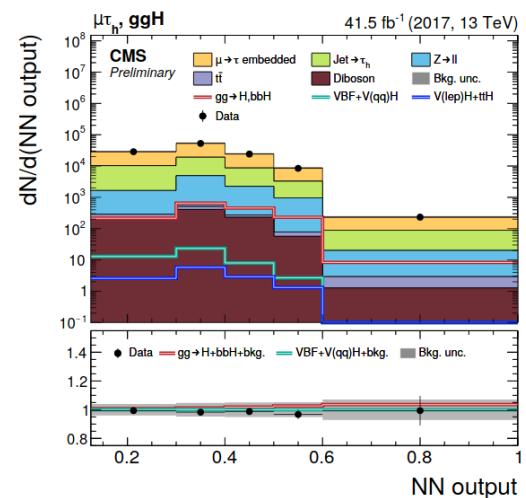
- eμ: Z → ττ + tt dominant bkg
  - e(μ)τ<sub>h</sub>: Z → ττ + W+Jets bkg
  - τ<sub>h</sub>τ<sub>h</sub>: QCD bkg
- } 90% bkg estimated from data-driven methods

→ Softmax conditional probabilities of events from multiclass NN used to separate 9-classes ([ggF,VBF] signal + 7 bkg):

→ Simultaneous binned likelihood fit:

- 21 bkg categories
- 4 lepton channels
- 3 signal models

→ Showing inclusive σ<sub>H→ττ</sub> fit results



→ **CMS**: parameterisation of anomalous HVV couplings via:

$$A(HVV) \sim \left[ a_1^{VV} + \frac{\kappa_1^{VV} q_1^2 + \kappa_2^{VV} q_2^2}{(\Lambda_1^{VV})^2} \right] m_{V1}^2 \epsilon_{V1}^* \epsilon_{V2}^* - \Lambda_1: \text{BSM scale}$$

$$+ a_2^{VV} f_{\mu\nu}^{*(1)} f^{*(2)\mu\nu} + a_3^{VV} f_{\mu\nu}^{*(1)} \tilde{f}^{*(2)\mu\nu} - a_3^{VV} \text{ CP-odd interaction}$$

$$- a_2^{VV} \text{ CP-even interaction}$$

→ HVV anomalous couplings measured using effective cross-section ratios  $f_{a_i}$ , and relative phase  $\Phi$ :

$$\phi_{a_i} = \arg\left[\frac{a_i}{a_1}\right] \quad f_{a_i} = \frac{a_i^2 \sigma_i}{\sum a_i^2 \sigma_i}$$

→ **ATLAS**: parameterisation of CP odd terms according to:

$$\mathcal{L}_{\text{eff}} = \mathcal{L}_{\text{SM}} + \bar{g}_{HAA} H \bar{A}_{\mu\nu} A^{\mu\nu} + \bar{g}_{HAZ} H \bar{A}_{\mu\nu} Z^{\mu\nu} + \bar{g}_{HZZ} H \bar{Z}_{\mu\nu} Z^{\mu\nu} + \bar{g}_{HWW} H \bar{W}_{\mu\nu}^+ W^{-\mu\nu},$$

Where:

$$\bar{g}_{HAA} = \frac{g}{2m_W} (\bar{d} \sin^2 \theta_W + \bar{d}_B \cos^2 \theta_W) \quad \bar{g}_{HAZ} = \frac{g}{2m_W} \sin 2\theta_W (\bar{d} - \bar{d}_B)$$

$$\bar{g}_{HZZ} = \frac{g}{2m_W} (\bar{d} \cos^2 \theta_W + \bar{d}_B \sin^2 \theta_W) \quad \bar{g}_{HWW} = \frac{g}{m_W} \bar{d},$$

→ Assume that  $\tilde{d} = \tilde{d}_B$  as indistinguishable with dataset

$$|\mathcal{M}|^2 = |\mathcal{M}_{\text{SM}}|^2 + \bar{d} \cdot 2 \text{Re}(\mathcal{M}_{\text{SM}}^* \mathcal{M}_{\text{CP-odd}}) + \bar{d}^2 \cdot |\mathcal{M}_{\text{CP-odd}}|^2$$

→ Transform between the two parameterisations:

$$\tilde{d} = \cos(\phi_3) \sqrt{\frac{f_3 \sigma_1}{(1-f_3) \sigma_3}} \quad \text{and} \quad f_3 = \frac{r_3^2}{1+r_3^2} \quad \text{Where:} \quad r_3^2 = \tilde{d}^2 \cdot \frac{\sigma_3}{\sigma_1}, \quad \text{sgn}(\tilde{d}) = \cos(\phi_3)$$

→ Comparison of transformed limits performed internally, regrettably can not be shown here today